

Human psychophysics of direct cortical stimulation of somatosensory cortex

Jeneva A. Cronin

A dissertation

submitted in partial fulfillment of the
requirements for the degree of

Doctor of Philosophy

University of Washington

2018

Reading Committee:

Jeffrey Ojemann, Co-chair

Rajesh Rao, Co-chair

Eric Chudler

Program Authorized to Offer Degree:

Bioengineering

© Copyright 2018
Jeneva A. Cronin

University of Washington

Abstract

Human psychophysics of direct cortical stimulation of somatosensory cortex

Jeneva A. Cronin

Co-chairs of the Supervisory Committee:

Jeffrey Ojemann

Department of Neurological Surgery

Rajesh Rao

School of Computer Science and Engineering

Feedback is a vital part of any control system, and somatosensory feedback is essential for efficient and precise movement. Thus, future rehabilitative brain-computer interfaces (BCIs), such as neuroprostheses, require the integration of somatosensory feedback for improved control. Such bidirectional BCIs (BBCIs) will both record from and stimulate the nervous system to restore function. Direct cortical stimulation (DCS) of the primary somatosensory cortex (S1) through electrocorticography (ECoG) electrodes is one possible method of providing sensory feedback to users. The future success of ECoG sensory stimulation will depend on our ability to elicit a wide range of useful tactile perceptions through stimulation. However, the field's understanding of the relationship between DCS parameters, a subject's ability to perceive DCS, and the percepts a subject experiences is limited. I have endeavored to address these

limitations using DCS via macro-ECoG electrodes in human subjects who can describe their perception and experience of DCS.

We first examined the psychophysics of DCS of S1, using bipolar, biphasic DCS waveforms characterized by their current amplitude, pulse phase width, pulse frequency, and stimulation train duration. We found that although perceptual thresholds vary between subjects, certain relationships between the stimulation parameters and their perceptual thresholds hold, including a previously reported finding in non-human primates and rats that perceptual charge thresholds decrease with decreasing pulse width and increasing pulse frequency. Next we assessed subjects' response times to S1 DCS compared to their response times to haptic stimuli and found that subjects respond significantly slower to S1 DCS than to haptic touch. Finally we considered how S1 DCS could perform in a future BCI by evaluating how S1 DCS would affect subjects' sense of ownership over an artificial limb and exploring how subjects could use S1 DCS as feedback in a motor-based task. We found that S1 DCS could indeed evoke a sense of ownership and be used as task feedback, but may not have been a trivial feedback signal to learn. These findings have implications in the development of somatosensory feedback for BCIs. Given that we observed similar trends in subject perception as is noted in studies using other electrical stimulation modalities, it is possible that we can apply what we have learned through these macro-ECoG DCS studies to other stimulation modalities.

1 Acknowledgments

I have worked with so many talented individuals during this time, all of whom have contributed in some way to my graduate school success and development, and I am immensely grateful for their help, encouragement, and friendship.

First, I would like to thank my advisors, Jeffrey Ojemann and Rajesh Rao for their guidance and support as I navigated graduate school and this research project. I would also like to thank my mentors, Kurt Weaver and Jared Olson, who helped conceive of and guide this research project, and who have encouraged me throughout the whole process. They all helped me hold on to my scientific curiosity and excitement throughout this arduous thesis research journey while also helping me learn to leave good enough alone. I also want to thank the rest of my supervisory committee - Eric Chudler, Geoffrey Boynton, and Chris Neils - who have helped guide my research and my graduate school experience. I am very grateful for all of their support in my endeavors including my non-research interests.

I additionally want to thank several other faculty members who supported me along the way – Andrew Ko, Larry Sorensen, Bing Brunton, and Nathan Kutz – were all tremendously helpful, be it with research advice or piquing my interest in other subjects.

By far one of the best things about graduate school was getting to work alongside amazing researchers through Grid Lab and the Center for Neurotechnology (CNT). I had the pleasure of working with many including: David Caldwell, Kaitlyn Casimo, Nile Wilson, James Wu, Kelly Collins, Kim Hua, Alainna Brown, Felix Darvas, Arvid Guterstam, Chao-hung Clark Kuo, Gabriel Obregon-Henao, Courtnie Paschall, Devapratim Sarma, Jeremiah Wander, and Nancy Wang. I also found tremendous support through other students at the CNT and those that I was privileged to serve with on the Student Leadership Council, including Katherine Pratt, Maggie Thompson, and Tim Brown. Thank you for all of the support, conversations about impostor syndrome, lessons in leadership, and friendship.

I want to especially thank David, Kaitlyn, Nile, and James, my lab/office mates over the past 4.5 years. David and I also did much of this sensory stimulation work together and I am so grateful for his collaboration and support. I think it's probably rare to get to work with a group of such driven and intelligent people for hours and hours every week (and on patient recording weekends), and still call them friends at the end of the day and be excited to find time to get together. They're the thing that I'll miss most about graduate school and have all taught me so much about life and what I want to do with mine.

I would also like to thank my family – my parents for encouraging me in math, science, and all aspects of life from an early age and my siblings for their love and support. Most importantly, I want to thank my husband, Justin, for his endless support and encouragement through every step of graduate school. He made sure that I always remembered the bigger picture and kept adventuring – I am eternally grateful for his perspective.

Finally, none of this research would have been possible without the patients that offered their time and energy to participate in this research and the clinicians that monitored it. Our research subjects deserve a huge recognition for their involvement and interest in progressing our research even though it wouldn't directly impact their medical condition. Thank you.

2 Contents

Table of contents

1	Acknowledgments	5
3	Introduction	9
3.1	Clinical and Societal Significance	9
3.2	Overview of BCIs	11
3.3	Why Sensory Feedback in Brain-Computer Interfaces	11
3.4	Relevant Somatosensory Physiology for stimulation	12
3.5	BBCIs and Somatosensory Feedback Approaches	15
3.6	Stimulation physiology	20
3.7	Human psychophysics and responses to DCS: Thesis contributions	22
4	General Methods	23
4.1	Subjects	23
4.2	Cortical reconstructions and electrode localization	23
4.3	Stimulation Hardware and Data Acquisition	24
4.4	Stimulation protocol	24
5	Direct Cortical Stimulation Psychophysics	26
5.1	Introduction	26
5.2	Methods	27
5.3	Results	34
5.4	Discussion.....	46
6	Response Timing	51
6.1	Introduction	51
6.2	Methods	53
6.3	Results	59
6.4	Discussion	63
7	Ownership of artificial limbs	67
7.1	Introduction	67
7.2	Methods	68
7.3	Results	69
7.4	Discussion.....	70
8	DCS for task-based feedback	72
8.1	Introduction	72
8.2	Methods	72
8.3	Results	75
8.4	Discussion.....	78
9	Conclusion	82
9.1	Review of Findings	82
9.2	Limitations.....	84
9.3	Future Work	85

9.4 Ethical Considerations.....	89
10 Appendix 1 - S1 DCS Psychophysics.....	94
11 Appendix 2 - Aperture task: Subjects 1 and 3	106
12 References	111

List of Figures

Figure 4-1. Sample of reconstructed electrode locations	24
Figure 4-2. Stimulation waveform parameters	25
Figure 5-1. Illustration of the double-interleaved 3-down 1-up staircase	30
Figure 5-2. Design of the charge discrimination experiment	33
Figure 5-3. Subjects' percept localization	36
Figure 5-4. Sample perceptual thresholding staircases and psychometric curves	39
Figure 5-5. All subjects' 79% perceptual thresholds for the baseline DCS train	40
Figure 5-6. Current amplitude and charge per phase 79% perceptual thresholds	41
Figure 5-7. Charge thresholds for Subjects 1-8 for all experiments	42
Figure 5-8. Just-noticeable differences for Subjects 6, 8, and 9.....	43
Figure 5-9. Charge discrimination results for Subject 6.....	45
Figure 6-1. Response timing experimental protocol	53
Figure 6-2. Response timing experimental progression by subject	57
Figure 6-3. Comparison of reaction times for four subjects and their DCS electrodes.....	59
Figure 6-4. Comparison of the two blocked sessions for three subjects	60
Figure 7-1. Rubber hand illusion setup.....	68
Figure 7-2. Rubber hand illusion results	70
Figure 8-1. Sample traces of hand position and DCS waveforms from aperture task	76
Figure 8-2. Subject 2's accuracy levels as a measure of performance	77
Figure 8-3. Subject 2's R^2 values as a measure of performance.....	78
Figure 10-1. Another sample of perceptual thresholding staircases	94
Figure 10-2. All subjects' psychometric curves for the baseline DCS train	95
Figure 10-3. Perceptual thresholds for baseline DCS trains on consecutive days.....	96
Figure 10-4. Perceptual thresholds for DCS trains with varied PW	97
Figure 10-5. Perceptual thresholds for DCS trains with varied PF.....	98
Figure 10-6. Charge discrimination results for Subject 8	99
Figure 10-7. Example of goodness of fit assessment for Subject 4	101
Figure 10-8. Example of bridging assumption assessment for Subject 6	104
Figure 11-1. Subject 1's accuracy levels as a measure of performance	107
Figure 11-2. Subject 1's R^2 levels as a measure of performance	107
Figure 11-3. Sample trace of Subject 1's hand aperture position and DCS waveforms.....	108
Figure 11-4. Subject 3's accuracy levels as a measure of performance	109
Figure 11-5. Subject 3's R^2 levels as a measure of performance	110
Figure 11-6. Sample trace of Subject 3's hand aperture position and DCS waveforms.....	110

3 Introduction

Somatosensation is essential for coordinating movements [1], grasping and manipulating objects [2–4], embodying limbs [5,6], and conducting human social interactions [7]. Yet this critical sensation of touch is impaired in many people with paralysis, amputation, and other neurological disorders or trauma. Because touch plays an integral role in our experience and interaction with our environment, restoring touch, or somatosensation, has been identified as a consumer design priority for prostheses [8] as well as a priority for individuals with paralysis [9] [10]. Accordingly, future rehabilitative technologies will need to integrate somatosensory feedback to improve control and function and meet end users goals. Brain-computer interfaces (BCIs), which allow for direct brain control of external devices, may be able to restore both motor and somatosensory functions by recording and decoding motor intentions from the nervous system, moving an end effector (e.g., a prosthetic limb), and electrically stimulating the user’s nervous system in an attempt to restore touch [11].

Useable sensory feedback via electrical stimulation of the nervous system will need to elicit perceptual experiences (percepts) that users can employ to facilitate coherent behavioral responses. As many natural tactile experiences are graded, varied, and time-bound, the future success of sensory stimulation will in large part depend on users’ abilities to quickly perceive a high number of unique percepts elicited by varied stimulation waveforms. Therefore, to develop successful rehabilitative devices, we need to consider a broad space of sensory feedback parameters, sensory percepts, and behavioral responses. My thesis work has employed direct cortical stimulation (DCS) via subdural electrocorticography (ECoG) electrodes to better understand the psychophysics of DCS of the primary somatosensory cortex (S1).

As detailed below, there is a great clinical and social need for a BCI that can restore both motor and sensory functions. After considering the significance of restoring somatosensation, I will discuss the development of BCIs, research to date with sensory feedback in BCIs, methods of delivering somatosensory feedback, and the sensory physiology and stimulation physics that are relevant to this work. Then in the following chapters, I will examine our recent research into the human psychophysics of DCS of S1 (Chapter 5), response times to DCS (Chapter 6), evoking a sense of ownership using DCS (Chapter 7), and using S1 DCS as feedback in a task (Chapter 8).

3.1 Clinical and Societal Significance

An estimated 5.5 million people in the United States alone are paralyzed to some degree, including approximately 1.8 million stroke survivors and approximately 1.5 million spinal cord injured individuals [12,13], and nearly 2 million people have lost a limb [14]. Currently these individuals, and those with other sensorimotor disorders, have limited rehabilitation options, and none of those options can completely restore function or sensation to the affected limbs. In 2004, Anderson [9] asked survey participants with spinal cord injuries to rank their priorities in regaining function. Those with tetraplegia responded that regaining arm and hand function were the most important, while paraplegics ranked regaining sexual function the highest followed by bladder and bowel function [9]. A critical barrier to restoring function to these individuals will be restoring somatosensory feedback from their limbs.

In addition to the impact of sensorimotor disorders on quality of life, function, and psychological well-being [15,16], these disorders also create an economic burden through direct costs such as medical care and indirect costs such as lost productivity. Considering spinal cord injury, a study from DeVivo et al. [17] estimated that average charges for the first year of care were \$523,089 (in 2009 US dollars), ranging from approximately \$311,000 to \$950,000 depending on the level of injury. Following initial expenditures, DeVivo et al. [17] estimated ongoing charges including those for rehospitalization, medical equipment, and attendant care at an average of \$79,759 per year with attendant care accounting for the greatest recurring cost. Using these data and a report from Cao et al. [18], the National Spinal Cord Injury Statistical Center estimated that the lifetime costs of spinal cord injury ranged from approximately \$1.5 to \$4.7 million dollars (in 2014 dollars) for an injury occurring at 25 years of age and from approximately \$1.1 to \$2.6 million (in 2014 dollars) for an injury occurring at 50 years of age [19]. In addition to these direct costs, indirect costs from decreased employment post injury have also been reported. A 2011 study of 515 participants reported employment rates of 83.3% at injury down to 24.5% approximately 3.8 years post injury [20]. Similarly, a 2012 survey of 70,000 households conducted by the Christopher and Dana Reeve Foundation found that almost 42% of respondents with paralysis reported that they were unable to work, and approximately 46% of respondents with paralysis reported an annual household income of less than \$25,000 per year [21]. There are inherent limitations in these cost studies, including the difficulty of estimating costs, self-reported data, and the limited samples of survey participants [17,18]; however, the economic impact of spinal cord injury is clear.

An analysis of the costs of care with and without a hand grasp neuroprosthesis demonstrated that by decreasing the amount of time an attendant was needed, cumulative costs of spinal cord injury could decrease [22]. Although reductions in cost will depend on the rehabilitation method implemented, BCIs and neurorehabilitative technologies have the potential to reduce overall costs and improve users' quality of life for individuals with paralysis and other sensorimotor disorders.

Although it is outside the scope of this work, which focuses specifically on DCS for somatosensory feedback, it should be noted that cortical stimulation could also benefit individuals with other neurological disorders or trauma. Other established and emerging cortical stimulation applications include: deep brain stimulation for movement disorders, traumatic brain injury, post-traumatic stress disorder, and neuropsychiatric disorders [23]; DCS to direct plasticity and alter connectivity [24]; and, both intracortical and surface stimulation for visual impairments [25]. This non-exhaustive list of applications employs different methods of stimulation and will necessarily target different brain regions, but as we will discuss, there is evidence that the principles underlying all cortical stimulation methods may be applied across modalities and across brain regions. Therefore, while this work concentrates solely on somatosensory stimulation, it has a broader clinical and societal significance as we continue to expand our understanding of cortical electrical stimulation.

3.2 Overview of BCIs

BCIs decode brain signals to infer or predict users' intentions and facilitate interaction with the environment via control of an end effector such as a computer cursor or prosthetic limb (see [11,26–31] for reviews of BCI progress). The primary methods and levels of recording electrical brain signals are electroencephalography (EEG) recorded at the scalp, electrocorticography (ECoG) recorded at the cortical surface, and local field potentials (LFPs) and single-neuron action potentials (single units) both recorded intracortically [32]. Beginning first in the late 1960s in non-human primates [33] and then in the 1990s in invasive human studies [34], BCI research has advanced steadily to address the limited rehabilitation options for people with severe neurological trauma and sensorimotor disorders [26] and as a tool for scientific discovery [11].

In 1969, Fetz trained non-human primates to increase the activity of arbitrary neurons recorded via intracortical electrodes in precentral cortex [33]. In 1973, Vidal outlined an experimental program to explore brain-computer communication with human EEG users [35]. Since then, BCIs have been used to direct cursors on a computer screen [36,37], control a BCI-speller [38,39], move paralyzed muscles [40,41], and control robotic arms [42–44]. Although still in research phases, such BCIs have been tested in human subjects with paralysis resulting from spinal cord injury or stroke [36,39,42] and subjects with amyotrophic lateral sclerosis (ALS) [34,45,46]. Much of the current motor BCI research has focused on decoding motor-correlated neural signals from sensorimotor areas, such as those in primary motor cortex following imagined or overt motor movement [27,29]. However, other control signals have also been demonstrated in humans including mental calculation (e.g., mathematical subtraction) to modulate gamma-power in the dorsolateral prefrontal cortex [47,48], mental object rotation to modulate 8-30 Hz signals in centro-parietal EEG electrodes [49], auditory perceptual imagery to modulate signals over temporal lobe [50], visual stimuli to modulate signals over the occipital cortex or centro-parietal regions [38], and motor imagery to modulate signals over posterior parietal cortex [51].

3.3 Why Sensory Feedback in Brain-Computer Interfaces

Given the advances in BCIs over the past two decades, one may wonder why we should still investigate the integration of somatosensory feedback into BCIs. Although not always obvious as we interact with our environment, somatosensory feedback plays a crucial role in our abilities to dexterously manipulate objects and interact seamlessly with our surroundings (see [52] for a thorough review of how tactile signals are used during object manipulation). Afferent tactile signals allow us to complete motor tasks by adjusting grip (perpendicular) and load (tangential) forces based on the shape and surface friction of an object [52]. Tactile signals and projections between the somatosensory and motor cortices have also been implicated in the ability of non-human primates to learn new motor skills [53]. Additionally, somatosensation makes limbs feel like one's own [5,54], and has significant emotional and social impact as a means of communicating via physical touch [7,55,56].

Various studies have demonstrated motor deficiencies after somatosensation is disrupted via a local anesthetic or by altering the function of neurotransmitters. When a local anesthetic is

applied to human subjects' fingertips, their initial grasp force applied to lift an object increases significantly and they have a higher rate of finger misalignment for a pinch grasp even with visual feedback [1]. Then while holding an object with anesthetized fingertips, subjects' grip force is often greater than without anesthesia but it decreases throughout 20-30 second trials and their drop rate increases significantly [2]. Similarly, non-human primates lose finger coordination and fine control of grip forces when regions of S1 are inactivated with a GABA_A-agonist injection [3].

Most motor-based BCIs have used users' intact visual [57] and/or auditory [58,59] systems for feedback, but have not fully integrated somatosensory feedback into a bidirectional BCI (BBCI) [60]. Prior work in non-human primates has demonstrated that performance on a BCI task is improved with visual feedback compared to with no feedback [61], but it is unlikely that visual feedback alone in future human BBCIs will fully compensate for subjects' loss of somatosensation and consequent motor impairments. There are cases of patients losing tactile and proprioceptive feedback after an infection or autoimmune reaction damages their sensory afferents, causing acute sensory neuropathy. Although their motor function and sense of pain and temperature remain intact, their motor movements including walking and dexterous hand movements never return to their former state when tactile processing was intact [4,54]. Visual feedback does help these patients and can improve their performance on motor tasks, but deficits still remain even with visual feedback [62,63].

In addition to the necessity of somatosensory feedback for interacting with one's environment, prior work has suggested that integrating somatosensory feedback into a BCI task can improve performance. In non-human primates, integrating external somatosensory feedback through a robotic exoskeleton with visual feedback improved performance on an intracortical motor-based BCI task over visual feedback alone [64]. Similarly, providing cortical sensory feedback through intracortical microstimulation (ICMS) in non-human primates improved BCI task performance as compared to task performance with auditory feedback or without any task feedback [65].

In humans, Pistohl et al. provided proprioceptive feedback noninvasively through a robotic manipulandum that passively moved the user's arm and increased human performance in a myoelectric-control task [66]. In EEG-based motor-imagery BCIs, proprioceptive feedback improved performance by enhancing sensorimotor desynchronization in the 8-25 Hz frequency range [67]. For upper limb amputees with myoelectric prostheses, somatosensory feedback via peripheral nerve stimulation has also improved performance in both blinded (i.e., subjects wore blindfolds) [68] and sighted object manipulation tasks [69]. Some subjects have also reported a decrease or loss of their phantom limb pain following somatosensory stimulation [69]. These results suggest that incorporating somatosensory feedback into BCIs and future neural rehabilitative devices will improve their functionality and users' quality of life.

3.4 Relevant Somatosensory Physiology for Stimulation

Before reviewing progress on sensory feedback in BCIs, we will briefly review the relevant somatosensory physiology to help guide discussion of current somatosensory interface

technologies. We will focus primarily on the peripheral mechanoreceptors that respond to somatosensory events and their ascending pathway into the primary somatosensory cortex (S1). A full examination of somatosensory physiology is outside of the scope of this work, but more detailed reviews can be found in [52,70,71].

There are four primary tactile afferents in glabrous skin that innervate specific mechanoreceptors which respond to cutaneous stimuli: fast-adapting type I (FA-I, sometimes referred to as rapidly adapting, or RA) which innervate Meissner corpuscles; slow-adapting type I (SA-I) which terminate in Merkel disks; fast-adapting type II (FA-II) which innervate Pacinian corpuscles; and, slow-adapting type II (SA-II) which innervate Ruffini endings [52,71–73]. Type I afferents terminate in the superficial skin with the highest density in the fingertips where they extract spatial features of dynamic mechanical events, such as rubbing a textured surface. Type II afferents terminate deeper in the skin and have a lower, but roughly uniform density, in the hand. They are seemingly involved in transient mechanical events such as when a handheld object makes or breaks contact with another object (e.g., when a handheld coffee cup makes contact with a table) and provide information about the shape and texture of objects. Some studies suggest that certain afferents are highly involved in specific tactile functions: SA-I in skin indentations, FA-I in low frequency skin vibrations (flutter), SA-II in skin stretch, and FA-II in high-frequency vibration [52,72,73]. However, others stress that all afferents respond to aspects of a tactile event (i.e., skin deformation) and together they shape our tactile perception [71].

Proprioceptive information primarily originates from proprioceptors in the muscles and tendons, muscle spindle afferents and Golgi tendon organs, respectively. Muscle spindle afferents convey information about the position and velocity of the body while Golgi tendon organs convey information about muscle tension [72]. There is also some evidence that Type II afferents affect proprioception as they respond to changes in skin strain that occur during joint movement [52].

Information from mechanoreceptors and proprioceptors in distinct parts of the body is relayed to the cortex via afferent neurons. These afferent nerve fibers are bundled together into fascicles which have a protective sheath, known as the perineurium. Groups of fascicles encircled by another supportive sheath, the epineurium, form a nerve. Nerves at the wrist (i.e., the median, ulnar, and radial nerves) contain between 20,000 to 35,000 nerve fibers, of which approximately 17,000 are cutaneous afferents carrying information from one or a small group of mechanoreceptors [73,74]. Nerves contain both ascending afferent fibers carrying somatosensory information, as well as descending efferent fibers which innervate muscles [73].

Primary afferents that encode tactile and proprioceptive information via mechanoreceptors branch in the spinal cord into both local and ascending projections. The ascending projections synapse in the medulla and then decussate (cross) to the contralateral side forming the dorsal column-medial lemniscal pathway. The secondary afferents (e.g., cuneate neurons) integrate input from primary afferents and terminate in the lateral portion of the ventral posterior (VP) nucleus of the thalamus, a subregion known as the VPL. The VPL and other subregions of the VP

thalamus are organized somatotopically [72]. Some ascending projections from primary afferents also convey somatosensory information to the cerebellum via spinocerebellar tracts [72].

Primary afferents may encode information through both their firing rates (i.e., rate coding) and their relative spike timing to one another in an ensemble (i.e., relative spike timing). A single primary tactile afferent can project its signal to thousands of cuneate neurons in the lower medulla (via the dorsal column) and each cuneate neuron may receive signals from several hundred tactile afferents such that approximately 11,000 second-order cuneate neurons may respond to stimuli at a single fingertip. One model for processing signals from tactile afferents involves second-order neurons uniquely encoding various patterns of primary afferents' relative spike timing that are representative of different contact-surface shapes [52].

From the thalamus, somatosensory information is carried via thalamocortical neurons to all areas of the primary somatosensory cortex (S1), which is somatotopically organized and arranged in cortical columns [72]. S1 is comprised of four areas which together process tactile and proprioceptive information: areas 3a, 3b, 1, and 2, moving posteriorly from within the central sulcus to the postcentral gyrus. Proprioceptive information from VP travels to areas 3a and 2, while tactile information from VP travels to areas 3b, 1, and 2. Within S1 there are also local projections with area 3b projecting to area 1, and area 3a projecting to area 2 [72]. The proprioceptive areas, 3a and 2, are only roughly organized by somatotopy compared to the tactile areas, 3b and 1 [70]. S1 then projects to the secondary somatosensory cortex (S2) on the superior bank of the lateral fissure [72] and directly and indirectly via the posterior parietal cortex to the primary motor cortex (M1) [72,75]. Within S1, information from submodalities of afferents seems to converge, with the majority of S1 neurons exhibiting both a sustained, SA-1 like response, and an off, FA-I like response [71].

Like S1, S2 is also organized somatotopically, but more roughly as the receptive fields for neurons in S2 seem to be larger [76,77]. For example, S2 exhibits separation of evoked responses to stimuli applied to the hand and foot but not to different fingers [78]. While tactile stimuli evoke potentials in only the contralateral S1, both the contralateral and ipsilateral S2 regions respond to stimuli on one side of the body [77–79]. This bilateral response of S2 seems to be due to both connections between hemispheres and neurons with bilateral receptive fields that receive input from the thalamus [76,77]. Some studies suggest that information is processed in S1 and then subsequently in S2 based on longer latency responses in S2 than in S1 [79] and others suggest both feedforward and feedback connections between S1 and S2 [78,80]; however, others suggest parallel processing of information in S1 and S2 [81,82]. S2 is thought to be involved in higher order processing, including sensorimotor integration, attention, and memory, and possibly integrating non-painful and painful stimuli [83]. Tactile discrimination studies in which stimuli were presented successively also suggest that S2 is involved in storing and integrating prior stimuli information [78]. Relatedly, S2 is believed to play a role in tactile learning and recognition, as lesions to S2 can result in tactile recognition deficits in humans, an effect known as tactile agnosia [76,84]. Connections between S2 and

motor areas may also enable active tactile exploration of an object by providing sensory feedback to direct movements [84].

Some studies have suggested that while S1 and other primary sensory areas such as the primary auditory cortex are involved in encoding information about a sensory-specific stimuli, S2 may begin to encode multimodal sensory events [78]. S2 may also be involved in integrating tactile inputs from functionally related body parts [76]. In addition to the involvement of S2, other multisensory integration areas, which combine information from various sensory modalities, are likely involved in tactile perception and forming a coherent representation of our environment [85–87]. These higher-level association or integration areas are not completely understood but may include ventral premotor cortex (PMv) [88–91], inferior parietal sulcus (IPS) [89], posterior parietal cortex (PPC) [86,92], inferior prefrontal cortex (inferior PFC) [86], ventral intraparietal area (VIP) [93], and posterior superior temporal sulcus [94] as reported in human and non-human primate studies [87]. Further examination of the current understanding of how the response of S1 and other somatosensory areas leads to a conscious tactile perception can be found in [52] and [71].

3.5 BCIs and Somatosensory Feedback Approaches

One of the best examples of a sensory BCI in wide use today, albeit not a sensorimotor BCI, is the cochlear implant, which as of 2008 had more than 120,000 users worldwide [95]. The cochlear implant electrically stimulates the tonotopically organized cochlea to address severe hearing loss and deafness. Users are able to learn to use and interpret signals from the device, although some aspects of typical auditory stimuli, such as music and conversations in noisy environments, are still difficult to interpret and are being addressed in ongoing research [95–97]. Cochlear implants rely on the auditory nerve to relay signals to higher cortical processing areas, and thus for deaf patients without an intact auditory nerve, cochlear implants do not work. For these individuals, auditory brainstem implants [98], and auditory cortex stimulation [99] are being researched. Other non-sensorimotor examples of sensory BCIs are also in development to address visual [25,100] and vestibular impairments [101].

To address the loss of sensorimotor function, a bidirectional sensorimotor BCI, or BBCI, should decode motor-related neural signals, execute a movement of an end effector, and encode sensory feedback that relays information about the end effector, for example the pressure a prosthetic limb is exerting on an object [60,72,102]. For such BBCIs, sensory feedback can be provided using electrical stimulation methods via both peripheral interfaces and cortical interfaces. These methods include peripheral nerve stimulation [69,103,104], targeted muscle reinnervation [105,106], intracortical microstimulation (ICMS) [60,65,107,108], and direct cortical stimulation (DCS) [109–113]. In the following sections we will discuss some examples of these interfaces used to provide somatosensory feedback and elicit somatosensory percepts. For a review of the types of physical electrode interfaces used in these modalities see [72] and [74].

Peripheral nerve interfaces

A number of studies have demonstrated the use of peripheral nerve interfaces to elicit somatosensory percepts in humans. Peripheral nerve interfaces can be extraneural (extrafascicular) or intraneural (intrafascicular) depending on whether or not they penetrate the nerve fascicles (i.e., the perineurium) [114]. Extrafascicular interfaces have been used chronically for several years in humans whereas intrafascicular interfaces have not demonstrated long term, stable use in humans [72,114]. Stimulation via peripheral nerve interfaces has elicited sensations of pressure, pulsing, tapping, buzzing, vibration, flutter, brushing, sandpaper, and motion among other percepts [69,73,114–116].

Using intrafascicular electrodes which stimulated the median and ulnar nerves in the forearm, Raspopovic et al. demonstrated that a human subject with a transradial amputation could modulate the grasp force exerted by an EMG-controlled prosthesis with sensors at the fingertips to enable feedback [103]. In other studies, intrafascicular implants were used to both decode different movements and to stimulate sensory afferents in order to produce percepts [116,117] or provide feedback on the grip strength and limb position of a prosthesis [104]; however, the decoding and stimulation were done separately and not in a closed-loop fashion.

Using extrafascicular nerve cuff electrodes, Tan et al. were able to elicit tactile perceptions including pressure and tapping in two subjects with transradial amputations for 16 and 24 months post implant [69]. In this study and another from the same group, with the two subjects then 32 and 40 months post implant, peripheral sensory stimulation improved their performance on motor based tasks using their usual myoelectric prosthesis [68,69]. Both subjects also experienced an increased sense of ownership over their prostheses [68] and reported that their phantom limb pain disappeared [69].

Targeted muscle reinnervation

Targeted muscle reinnervation (TMR) is another peripheral approach to restoring sensorimotor function in amputees whereby residual motor and sensory nerve fibers that had innervated the amputated limb are surgically redirected to denervated muscles and skin, often in the chest [72,73,118]. Two subjects who underwent TMR 9 and 15 months post amputation, referred sensations from touching their reinnervated chests to specific areas of their amputated hands [105]. Their tactile acuity of the reinnervated skin, measured by grating orientation thresholds and point localization thresholds, was similar to or better than that of the normal chest skin [119]. In a separate study, three subjects were able to control the movements of an advanced prosthesis using EMG recordings from their reinnervated skin following TMR surgery [120]. In a proof of principle study, sensory feedback and motor control were combined such that a TMR subject was able to operate a myoelectric tool using native and reinnervated muscle sites on the residual limb while receiving somatosensory feedback to volitionally grip and drop a ball [106].

While peripheral nerve interfaces [69,103,104], and targeted muscle reinnervation [105,106] have shown success in providing sensory feedback to human users with upper limb amputations, peripheral interventions would not work in someone with a spinal cord injury or

other sensorimotor disorder of the central nervous system. For those individuals, cortical interventions, such as intracortical microstimulation (ICMS) or direct cortical stimulation (DCS) will need to be developed.

Intracortical microstimulation

In non-human primates, ICMS sensory feedback, via microelectrodes that penetrate into the cortex, has been used to deliver stimulation proportional to the force exerted on a sensorized prosthetic fingertip [107] and to create closed-loop BCIs, decoding motor intention and encoding sensory feedback [65,108]. Numerous studies have demonstrated that non-human primates can learn to use the signal from ICMS of S1 to perform a task (see [60] for a review). Some studies have tried to deliver biomimetic stimuli, which replicate innate processing patterns, using ICMS signals that are believed to have some naturalistic component. For example, Tabot et al. had non-human primates perform tactile discrimination tasks using both mechanical stimuli and ICMS stimulation of area 3b and considered how information about contact location, pressure, and timing should be conveyed [121]. Other studies have not tried to mimic natural sensations and instead have used ICMS to provide feedback on the distance to a target [122] or on the direction to move a cursor [123]. Still others have purposefully demonstrated sensory substitution or augmentation, using ICMS to convey information from a head-mounted infrared sensor to rats during a discrimination task [124].

All of these studies have demonstrated subjects' ability to apply the novel ICMS stimuli to a task. Dadarlat et al. [122] have demonstrated that non-human primates can not only learn to use ICMS stimulation as feedback, but they can also integrate a learned, artificial signal from S1 ICMS with a visual signal to perform a task. Depending on the reliability of the visual feedback the animals can perform better with ICMS and visual feedback combined [122]. Prior work has also considered how varying ICMS stimuli can be differentiated, and has suggested that non-human primates can discriminate ICMS with different temporal [125–129] and spatiotemporal patterns [126].

Additional studies have demonstrated that the ICMS feedback signal can be used in a BCI-controlled task, thus closing the loop between decoding motor signals and encoding sensory feedback. O'Doherty et al. was the first to describe a BBCI in a non-human primate in which the animal controlled a cursor using motor cortical activity and chose the right or left target based on S1 ICMS signals [123]. In the same study, the authors demonstrated that the animal could eventually perform equally well on the open-looped, somatosensory feedback portion of the task with ICMS feedback or vibrotactile feedback (using a joystick to control the cursor). In another BBCI study from this group, they decoded motor signals from M1 to move a virtual arm and stimulated S1 to provide feedback about the "tactile properties" or "textures" of potential targets displayed on a screen [108]. Klaes et al. demonstrated that a non-human primate could use feedback from ICMS of S1 better than auditory feedback to find an invisible target in a virtual space using a joystick [65]. In a BBCI experiment, they then decoded motor-related signals from posterior parietal cortex to control a virtual arm and allow the non-human primate to select the correct target from two choices (correct target evoked ICMS stimulation, whereas the incorrect target did not) [65].

While the above studies have focused on stimulating tactile regions of S1 such as area 3b [121,127,128] and area 1 [121], other studies have considered ICMS of proprioceptive areas 3a [129] and 2 [70]. One study demonstrated that stimulating area 2 via ICMS, could bias a non-human primate's perception of hand motion, suggesting that stimulating proprioceptive-specific cortical areas could provide efficacious proprioceptive feedback [70].

In humans, ICMS has been delivered to elicit tactile sensations [130] and proprioceptive sensations [131] in subjects with tetraplegia (one subject in each study). The majority of tactile sensations were categorized as "possibly natural" with somatosensory qualities of "pressure," "tingle," and "electrical" [130].

Direct cortical stimulation

Direct cortical stimulation (DCS), which applies electrical current directly to the surface of the cortex either epidurally or subdurally, has been used extensively in humans for both clinical treatment and research [132]. DCS was first applied to a living human subject as early as 1874 by Robert Bartholow who elicited muscle contractions in his patient. In the early 1900s, DCS was used to localize epileptic foci and map brain regions [133], and in 1934 an intraoperative technique for recording from and stimulating through electrocorticography (ECoG) electrodes was developed [132]. In the 1940s and following, Penfield and colleagues used DCS to create motor and sensory maps in human patients, while others explored if DCS could be used to provide feedback for a visual prosthesis [134–136]. Its use has continued in clinical practice to identify critical functional brain areas in patients with tumors and epilepsy, and in research to map other brain regions and their function [132].

In humans, DCS of somatosensory areas has been used to map these areas and to deliver somatosensory feedback. In 1964, Libet et al. reported on DCS parameters and their effect on conscious somatosensation in humans [112]. This work has been followed by more studies on the perception of DCS of S1 that have delivered stimulation through macro-ECoG electrodes [109,110,112,113,137] and more recently through high-density, micro-ECoG electrodes [111,138,139]. Macro-ECoG electrodes, which are used clinically, often have exposed surfaces of several millimeters in diameter with a center-to-center spacing of approximately 1 cm. High-density or micro-ECoG electrodes often have similarly-sized exposed surfaces of approximately 2 mm with a center-to-center spacing of several millimeters.

In our lab's experience, macro-ECoG DCS of sensory areas has elicited abstract sensations sometimes described as "vibration", "buzzing", "pressure", and "wind running down the hand" (Table 5-3) [109,110]. It is not surprising that DCS elicits abstract sensations as we may be affecting up to 500,000 neurons in a non-biomimetic fashion (this number of neurons stems from an estimation of the neuronal density in non-human primates [140] and the ECoG electrode surface area). As the work presented in this document will focus on DCS of S1 in human subjects, this prior work will be discussed in more detail in the following sections, particularly in Chapter 5.

Other somatosensory stimulation methods

Although we will focus on DCS and compare our results to those from other electrical stimulation research (primarily with ICMS or high-density DCS), it is worth noting that there are other methods of neural stimulation in development. As deep brain stimulation (DBS) for clinical treatment has become more prevalent [23], research groups have experimented with thalamic stimulation for somatosensory feedback with a DBS lead that is implanted for clinical purposes (e.g., treatment of essential tremor) [141,142]. Most percepts elicited in these studies were described as a “tingle” and were “rather unnatural” [109].

Other groups have considered stimulating parts of the spinal cord or the dorsal root ganglia (DRG) to restore motor abilities and somatosensation. Gaunt et al. applied intraspinal microstimulation to cats and found that sensory axons were activated at lower currents than motoneurons [143]. In anesthetized cats electrical stimulation of the DRG via penetrating electrodes recruited a range of afferent fibers, as measured with a nerve cuff electrode at the sciatic nerve [144]. Unlike peripheral nerves, DRG only contain afferent fibers so stimulating only afferents and not efferent fibers could be more feasible than in intra- and extra-neural peripheral implants. However, the surgery to access and implant a device in the DRG is more invasive and dangerous than implanting other peripheral devices (e.g., a nerve cuff) [73]. In a noninvasive human study, transcutaneous cervical spinal stimulation of an individual with tetraplegia resulted in not only improved motor functioning, but also improved sensory functioning primarily during the weeks with stimulation [145].

There are also non-electrical stimulation methods that are in early stages of development, but could eventually provide a more spatially specific and cell type specific method of stimulation. These include optogenetic stimulation [146–148] possibly using probes that allow for simultaneous recording [149], focused ultrasound [150–152], temporal interference of high-frequency oscillating electric fields [153], and magnetic nanoparticles to induce magnetothermal membrane depolarization [154].

Choosing a somatosensory feedback approach

As previously discussed, cortical stimulation could benefit individuals with paralysis or other neurological disorders or trauma, and we will therefore focus on cortical somatosensory feedback over peripheral options. Specifically, we will focus on DCS via macro-ECoG electrodes because of the three cortical-level interfaces (macro-ECoG, micro-ECoG, and ICMS) only macro-ECoG is regularly implanted for clinical purposes. Unlike ICMS and micro-ECoG sensory stimulation research, which has only been conducted on several human subjects with paralysis, macro-ECoG sensory stimulation research can be conducted on many more subjects who consent to research after a macro-ECoG grid is implanted for clinical purposes (see General Methods).

In addition to the greater prevalence of human macro-ECoG subjects, subdural ECoG grids may also offer some benefits in long-term implantation over penetrating intracortical electrodes, including stability and a less invasive implantation [26]. Implantation of intracortical electrodes can trigger an inflammatory response, recruiting microglia and astrocytes to the site and

encapsulating the probe. This encapsulation seems to increase the electrical impedance and eventually prevent recording nearby neurons. It may also result in chronic neuronal loss [32,155]. Intracortical recordings have been completed up to nearly six years post implant, but most recording durations are between one to two years long, and over that time the number of recorded units declines [156–158]. In contrast to intracortical recordings, intracortical stimulation may remain effective for a longer period of time. A study of the stability of percepts elicited by S1 ICMS in non-human primates demonstrated that the ability to perceive ICMS stimuli can remain stable for several years, and perceptual thresholds may even decrease [159]. Other studies of ICMS in visual cortex have suggested that perceptual thresholds remain stable over time [160] or increase with time [161], but are still elicited.

Although encapsulation of the penetrating electrodes and the resultant increase in impedance primarily affects recording neural activity and not the efficacy of electrical stimulation, we still desire a system that can both record and stimulate neurons for a substantial amount of time. Surface electrodes, such as those used in DCS, do not evoke a strong inflammatory response because they do not penetrate the cortex and have been demonstrated in recordings lasting up to 766 days in humans [162]. Longer-term recordings using ECoG electrodes in humans may be possible, but generally are not done for clinical purposes so the available research on this point is limited.

In future BBIs, we desire a stimulation method with high spatial resolution that elicits natural sensory percepts localized to small areas on the target limb. For such high resolution, ICMS or micro-ECoG stimulation is likely to be used over macro-ECoG stimulation, due to their smaller electrode surface areas and higher electrode density. However, the potential future use of ICMS and micro-ECoG for sensory feedback does not diminish the current research benefit of macro-ECoG stimulation. Thus, in the chapters that follow we present our results on DCS via macro-ECoG electrodes for somatosensory feedback.

3.6 Stimulation Physiology

Before reviewing our work on S1 DCS for somatosensory feedback, we will briefly review how cortical stimulation (ICMS or DCS) evokes neural activity and generates a response. This process is not wholly understood, and questions still remain regarding the cortical volume that is activated during stimulation and what cell types respond. However, since the variability of the physical neural responses to DCS most likely impacts our psychophysical results, we will quickly review some of the current literature.

Electrical stimulation acts by changing the charge of the extracellular space leading to hyperpolarization or depolarization of the cell membrane. At the anode (the electrode that is driven to a more positive potential), the cell membrane is hyperpolarized as current flows into the cell, whereas at the cathode (the electrode that is driven to a more negative potential) the cell membrane is depolarized as current flows out through the cell membrane [163,164]. As current flow must be balanced throughout the cell, the local hyperpolarization and depolarization at the anode and cathode, respectively, must also be locally balanced. Thus, as current flows outward at the cathode and the neural fiber is locally depolarized, current must

also flow inward in the surrounding region creating a hyperpolarized, ‘anodal’ surround. Similarly, as current flows inward at the anode and the fiber is locally hyperpolarized, current must also flow outward creating a depolarized surrounding region [164,165]. In the case of the anode, the depolarized surround region is more spread out than the concentrated depolarized region under the cathode. The densely depolarized region under the cathode is more likely to generate an action potential than the depolarized surround around the anode, so cathodal-first stimulation often requires less current to elicit a response [166]. However, if the surrounding hyperpolarization around the cathode is too large, then an action potential due to the local depolarization will not be able to propagate through the anodal surround [164–166].

Multiple studies and models have suggested that many aspects of stimulation affect the neural responses. For one, a neural response will only occur when there is an extracellular voltage gradient in the direction of the axon [166], so the orientation of axons relative to the stimulating electrodes (which is usually unknown) will impact neural responses [167]. Similarly, the distance between the electrode and the neural elements will affect responses by dictating the current that reaches the neurons or the region of interest [166]. The dendritic arbor structure and the axonal branching structure will also affect responses [167]. Additionally, specific cell-type responses seem to be affected by the polarity of stimulation and at a given stimulation current, the depth of recruitment may be cell-type specific [167].

During ICMS, there is evidence that stimulation evokes a sparse pattern of activation primarily around the electrode tip, and increasing the current activates more cells within that region rather than simply enlarging the region [132,168]. There is also some evidence that microstimulation evokes a short excitatory response followed by a longer period of inhibition, possibly due to synaptic inhibition, which may disrupt processing [132,169]. However, observations in microstimulation may not translate directly to surface stimulation [170].

During DCS, because the resistivity of gray matter is greater than that of cerebrospinal fluid (CSF) [166], a significant percentage of the current may be shunted through the CSF and not flow into the cortex where it can evoke a neural response (~45% based on one model [171]). The electric potential during bipolar DCS, in the case where the distance between the dipole and point of interest is great, falls off with the square of the distance [132,172]. About half of the current will flow deeper than half of the distance between the two stimulating electrodes [173], but the amount of CSF between the electrodes and the tissue will affect the current density [174]. Increasing the current delivered likely increases the number of neurons that are activated within a region and increases the region of activation (in part through synaptic connections) [132]. During stimulation the most likely sites of neural activation are the axon initial segment and the nodes of Ranvier because they have the highest sodium channel concentrations [132,175], but it is still difficult to predict responses to DCS as they depend on the exact morphology of the stimulated cortical region [132]. Finally, DCS can elicit remote effects, potentially due to current volume conduction or synaptic projections [132]. In one study in a human, DCS of the basal temporal area caused aphasic deficits; however, after resecting the basal temporal area, no language deficits occurred, suggesting that the aphasia was caused by remote spread of the DCS [132].

3.7 Human Psychophysics and Responses to DCS: Thesis Contributions

Although a number of studies have delivered sensory feedback to human subjects via electrical stimulation of the cortex or peripheral nerves [11,72], there is a sizeable gap in our understanding of efficacious somatosensory stimulation. What stimulation parameters can convey a wide range of uniquely discernable percepts? How natural does DCS of S1 feel and where do the percepts localize? What S1 DCS patterns can subjects discriminate between? How quickly can subjects perceive and respond to S1 DCS? Can it evoke a sense of ownership as peripheral stimulation can? Can subjects use DCS as feedback in a motor task, as would be required for many rehabilitation uses? Considering these questions will elucidate the potential of DCS for somatosensory feedback, which must allow users to quickly perceive a high number of unique percepts that they can employ to facilitate coherent behavioral responses. My thesis work has endeavored to address these open questions using DCS via ECoG electrodes in human subjects who can describe their perception and experience of DCS.

In the following studies we first examine the psychophysics of DCS of S1, using bipolar, biphasic DCS waveforms characterized by their current amplitude, pulse phase width (PW), pulse frequency (PF), and stimulation train duration (TD) (Figure 4.2). We consider subjects' perceptual thresholds, their just-noticeable differences, and the effect of charge on their perception of the stimulus intensity (Chapter 5). We then consider subjects' response times to S1 DCS as compared to haptic stimulation and find that subjects respond significantly slower to S1 DCS than to haptic touch (Chapter 6). Given that we desire a somatosensory feedback approach that users will want to engage with, we then assess whether DCS of S1 can induce a sense of prosthesis ownership using a novel version of the traditional rubber hand illusion (Chapter 7). After discussing these qualitative and quantitative human responses to DCS, we look at how subjects may use DCS as feedback in a motor task (Chapter 8). I begin the discussion of this research with an overview of the general methods used in these experiments (Chapter 4). Finally, I explore the limitations of this research and conclude by proposing future avenues of research to build from this work (Chapter 9).

4 General Methods

Specific methods for each DCS experiment differ and are detailed within each chapter, but the methods consistent for all DCS experiments are outlined below.

4.1 Subjects

Human subjects implanted with macro-scale ECoG grids for clinical monitoring of intractable epilepsy at the University of Washington Regional Epilepsy Center at Harborview Medical Center (Seattle, WA) participated in DCS studies just prior to surgical resection (see, e.g., Leuthardt et al. [176]). Subjects are primarily implanted with grids or strips of platinum subdural ECoG electrodes with a 2.3 mm exposed diameter and 10 mm center-to-center spacing (Ad-tech Medical, Racine, WI, USA). Clinicians determined grid placement based on clinical needs without consideration for research, and subjects remained hospitalized for approximately seven days for clinical monitoring of epilepsy. During this time they could consent to participate in research studies. All DCS studies were conducted after subjects had resumed taking antiepileptic medications, after approximately six days of hospitalization. Prior to resuming taking this medication, subjects can and often do participate in recording studies that do not involve cortical stimulation.

The clinical environment in which these experiments are conducted can restrict the number of studies that we are able to perform with an individual subject. After waiting until subjects have resumed taking antiepileptic medication to avoid the risk of evoking a seizure during stimulation, we usually have 1-1.5 days to conduct stimulation studies. Subjects' clinical and personal needs during that time, including standard-of-care clinical mapping and rest, limit our time and the experiments that we can run with each subject.

All of the experiments presented here were approved by the Institutional Review Board of the University of Washington, and all subjects gave written, informed consent.

4.2 Cortical Reconstructions and Electrode Localization

We localized electrodes using a preoperative MRI scan, a post-operative CT scan, and custom MATLAB processing scripts as described previously [177–179]. We then identified a pair of adjacent electrodes over the hand sensory cortex to use for DCS based on reconstructions and subject responses to standard-of-care clinical mapping and SSEP phase-reversal.

Clinical mapping results often helped identify electrodes over hand and arm sensory cortex that can be used for DCS (Figure 4-1). Electrodes lying over the seizure focus were avoided during DCS. Some experiments presented here used a pair of control electrodes for 'off-target', non-sensory stimulation. These electrodes were chosen outside of S1 and away from the seizure focus, to minimize the chance of either a perceptual experience or a seizure.

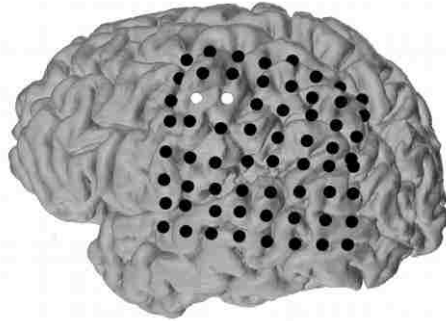


Figure 4-1. Sample of reconstructed electrode locations

Left hemisphere implanted ECoG grid with two electrodes that were used for bipolar stimulation of hand S1 highlighted in white.

4.3 Stimulation Hardware and Data Acquisition

We used an IZ2H-16 stimulator and a LZ48-400 battery pack (Tucker-Davis Technologies, Alachua, FL, USA) to deliver constant-current, bipolar, biphasic, symmetric, square pulse stimulation trains. All experiments were controlled with custom software using OpenEx (Tucker-Davis Technologies) and MATLAB. Neural data was acquired using the Tucker Davis Technologies System 3 with an RZ5D BioAmp Processor and a PZ5 Neurodigitizer.

4.4 Stimulation Protocol

Stimulation waveforms are defined by five parameters: current amplitude, pulse width (PW), pulse frequency (PF), train duration (TD), and the inter-train interval (ITI). Figure 4-2 illustrates how each of these parameters is defined. We began all stimulation studies by establishing a value for the suprathreshold current amplitude that would result in a conscious perception of the DCS. See each chapter for the specific methodology used for each experiment. If subjects did not perceive the initial attempt of S1 DCS identified as described above, or if DCS generated muscle contraction, we selected another set of anatomically appropriate stimulating electrodes until we found a pair of adjacent electrodes that elicited a sensation on the subject’s hand.

Our stimulation waveforms were always below the Shannon limits - a threshold in the relationship between charge per phase and charge density per phase above which experimental data has demonstrated tissue damage [164,180].

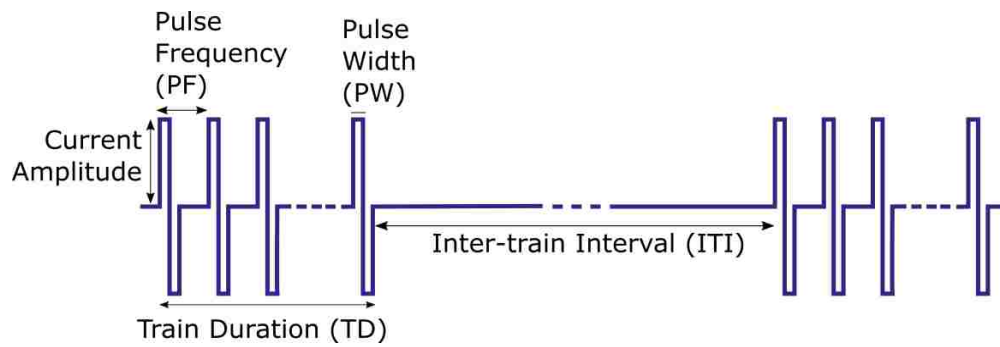


Figure 4-2. Stimulation waveform parameters

Single DCS trains are characterized by their current amplitude, pulse width (PW), pulse frequency (PF), and train duration (TD). Multiple DCS trains in succession are additionally characterized by the inter-train interval (ITI) between two stimulation trains.

5 Direct Cortical Stimulation Psychophysics

To begin our study of the potential of DCS for somatosensory feedback in BBCIs, we examined the psychophysics of S1 DCS by delivering bipolar, biphasic DCS trains to the hand region of S1. As we have discussed, due to the varied and graded nature of typical tactile experiences, the future success of ECoG sensory stimulation will depend on our ability to elicit a wide range of distinguishable tactile percepts through stimulation. However, despite recent research on cortical stimulation for sensory feedback, our understanding of the relationship between DCS parameters, human subjects' perceptual thresholds, and the percepts a subject experiences is still limited.

Here we employed traditional psychophysics methods to investigate the perceptual dynamics of S1 DCS in nine human subjects with indwelling, macro-scale ECoG grids while varying current amplitude, pulse phase width, and pulse frequency. Using a baseline bipolar DCS train of 205 μ s pulse width, 200 Hz pulse frequency, and a 200 ms train duration, we found subjects had perceptual thresholds ranging from 0.47 to 3.76 mA. Increasing the pulse width or pulse frequency caused the perceptual amplitude threshold to decrease. Increases to the pulse frequency also required less charge per phase to reach perceptual thresholds, whereas increases to the pulse width required greater charge per phase to reach threshold. In two subjects we tested their current amplitude just-noticeable differences (JNDs) and found that a change of 120-149 μ A was sufficient to distinguish S1 DCS trains, but as predicted by defined psychophysical laws JNDs seem to be dependent on the intensity of the baseline stimuli. Furthermore, in one subject, we demonstrate that DCS trains with equal total charge are discriminable on the basis of individual parameters. Our findings suggest that DCS of primary somatosensory cortex may be an effective method of providing sensory feedback. Although stimulation thresholds vary from subject to subject, more efficient stimulation may be achieved with smaller pulse widths and higher pulse frequencies based on the charge required to reach perceptual discrimination criteria.

The following chapter is in preparation and will be submitted for publication as:

Cronin, J.A., D.J. Caldwell, K. Hua, K. Collins, G. Boynton, J.D. Olson, J. Tsai, A.L. Ko, K.E. Weaver, R.P.N. Rao, J.G. Ojemann. Psychophysics of direct cortical stimulation for encoding somatosensory sensation in humans.

5.1 Introduction

Bidirectional brain-computer interfaces (BBCIs) that can both decode motor intentions and encode sensory feedback by stimulating the nervous system offer the potential to restore or improve both motor and sensory function after central nervous system injury. Given that somatosensation is essential for coordinating movements [1], grasping and manipulating objects

[2–4], embodying limbs [5], and conducting human social interactions [7], it is predicted that artificial somatosensory feedback is a critical factor to the ultimate success of rehabilitative neuroprostheses. In addition to providing critical sensory feedback, artificial sensory restoration may also improve overall BCI performance. In non-human primates, both integrating external somatosensory feedback through a robotic exoskeleton [66] and providing cortical sensory

feedback through intracortical microstimulation (ICMS) [65] improved BCI task performance relative to task performance without the additional sensory feedback.

Although researchers have yet to demonstrate a fully functional BCI in humans, progress has been made toward closing the BCI feedback loop via electrical stimulation. At the cortical level, artificial somatosensory feedback has been delivered to humans via direct cortical stimulation (DCS) of primary somatosensory cortex (S1) through macro-electrocorticography (ECoG) electrodes [109,110,112,113,137], and more recently via DCS through micro-ECoG electrodes [111,138,139] and via intracortical microstimulation (ICMS) through microelectrode arrays [130,131]. Electrical stimulation through all of these modalities has demonstrated that subjects can experience and discriminate percepts with varying intensity and qualia based on the stimulation parameters [110,111,130,131,139], localize stimulation from different electrode pairs to different areas of the hand and arm [111,130,131,137,139], and use the somatosensory feedback to perform a motor-based task [109,139].

Efficacious BBIs will need to provide sensory feedback that users can employ to facilitate coherent behavioral responses. As many natural tactile experiences are graded, varied, and time-bound, to adequately substitute for natural sensation sensory stimulation will need to enable users to quickly perceive and distinguish a large number of unique percepts elicited by varied stimulation waveforms. While recent research on sensory stimulation has elucidated some aspects of the relationship between perception and stimulation parameters, there remains a gap in our understanding of the stimulation parameters that may be used to convey a range of uniquely discernable percepts. A primary goal of this study was to describe the S1 DCS psychophysical parameter space in humans, as has been done in non-human primates with ICMS stimulation [181]. Here we present results from nine subjects on the psychophysics of S1 DCS, including DCS percept reports, psychometric functions under varied parameter values, and in two subjects, just-noticeable differences and charge discrimination results. Through macro-scale ECoG, our results confirm previous reports that perceptual amplitude thresholds decrease as pulse width or pulse frequency increase, but threshold levels of charge per phase depend on the pulse width and pulse frequency [138,181]. Our charge discrimination results also suggest that while total charge delivered may impact perceptual thresholds, S1 DCS trains of equal total charge are still discriminable on the basis of individual parameters, especially current amplitude.

5.2 Methods

Subjects

Human subjects (n=9) implanted with macro-scale ECoG grids for clinical monitoring of intractable epilepsy at the University of Washington Regional Epilepsy Center at Harborview Medical Center (Seattle, WA) participated in DCS studies just prior to surgical resection, following the general methods outlined in Chapter 4. Subject demographics and epileptic foci are provided in Table 5-1. Subjects 1-7 and 9 were implanted with Ad-tech ECoG grids with a 2.3 mm exposed diameter and 10 mm center-to-center spacing as described in the general methods, Chapter 4. Subject 8, however, only had depth electrodes implanted, rather than a

grid of electrodes, with circumferential electrodes 0.8 mm in diameter and 2 mm in length with center-to-center spacing of 3.5 mm (PMT Corporation, Chanhassen, MN, USA).

Subject	Gender	Age	Handedness	Coverage
1	male	37	right	Left hemisphere grid
2	male	26	right	Right hemisphere grid
3	male	34	right	Left hemisphere grid
4	male	28	right	Left hemisphere grid
5	male	19	right	Right hemisphere grid
6	female	31	right	Right hemisphere grid
7	female	45	right	Right hemisphere grid
8	male	42	left	Left hemisphere depth electrodes
9	male	39	left	Left hemisphere strips and depth electrodes

Table 5-1. Subject demographics

Demographics for all patients in this study, including their ECoG grid coverage.

Cortical Reconstructions

Cortical reconstructions and electrode localization were performed as outlined in Chapter 4.

Direct Cortical Stimulation Protocol

We used the stimulation hardware and protocol described in Chapter 4.

Baseline S1 DCS Parameter Values

All nine subjects completed a perceptual thresholding test for our baseline stimulation train, defined as a DCS train with 205 μ s pulse widths (PW) per phase (i.e., 205 μ s for both the cathodal and anodal phases), a 200 Hz pulse frequency (PF), and a 200 ms train duration (TD). For four of the subjects, we had sufficient experimental time to complete additional perceptual threshold experiments with varied PW (Subjects 4, 5, and 8) or varied PF (Subjects 6 and 7).

Percept Descriptions

After finding subjects' perceptual thresholds (described below), subjects were asked to describe the sensation elicited by S1 DCS and the location of the percept. Subjects 1-3 verbally described where they felt the sensation. Subjects 4-9 drew where they felt the stimulation on a digital hand diagram (as in Figure 5-3) using either a touchscreen tablet or a computer and mouse, while they verbally described the sensation. We neither provided subjects with a questionnaire regarding the stimulation percept nor verbally suggested any descriptors to avoid biasing the subject. Subjects were, however, told that the S1 DCS may feel abstract or different than

natural touch prior to beginning any stimulation studies to prevent unnecessarily surprising or startling subjects naive to S1 DCS.

In addition to digitally indicating (i.e., drawing) their percept location on the hand, Subjects 5, 6, and 8 rated how natural the sensation felt ranging from 1 to 7: 1) Not at all natural; unnatural; 2) Hardly natural; 3) Partly natural; 4) Moderately natural; 5) Quite natural; 6) Highly natural; and, 7) Completely natural. We used a 7-point rating scale rather than the 5-point rating scales used [130] and proposed [182] elsewhere, to give subjects more levels within the middle of the scale after noting that the ICMS subject in Flesher et al.'s study described 233 out of 250 stimuli as "possibly natural" [130]. Based on an anecdotal report of subject perception of verbal qualifiers, these qualifiers categorize increasing intensity [183]. The rating scale was displayed below the hand image, and subjects could either circle their answer or respond verbally.

Perceptual Thresholds

We used a staircase method, an adaptive perceptual thresholding approach in which the current amplitude is stepped up or down based on subjects' responses to the preceding trials, to estimate subjects' perceptual thresholds (in current amplitude). The staircase method provides a relatively simple adaptive approach to efficiently identify thresholds without prior knowledge of a subject's perceptual performance [184,185]. Nine subjects completed a k-down 1-up perceptual staircase, with varied values of k as we determined what pattern worked best for our particular subjects (Subject 1: 1-down 1-up; Subject 2: 6-down 1-up; Subjects 3-9: 3-down 1-up; Table 5-3). If a subject reported feeling the DCS k times in a row, the amplitude was decreased, while if they reported not feeling the DCS in a single trial, the amplitude was increased. Each staircase primarily used four steps of 250 μ A each, then eight steps of 100 μ A, followed by 50 μ A steps for the remainder of the staircase; however, at times a larger step size was added to help subjects reach their perceptual threshold more quickly. Subjects 1-3 completed a single staircase using their k-down 1-up pattern with 50 trials (Subject 1) or 60 trials (Subjects 2 and 3). Subjects 4-9 used a 3-down 1-up, double-interleaved staircase method, consisting of two interleaved staircases each with 25 experimental trials and 5 catch trials, for a total of 60 trials (Figure 5-1). The interleaved pattern was used to decrease the likelihood of a subject learning the 3-down 1-up pattern [184,185].

In general, for each trial, an audio cue of two 200 ms beeps separated by 300 ms were presented beginning 1 s prior to the DCS onset. After the DCS was delivered, subjects were required to indicate whether or not they perceived the DCS train. Subjects 1-4 verbally responded whether or not they felt the stimulus and experimenters manually entered their responses into custom software. Subjects were instructed to respond "yes" or "no" to each trial. To speed up perceptual testing, we implemented a graphical interface for Subjects 5-8 using MATLAB's PsychToolbox and a monitor and keyboard positioned in front of each subject. Our intention was to give subjects full control over the progression of the perceptual thresholding trials to further encourage them to quickly respond to the perception question and proceed to the next trial. Each trial for Subjects 5-8 continued to use the double beep audio indicator, but added a visual fixation cross displayed on the screen for 1.5 s (1 s prior to the DCS and during the audio cue, 200 ms during the DCS train, and 300 ms after the stimulus). The

screen then flipped to a perception question, reading “Did you feel the stimulation?”. Subjects used the left and right arrow keys to indicate whether or not they perceived the stimulus. Once they answered, their response (yes or no) was highlighted on the screen for 0.5 seconds, and then the visual fixation cross appeared for 1.5 seconds before another trial was triggered, beginning once again with the audio cue and visual fixation. The interstimulus interval (ISI), defined as the time between the end of one DCS train and the beginning of the next DCS train varied between and within each subject as it was dependent on how quickly they responded to the preceding trial, with medians of approximately 3.7, 4.3, 4.8, 8.7, 3.7, 3.8, 4.5, 4.2, and 4.8 s for Subjects 1-9, respectively.

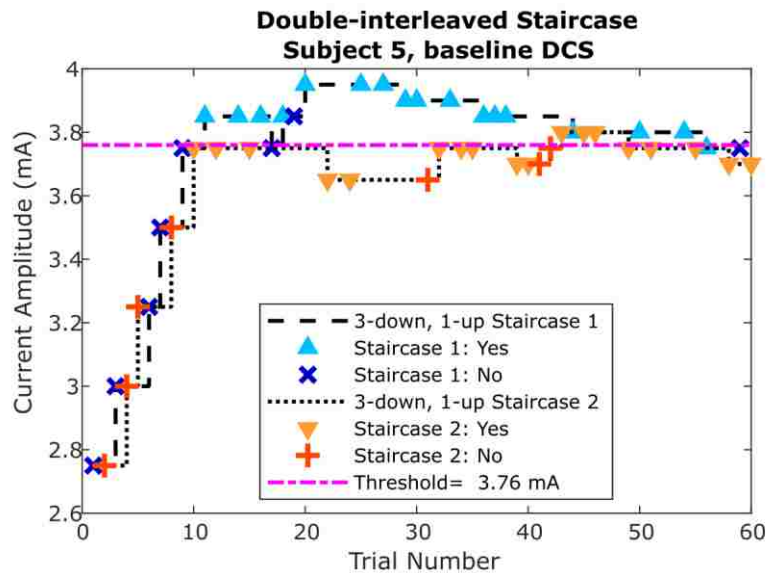


Figure 5-1. Illustration of the double-interleaved 3-down 1-up staircase

This procedure was used with Subjects 4-9. In this adaptive perceptual threshold approach, two staircases are randomly interleaved to prevent subjects from learning the 3-down 1-up pattern of a single staircase. Ten catch trials in which no stimulation was delivered were also interleaved (5 per staircase), but they do not affect the up-down pattern and are not illustrated here.

To estimate false positive rate, Subjects 4-9 completed ten catch trials (5 from each of the two interleaved staircases) during which no stimulation was delivered but the other trial components indicating the start of a trial (i.e., the visual fixation cross and/or the audio cue) were consistent with non-catch trials. Subjects’ perceptual responses to catch trials were not included in the 3-down 1-up staircase pattern. Instead, subjects’ performance on catch trials was used solely to estimate their false positive rate and set the lower bound for their psychometric function (see Psychometric Functions section).

Psychometric Functions

Resultant data from subjects’ perceptual threshold staircase experiments were fit with a Weibull function to estimate their psychometric curve. We applied a maximum likelihood

approach, which maximized the probability of obtaining the experimental data given a Weibull function parameterized with a threshold and slope, as described by Wichmann and Hill [186,187]. Subject data was well fit by a Weibull function as estimated using a goodness of fit approach described by Wichmann and Hill [186] (see supplemental methods for details and sample results. We used a previously described (Wichmann and Hill, 2001 [187]) parametric bootstrap method for psychophysical data with 10,000 simulations to estimate subjects' 68% bias-corrected and accelerated (BC_a) confidence intervals (CIs) for the 79% perceptual threshold parameter [187].

Within subjects perceptual thresholds were compared using a difference in medians permutation test with 10,000 permutations of the threshold parameter distributions obtained during the parametric bootstrap. A p-value of 9.999e-5 is the lowest p-value possible using a test with 10,000 permutations.

We also considered how confidence intervals from the parametric bootstrap would describe the true, underlying, and unknown parameter vector that describes the subject's psychometric curve (i.e., the bridging assumption, [187]). Our results, which are included in Appendix 1, suggest that the estimated BC_a confidence intervals should generally be a valid estimate of the variability of the true, underlying function.

Just-Noticeable Differences

To estimate subjects' JND, we used a two-alternative forced choice (2AFC) task design in which subjects had to identify which of two S1 DCS trains (A or B) felt more intense. A MATLAB and PsychToolbox-based graphical interface was again used to present the experiment. A fixation cross was displayed on the screen for 1.5 ms prior to the first 2AFC train, and then the letter "A" was displayed accompanied by the double beep audio tone before and during DCS with Train A. An inter-stimulus fixation cross was then displayed for 0.5 seconds followed by the letter "B" - again accompanied with the audio cue - displayed before and during DCS with Train B. For each trial, Train B started two seconds after the end of Train A. 300 ms after Train B was delivered, the question, "Which train felt more intense?," was visually presented, directing subjects to indicate train "A" or "B" using the left or right arrow keys, respectively. Their response was highlighted on the screen for 0.5 seconds, before triggering another trial.

Throughout each current amplitude JND experiment, one stimulation amplitude was held constant (the static amplitude) and the other amplitude was varied (the varied amplitude). The static and varied amplitudes were randomly assigned to Train A or Train B. For the two subjects who completed this task, we first tested static amplitudes (defined as, s) against varied amplitudes with deltas of $s+10$, 70, 130, 190, 250 μA or $s+10$, 80, and 150 μA for Subjects 6 and 8, respectively, with two trials per static-varied amplitude pair. Based on the results to this screening, we chose to continue the experiment with a smaller range of deltas for Subject 6 and a larger range of deltas for Subject 8 to better explore responses near their expected JNDs. For the full experiment with Subject 6, we tested two static amplitudes of $s=1250$ and $s=2000$ μA interleaved with one another with varied amplitudes of $s+10$, 45, 80, 115, and 150 μA from the two static amplitudes. For Subject 8, due to time constraints, we tested only one static

amplitude of $s=750 \mu\text{A}$ with varied amplitudes of $s+50, 100, 150, 200,$ and $250 \mu\text{A}$ from the static amplitude.

Subject 9 completed a pulse frequency JND experiment in which one stimulation PF was held constant (the static PF) and the other PF was varied (the varied PF). Because we had a range of PF deltas that we were interested in testing, we did not run a screening trial with this subject and instead ran the full experiment immediately. Using a static PF of $s=200 \text{ Hz}$ and a suprathreshold current amplitude of 3.7 mA , we tested varied PFs of $s+40, 70, 100, 130,$ and 160 Hz . All subjects completed ten trials per static-varied amplitude of PF pair for the full experiment.

Charge Discrimination

Using a 2AFC task in which subjects had to identify which of two trains felt more intense, we tested how the total charge delivered in a DCS train affected subjects' subjective experience of intensity. We varied the amplitude, PW, and PF either singly or jointly to alter the total charge delivered between the 2AFC trains. For each trial, a pair of S1 DCS trains were presented: one baseline train ($205 \mu\text{s}$ PW, 200 Hz PF, and 200 ms TD) with a suprathreshold current amplitude and one comparison train which differed from baseline in one or two parameters. For the comparison trains we changed each parameter alone and with each of the other two parameters (e.g., PW alone, PW + amplitude, or PW + PF) for a total of 9 comparison DCS trains. In three of the nine comparison DCS trains, we increased the total charge delivered from the baseline to the comparison trains by increasing only one parameter by 25% (amplitude and PF) or 20% (PW). Due to the limited clock rate of our hardware and the low number of samples in a baseline PW of $205 \mu\text{s}$, we were limited in the changes we could make to the comparison PW and could not obtain a 25% change in PW. In the other six comparison DCS trains, we varied two parameters at a time, increasing one by 20 or 25% and decreasing the other, to hold the total charge delivered constant (i.e., a 0% change in total charge delivered). Again, due to the limited clock rate of our hardware, we were unable to obtain a 0% change in total charge delivered for the PW + PF pair, and instead had to settle on a -1% change in the total charge delivered. Figure 5-2 illustrates our set of baseline-comparison DCS trains and Table 5-2 provides their parameter values with six comparison trains that conserved charge and three comparison trains that did not conserve charge. A total of ten 2AFC trials were presented for each of the nine comparisons. The presentation order of the baseline and comparison trains was randomized across the experiment and the baseline and comparison trains were each randomly presented as Train A in 50% of the 2AFC trials.

As in the JND task, a MATLAB and PsychToolbox-based graphical interface was used to direct the 2AFC experiment. Following the delivery of both DCS trains with the same timing as the JND experiment, subjects were asked the intensity question, "Which train felt more intense?," and responded using the left and right arrow keys. Subjects were then asked a second question, "Did the stimulation feel the same or different?," and indicated "Same" or "Different" using the left and right arrow keys, respectively. Both responses were highlighted on the screen for 0.5 seconds before either displaying the second question or starting a new trial beginning with the fixation cross.

Results of the charge discrimination experiment were compared to expected chance levels as estimated based on a binomial distribution with 10 trials and probability of an event (picking the comparison train as the more intense train) equal to 0.5. With a significance level of 0.5, choosing 8, 9, or 10 comparison trains out of 10 trials would not be expected by chance with $p=0.0439$, $p=0.0098$, or $p=9.77e-4$, respectively. Likewise, choosing only 2, 1, or 0 comparison trains out of 10 trials would also be unexpected, as this is equivalent to choosing 8, 9, or 10 baseline trains out of the 10 trials, and would therefore have the same p -values as listed above.

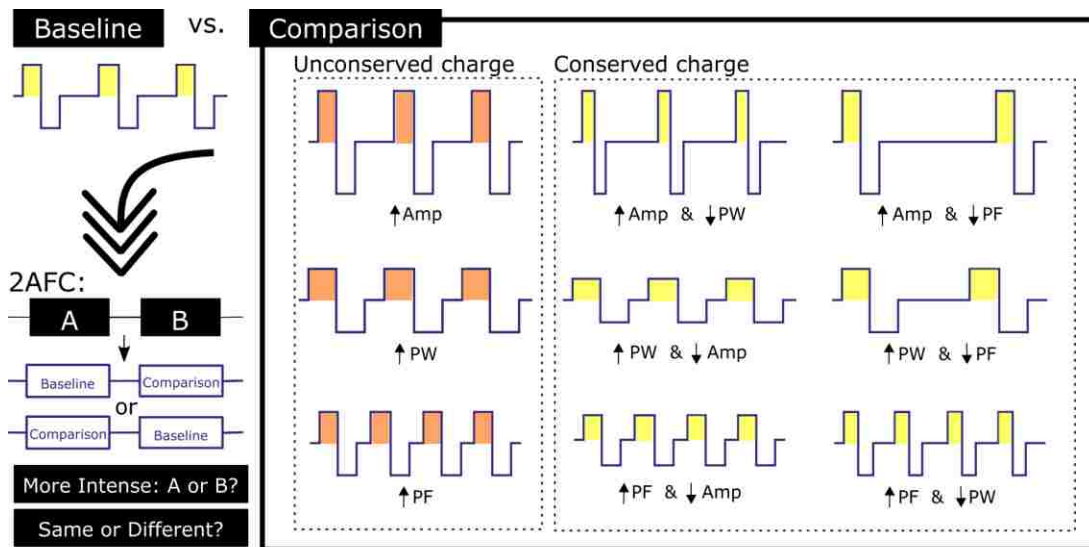


Figure 5-2. Design of the charge discrimination experiment

We tested a total of nine pairs of DCS trains (baseline + comparison), three with equal total charge in the baseline and comparison trains (indicated with yellow shading), and six with unequal total charge in the two trains (indicated with orange shading). By varying only one parameter from baseline we increased the total charge delivered in the comparison train compared to the baseline train (e.g., increasing current amplitude in the comparison train, increased the total charge delivered compared to the baseline train). When varying two parameters from baseline we held the total charge delivered in the baseline and comparison train pairs constant by increasing one parameter and decreasing the other. For example, when increasing the current amplitude we also decreased the PW or the PF (top row of the comparison trains). The baseline and comparison trains were randomly assigned to Train A or Train B for the 2AFC task. Subjects completed 10 trials for each of the nine baseline-comparison pairs, and were asked two questions at the end of each trial: 1) “Which train felt more intense?”, and 2) “Did the stimulation feel the same or different?”.

Train type	Amp	PW (μ s)	PF (Hz)	TD (ms)	TD perceived (ms)	% Change in total charge from baseline
Baseline	x	205	200	200	195	N/A
↑Amp	1.25x	205	200	200	195	25%
↑Amp + ↓PW	1.25x	164	200	200	195	0%
↑Amp + ↓PF	1.25x	205	161	199	193	0%
↑PW	x	246	200	200	195	20%
↑PW + ↓Amp	(1/1.2)x	246	200	200	195	0%
↑PW + ↓PF	x	246	166	199	193	-1%
↑PF	x	205	249	201	197	25%
↑PF + ↓Amp	(1/1.25)x	205	249	201	197	0%
↑PF + ↓PW	x	164	249	201	197	0%

Table 5-2. Set of baseline and comparison DCS train parameters for the charge discrimination task
Amplitudes depended on the subject’s perceptual threshold, but all other parameters were set ahead of time. A suprathreshold amplitude was set for the ‘x’ variable, and other amplitudes were calculated from that baseline. Subject 6 used a baseline amplitude of 1250 μ A while Subject 8 used a baseline amplitude of 750 μ A. Rows highlighted in gray did not conserve charge and correspond to the orange highlighted comparison trains in Figure 5-2. The TD was calculated as $(2 \cdot PW + \text{inter-pulse interval}) \cdot \text{number of pulses}$, and thus includes the period of time which follows the final pulse in the DCS train. In comparison, the ‘TD perceived’ column only includes the amount of time from the start of the first pulse to the end of the final pulse and therefore does not include the final inter-pulse interval. We have not tested the temporal duration of subjects’ S1 DCS percepts, but wanted to ensure that both TD measures were similar across the tested trains to avoid a potentially confounding variable for subject discrimination.

5.3 Results

DCS Percepts

As we purposefully targeted the hand primary sensory cortex, all nine subjects reported the S1 DCS sensation to their hand, although the specific area and size of the sensation varied between subjects (Figure 5-3). The size and location of the perceived artificial somatotopic sensation varied from a single fingertip (Subject 6) to large areas of the palm (Subjects 3 and 4). Generally subjects localize the S1 DCS sensation to one continuous area of their hand, but one subject (Subject 2) localized the sensation to three fingertips. Some subjects localized the sensation to a single side of their hand while others experienced the sensation on both sides of their hand. Percept locations were generally stable throughout stimulation experiments with consistent DCS parameters, but Subject 1 initially reported the location of the sensation from

the baseline DCS as changing. We therefore chose a different electrode pair for subsequent experiments including perceptual thresholding. Subject 4 reported a percept location for the baseline DCS train on the palmar side of his hand on the first day of testing (6 days post implant), but then reported a percept location on both sides of his hand on the second day (7 days post implant).

In Subjects 4-8, we investigated whether altering PW (Subjects 4, 5, and 8) or PF (Subjects 6 and 7) impacted the S1 DCS perception. Subjects 4, 5, 7, and 8 reported noticeably different locations of sensation under different parameters. Specifically, Subject 4, who had reported perceiving the baseline DCS percept on both sides of his hand with a greater sensation on the palmar side on the second day of testing, reported that with a 410 μ s PW DCS train he felt the percept more on the back of his hand than on the palm. From his hand drawing, he indicated an approximately 25% larger sensation area with the 410 μ s PW than the baseline DCS on the second day. Subject 5 reported that although all of the sensations qualitatively felt the same, the 410 and 819 μ s PW DCS percepts localized to his thumb, whereas the baseline DCS percept with 205 μ s PW localized to the proximal portions of his second and third fingers. Subject 7 reported that the 100 Hz PF DCS percept localized to a smaller area than did the baseline, 200 Hz PF DCS, and indicated an approximately 44% smaller sensation area on the hand drawing. Subject 7 also reported that she felt the 50 Hz sensation in a different location than the 100 and 200 Hz PF trains. Subject 8 reported that the 410 and 82 μ s PW DCS localized more distally on his second finger than did the baseline 205 μ s PW (Figure 5-3).

Subjects generally described abstract sensations from the S1 DCS and used terms such as, “pulsing,” “twitch,” “tingling,” and “buzz” to describe the percept (Table 5-3). Subjects 5, 6, and 8 also rated the naturalness of some of their percepts. Subjects 5 and 8 indicated that the baseline DCS train felt “moderately natural,” while Subject 6 indicated that the baseline train felt “hardly” or “partly natural”. Intriguingly, Subject 6 found S1 DCS trains more natural as the PF was decreased from 200 to 100 to 50 Hz, indicating that the 50 Hz train felt “moderately” or “quite natural” (Table 5-3). Subject 8 reported that DCS trains with 410 or 82 μ s PW were “hardly natural”.

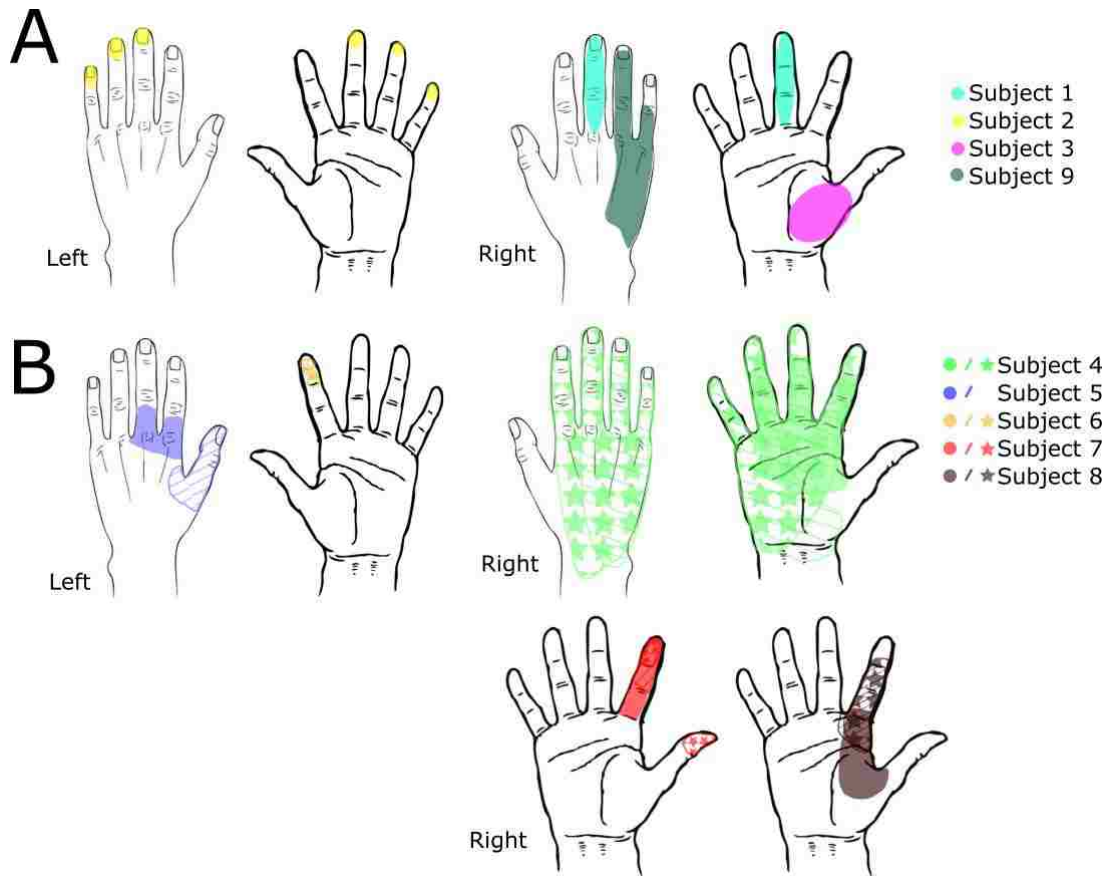


Figure 5-3. Subjects' percept localization

Subjects 1-3 verbally described where they felt the sensation as researchers took notes. Subjects 4-9 drew where they felt the stimulation on a digital hand image. All subjects described the sensation and location elicited by the baseline DCS train (205 μ s PW, 200 Hz PF, 200 ms TD), and Subjects 4-8 described additional DCS waveforms. **A)** Sensation locations for the subjects that only completed a baseline DCS train experiment. **B)** Sensation locations for Subjects 4-8, who reported a sensation location for the baseline train and one or two additional trains. Patterning in the color distinguishes the parameters tested as follows: **Subject 4:** *solid*) 1st day baseline train with 205 μ s PW; *lines*) 2nd day baseline train with 205 μ s PW; *stars*) 2nd day train with 410 μ s PW. **Subject 5:** *solid*) baseline train with 205 μ s PW; *lines*) train with 410 μ s PW (also stated that the train with 819 μ s PW felt the same as the 410 μ s PW train, but did not draw it). **Subjects 6 and 7:** *solid*) baseline train at 200 Hz; *lines*) train at 100 Hz; *C*) train at 50 Hz. **Subject 8:** *solid*) baseline train with 205 μ s PW; *lines*) train with 410 μ s PW; *stars*) train with 82 μ s PW.

Subject	Percept	Perceptual Threshold	Naturalness rating
From other stimulation experiments			
Subject A	“vibration,” and “an intention to move”	Roughly 2.25 mA	
Subject B	“felt like a soft line straight across the bottom”	Roughly 1.75 mA	
Subject C	“little pulse,” and “Noticeable... if I was at a ballgame it’d be noticeable like hair tickling your face”	Roughly 1.75 mA	
Subject D	“a teeny poke, or like pins and needles but very, very, very low”	Roughly 2.25 mA	
Perceptual threshold single staircase results			
Subject 1	1 st pair of stim electrodes: “Feels really light, but like when you hit funny bone, tingling” 2 nd pair (used in testing): “Feels like a buzz, like something brushed up against it”	0.87 mA (0.84, 0.91)*	
Subject 2	“tingling”	1.38 mA (1.36,1.39)*	
Subject 3	“like a pulse”	1.31 mA (1.22,1.55)	
Perceptual threshold double-interleaved staircase results (all 3-down, 1-up)			
Subject 4	1 st day, 205 μs PW : “Almost warm, maybe like pulsing feeling”	1.29 mA (1.27,1.32)*A	
	2 nd day, 205 μs PW : “Almost like hand twitched a little bit. A little bit warm, mainly like a jolt or a twitch”	0.88 mA (0.86 ,0.92)*B	
	2 nd day, 410 μs PW : Felt in slightly different area, but felt the same as 205 μs PW	Could not fit *C	
Subject 5	205 μs PW : “Kind of like a little jolt (but not like actually being shocked) [he's done that accidentally and says it's not the same]”; “Kind of like a vibrating feeling”	3.76 mA (3.73 ,3.80)*A	205 μs PW: 4
	410 μs PW : Same sensation, different location than 205 μs PW sensation	Could not fit *B	
	819 μs PW : Same sensation and location as 410 μs PW sensation	2.56 mA (2.52 ,2.64)	
Subject 6	1 st day, 200 Hz PF : “It felt like a pulse... like a quick little throb”	1.02 mA (0.98 ,1.07)*A	200 Hz PF: 2 or 3
	1 st day, 100 Hz PF : “Felt the same as the last one, maybe a little bit faster and therefore easier to feel, but same throb like feeling”	1.30 mA (1.28,1.33)*B	100 Hz PF: 3
	1 st day, 50 Hz PF : Similar sensation to 100 Hz	1.94 mA (1.89 ,2.08)*C	50 Hz PF: 4 or 5
	2 nd day, 200 Hz PF : “Kind of like a pulse or a throb... pretty light [comparable in strength to 1 st day]”	0.92 mA (0.89,0.97)	200 Hz PF: 3
Subject 7	200 Hz PF : “Felt almost like I put my fingers on something and it zapped them, but not like static shock... it’s weird and strange”	1.07 mA (1.02,1.15)*A	
	100 Hz PF : “It wasn’t as sharp feeling [as the 200 Hz]; a little less like that zap or jolt feeling”; she could tell that this DCS percept felt less spread out than the previous one	1.76 mA (1.59,2.52)*B	

	50 Hz PF: Similar sensation to 100 Hz, but she found it interesting that she felt it in a different spot	2.25 mA (2.06 ,3.21)*C	
Subject 8	205 μs PW: “Like something rubbed against your finger,” also thought the sensation felt like it moved from the base towards the tip of the finger	0.47 mA (0.46 ,0.49)*A	205 μ s PW: 4
	410 μs PW: “A lot softer [than 205 μ s PW]... hardly able to feel it;” he felt this sensation more distal on the finger	0.35 mA (0.33 ,0.35)*B	410 μ s PW: 2
	82 μs PW: “really, really light and slower... in the same general area... like something is under your skin pushing up, really soft”	0.89 mA (0.87 ,0.92)*C	82 μ s PW: 2
Subject 9	Baseline: “Gripping or squeezing sensation, or like you'd bumped something”	3.54 mA (3.48, 3.61)*	

Table 5-3. Qualitative descriptions of the DCS percept and their corresponding perceptual thresholds

Subjects 1-9 completed this study and correspond to those in Figure 5-3, while Subjects A-D completed prior studies from our group [109,137], and are included to illustrate the full range of reported percepts. All information is presented in the order in which we tested the stimulation parameters. Perceptual threshold current amplitudes and 68% BC_a confidence intervals, as measured by the staircase method and subsequent parametric bootstrap and permutation test, are provided (confidence intervals are in parentheses). Unless otherwise noted the descriptions are for the baseline stimulation train (205 μ s PW, 200 Hz PF, 200 ms TD). Only parameters that differed during a set of experiments for a given subject are listed in the table. For example, Subject 4 completed three staircases with varied PW; the first two staircases used the baseline PW of 205 μ s, while the third staircase used a longer PW of 410 μ s. Trials with an asterisk next to their perceptual amplitude threshold completed a hand drawing or described where they perceived the DCS location after the perceptual staircase (Figure 5-3). Subjects 4-8 have letters following the asterisks to indicate which patterned color in Figure 5-3 the trial corresponds to. Subjects 5, 6, and 8 additionally indicated a naturalness rating for some of their percepts with a range of 1 to 7 as follows: 1) Not at all natural; unnatural; 2) Hardly natural; 3) Partly natural; 4) Moderately natural; 5) Quite natural; 6) Highly natural; 7) Completely natural.

Perceptual thresholds

S1 DCS perceptual thresholds were determined using standardized adaptive staircase methodology. Subjects' 79% perceptual thresholds for the baseline DCS train (205 μ s PW, 200 Hz PF, and 200 ms TD) ranged from 0.87 to 3.76 mA for surface macro-scale ECoG electrodes (Subjects 1-7, and 9) and was 0.47 mA for the depth electrodes in Subject 8 with 68% BC_a confidence intervals approximately 0.2 mA wide on average (Table 5-3 and Figure 5-5, including 68% BC_a CIs for each parameter set). Subject 8's thresholding staircases and psychometric curves can be found in Figure 5-4 and are representative of how we completed staircases and curve fitting for all subjects. Subjects 1-3 completed 50-60 trials without any catch trials, so we estimated their false positive rate (i.e., their guess rate) to be 10% constituting the lower bound of their fitted psychometric curves (Figure 5-4). Subjects 4-9 completed 60 trials, including 10 catch trials each, from which we calculated a false positive rate of 20% for Subjects 4 and 9 and 0% for Subjects 5-8 (Figure 5-4). With Subjects 4 and 6 we were able to run stimulation experiments over two consecutive days with the baseline DCS train. For both subjects we found a significantly decreased 79% perceptual threshold from the first day to the second day. Subject 4's perceptual threshold decreased from 1.29 to 0.88 mA from the first to the second day for the baseline DCS train ($p=9.999e-5$, permutation test, Table 5-3). Subject 6's perceptual threshold decreased from 1.02 to 0.92 mA from the first to the second day for the baseline DCS train ($p=9.999e-5$, permutation test, Table 5-3).

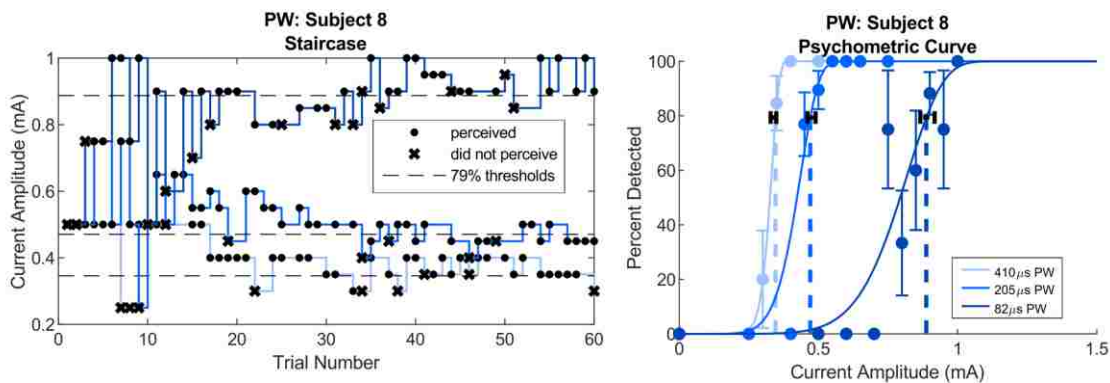


Figure 5-4. Sample perceptual thresholding staircases and psychometric curves

Left: Subject 8 completed three perceptual thresholding staircases with PWs of 82 μ s, 205 μ s, and 410 μ s, and other baseline parameters of 200 Hz PF and 200 ms TD. Significantly lower perceptual thresholds were achieved with longer PWs ($p=9.999e-5$). Subject 8's thresholding tests used a double-interleaved 3-down 1-up staircase as in Figure 5-1, but the staircases are merged together for each of the tested parameter sets for visualization. **Right:** Subjects' staircase results were fit with a Weibull function parameterized with a slope and threshold using a maximum likelihood approach to estimate their psychometric curves. We used Subject 8's catch trial results to set the lower bound of the psychometric functions to his false positive rate. Vertical error bars represent the standard deviation of the sample of yes/no responses. Black horizontal error bars represent the 68% BC_a confidence intervals around the estimated amplitude threshold (these are also provided in Table 5-3).

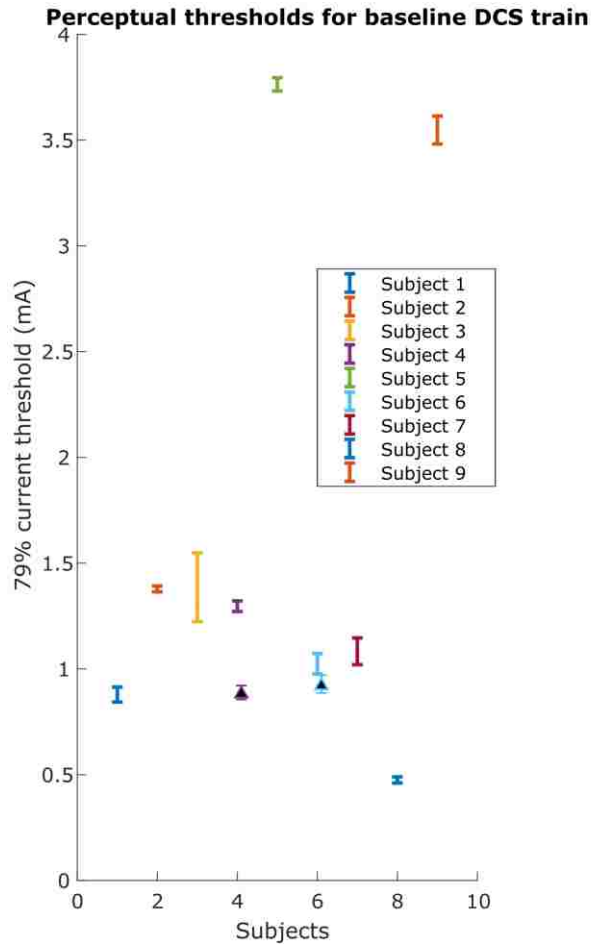


Figure 5-5. All subjects' 79% perceptual thresholds for the baseline DCS train

All nine subjects thresholding staircases were fit as described in Figure 5-4 and the Methods to estimate the subjects' 79% perceptual thresholds. Horizontal error bars represent the 68% BC_a confidence intervals around the estimated amplitude threshold (also provided in Table 5-3). Subject 8, who had depth electrodes implanted, had the lowest perceptual threshold of 0.47 mA. Outlined black triangles represent the second day of testing for Subjects 4 and 6. Subjects' psychometric curves, based on a best-fit Weibull function are provided in Appendix 1, Figure 10-2.

Subjects 5 and 8 completed multiple perceptual thresholding trials in which the PW was varied. Both subjects required a significantly lower current amplitude to perceive S1 DCS trains with longer PWs (Table 5-3, Figure 5-6A, $p=9.999e-5$, permutation test, for both subjects) but a significantly higher threshold charge for longer PWs (Figure 5-6B, $p=9.999e-5$ for both subjects). Subject 5 had a 79% perceptual threshold of 3.76 mA with a 205 μ s PW as compared to 2.56 mA with a 819 μ s PW. Similarly, Subject 8 had a 79% perceptual threshold of 0.89 mA with 82 μ s PWs, 0.47 mA with 205 μ s PWs, and 0.35 mA with 410 μ s PWs ($p=9.999e-5$ for permutation tests of 82 vs. 205 μ s PW and 205 vs. 410 μ s PW). Like Subject 8, Subject 5 also completed thresholding tests with 82 μ s PWs and 410 μ s PWs, but was not able to feel the 82 μ s PW DCS with up to 6 mA of current, and we were unable to fit the resultant data from the 410 μ s PW

test with a Weibull function as described in the Methods likely due to insufficient sampling at suprathreshold amplitudes. Subject 4 also completed an additional PW perceptual thresholding test with 410 μs PW, but his false positive rate was 0.8, so we were unable to ascertain his perceptual threshold.

Subjects 6 and 7 completed multiple perceptual thresholding trials with three different PFs: 200, 100, and 50 Hz. Both subjects' perceptual thresholds increased significantly as the PF decreased (Table 5-3, Figure 5-6A, $p=9.999e-5$, for 200 vs. 100 Hz, and 100 vs. 50 Hz). A significantly decreased charge was also required to reach threshold with increasing frequency (Figure 5-6B, $p=9.999e-5$, permutation test). Subject 6's 79% perceptual thresholds were estimated as 1.02 mA at 200 Hz, 1.3 mA at 100 Hz, and 1.94 mA at 50 Hz (Figure 5-6A). Similarly, Subject 7's 79% perceptual thresholds were estimated as 1.07 mA at 200 Hz, 1.76 mA at 100 Hz, and 2.25 mA at 50 Hz (Figure 5-6A).

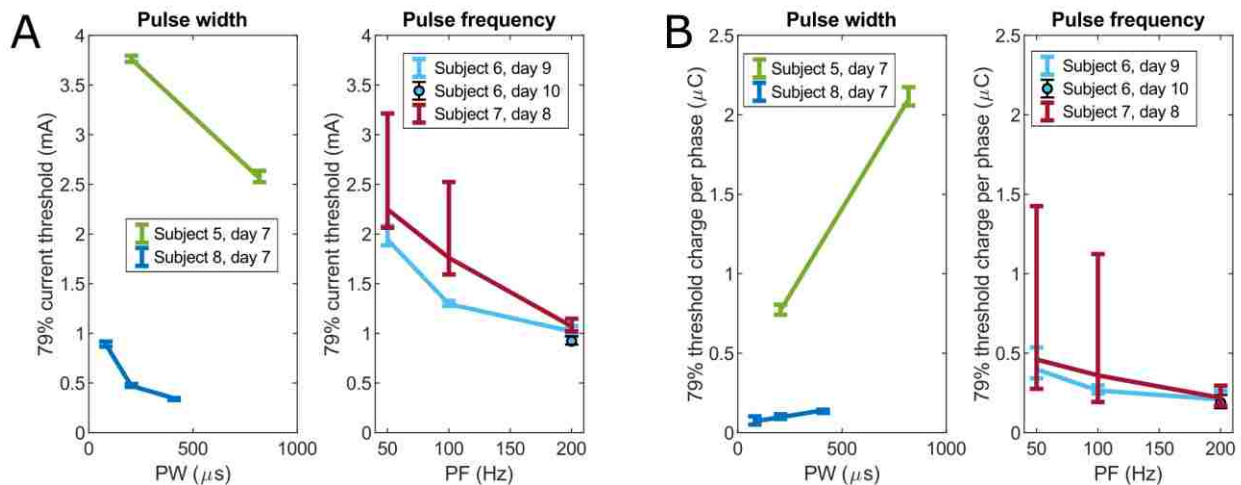


Figure 5-6. Current amplitude and charge per phase 79% perceptual thresholds

A. Current amplitude thresholds for subjects that completed tests with varied PWs or PFs. Subjects 5 and 8 completed tests with varied PWs (left subplot). Subject 5 completed tests with PWs of 205 μs and 819 μs , while Subject 8 completed tests with PWs of 82 μs , 205 μs , and 410 μs . The varied PW tests used a baseline PF of 200 Hz. Subjects 6 and 7 completed tests with varied PFs of 50, 100, and 200 Hz (right subplot). The varied PF tests used a baseline PW of 205 μs . All tests used a baseline train duration of 200 ms. Error bars for the 68% BC_a confidence intervals around the estimated amplitude threshold are provided. Perceptual amplitude thresholds decreased significantly ($p=9.999e-5$) as both PW and PF increased. **B.** The threshold charge per phase in μC , defined as the 79% perceptual amplitude \times PW ($\text{mA} \times \mu\text{s} / 1000$), was calculated for the subjects that completed perceptual threshold tests under various PWs or PFs. Subjects 5 and 8 required significantly increased charge to reach their perceptual threshold with increased PW ($p=9.999e-5$, left subplot). Subjects 6 and 7 required significantly less charge to reach their perceptual threshold with increased PF ($p=9.999e-5$, right subplot). Error bars for the 68% BC_a CIs around the estimated amplitude threshold are provided. As the charge per phase is calculated as the perceptual amplitude \times PW, and the PW is a known value, the amplitude threshold CIs can be applied to the estimate of the threshold charge per phase.

In Figure 5-7 we show the charges used in all S1 DCS sensory stimulation experiments and whether or not they perceived or responded to the stimuli. Specifically, we plot the charge per phase of the first pulse used in the train against the total charge delivered in the DCS train. Charge per phase was defined as the current amplitude x the PW for the first pulse, while the total charge (or the charge exchange per train) was defined as the amplitude x PW x the number of pulses (where the number of pulses = PF x TD).

Additional figures of subjects' psychometric functions are included in Chapter 10, Appendix 1 to provide a complete picture of our results.

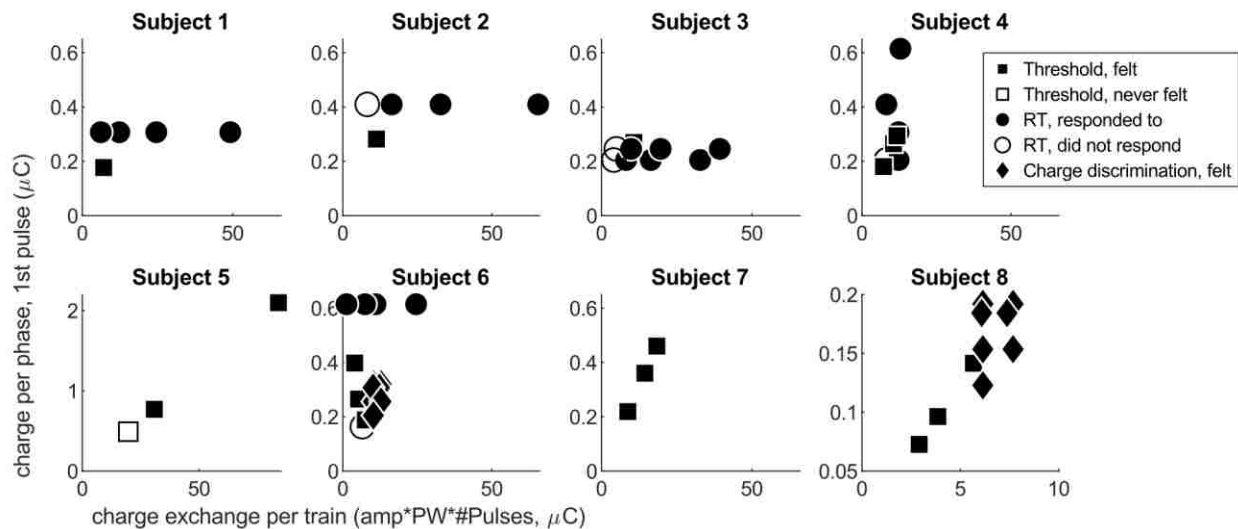


Figure 5-7. Charge thresholds for Subjects 1-8 for all experiments

Here we show the charge per phase of the first DCS pulse plotted against the charge exchange per train (total charge delivered) for Subjects 1-8 for all of the sensory stimulation experiments they completed. Subject 9 is not included as he only completed one threshold experiment followed by JND experiments with the same baseline waveform. Stimulation parameters that were not perceived or responded to are shown in white, while those that were responded to are shaded in black. Symbols correspond to the experiment type (squares: threshold experiments; circles: response timing experiments (Chapter 6); and, diamonds, charge discrimination experiments). Note that all subplots have the same axes limits, except for Subjects 5 and 8 who had much higher and lower perceptual thresholds, respectively, than the other six subjects.

Just-Noticeable Differences

In addition to the perceptual threshold experiments, Subjects 6, 8, and 9 also had time to complete a JND experiment. Using a 2AFC task in which subjects had to identify which of two DCS trains felt more intense we estimated the JND for two static amplitudes for Subject 6 and one static amplitude for Subject 8. Subject 6 had 79% JND thresholds of 125 μ A with a static amplitude of 1.25 mA and 149 μ A with a static amplitude of 2.0 mA. Subject 8 had a 79% JND threshold of 120 μ A with a static amplitude of 0.75 mA (Figure 5-8). Subject 9 completed a PF JND and had a 79% JND threshold of 161 Hz with a static PF of 200 Hz and a suprathreshold current amplitude of 3.7 mA (Figure 5-8).

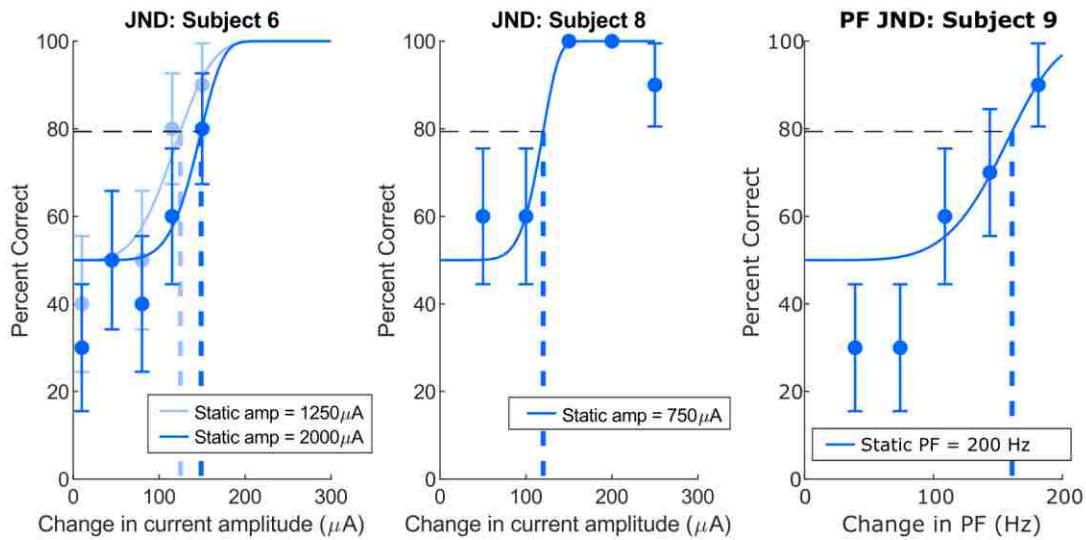


Figure 5-8. Just-noticeable differences for Subjects 6, 8, and 9

Left: At a static amplitude of 1.25 mA, Subject 6's 79% current amplitude JND threshold was 125 μA, while at a higher static amplitude of 2.0 mA, Subject 6's 79% current amplitude JND threshold was also greater, at 149 μA. **Middle:** At a static amplitude of 0.75 mA, Subject 8's 79% current amplitude JND threshold was 120 μA. **Right:** At a static PF of 200 Hz with a suprathreshold current amplitude of 3.7 mA, Subject 9's 79% PF JND threshold was 161 Hz. For all subplots: Vertical error bars represent the standard deviation of the sample of correct and incorrect responses on the 2AFC trials.

Charge Discrimination

Following the JND task, Subjects 6 and 8 were willing to continue research and completed a charge discrimination task, again using a 2AFC experimental design. For three of the nine tested DCS train pairs, we varied the total charge delivered with a higher total charge in the comparison train than the baseline train (Figure 5-2 for methods). For the other six pairs, the baseline and comparison DCS trains had an equal or nearly equal total charge delivered.

During 2AFC trials comparing the intensity of the baseline and comparison trains, Subject 6 consistently identified the DCS train with a greater amplitude as more intense whether or not the charge between the baseline and comparison trains was consistent (Figure 5-9). Specifically, Subject 6 identified the higher amplitude DCS train as more intense in: 10/10 trials for amplitude alone, 18/20 trials for amplitude and PW, and 18/20 trials for amplitude and PF, with the latter two groups having equal total charge in the two DCS trains. Whenever amplitude was varied as the primary parameter, with or without another parameter, Subject 6 selected the higher amplitude comparison train as more intense more often than would be expected by chance (binomial distribution with 10 trials and $P(\text{event})=0.5$, $p<0.05$). When amplitude was varied as the secondary parameter (i.e., PW or PF increased and amplitude decreased), Subject 6 still tended to identify the baseline train with the higher amplitude as more intense. Subject 6 also identified comparison trains with an increase in PW alone as having greater intensity more often than would be expected by chance, but when PW was varied with another parameter, Subject 6's performance was no longer different than chance.

During this experiment with Subject 8, he frequently mentioned that a difference between the DCS trains was minimally discernible; however, we did not adjust the parameters. We chose to keep the PW and PF parameters consistent with those tested in Subject 6, and did not want to increase the current amplitude above the 750 and 937.5 μA in the baseline and comparison trains, respectively, as amplitudes above 1 mA seemed to elicit a motor response in this subject. When increasing parameters on their own, and thereby increasing the total charge delivered in the comparison train, Subject 8 did not indicate that any train was more intense (first question) or different (second question) than the other train more often than would be expected by chance (see Appendix 1, Figure 10-6). This indicates that as Subject 8 expressed, he was unable to perceive a substantial difference in the intensity of the baseline and comparison trains.

After comparing the DCS trains' intensities, subjects were asked to indicate whether the two trains felt the same or different. Subject 6 responded that DCS trains felt different from one another more often than would be expected by chance in only two of the 2AFC sets in which amplitude was increased alone or along with a decreased PF (Figure 5-9). Subject 8, as in his intensity responses, did not indicate that any trains felt different more often than would be expected by chance.

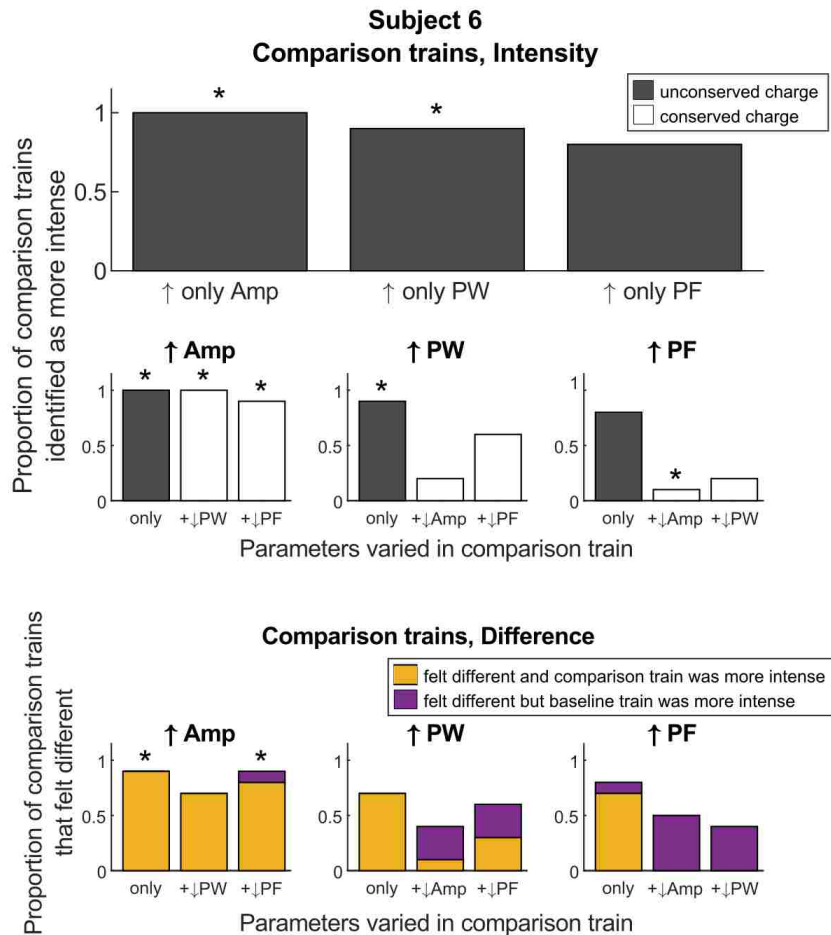


Figure 5-9. Charge discrimination results for Subject 6

The top two rows illustrate the subject's responses to the question of intensity (i.e., "Which train felt more intense?"). A higher proportion indicates that the subject frequently responded that the comparison train was more intense than the baseline train. The top row illustrates just the three baseline-comparison DCS train pairs in which only one parameter was altered and the charge was not conserved. The second row illustrates all nine of the baseline-comparison DCS sets in which two parameters were altered and the charge was conserved. Subplots are separated based on the parameter which was increased, with each bar representing either that parameter increased alone, or along with a decrease in one of the other two parameters. Asterisks highlight the sets with results that are unexpected due to chance based on a binomial distribution expected for 2AFC tasks (10 trials per set with $P(\text{event}) = 0.5$, $p < 0.05$). The bottom row illustrates the subject's responses to the question of difference (i.e., "Did the stimulation feel the same or different?"). Again subplots are separated based on the parameter which was increased. Yellow bars indicate the proportion of baseline-comparison train pairs which felt different from one another and the comparison train was identified as more intense, whereas purple bars indicate the proportion of trains that felt different but in which the baseline train was more intense. We would expect sets with significant results in the intensity question to also have significant results in the difference question, as we expected subjects to notice a difference between any trains they could identify as being more or less intense.

5.4 Discussion

It is necessary to describe the S1 DCS parameter space that can elicit discernable percepts and the interplay of stimulation amplitude, pulse width, pulse frequency, charge, and DCS perception to fully consider the feasibility of S1 DCS as a sensory feedback approach for closed loop neuromodulation. In this study we employ traditional psychophysics methods to investigate how nine subjects with acutely implanted standard clinical ECoG grids perceive DCS with varied current amplitude, PW, and PF. We observed that neither amplitude, PW, PF, nor charge delivered can predict near-threshold perception alone, but that there is a clear interaction between current and charge thresholds and the PW and PF. Consequently consideration of these parameters collectively will better render efficient and clinically efficacious stimulation waveforms. Further, a complete characterization of the interactions across DCS parameters may elucidate consistencies in subject perception. This hypothesis is in line with our current results revealing that: (i) although charge affects subject perception of DCS, DCS percepts are not solely dependent on charge delivered; and, (ii) amplitude may be the predominant parameter in the subjective experience of intensity. These results support previous findings of the dependence between current and charge perceptual thresholds and the PW and PF, and the psychophysical law that JNDs are dependent on the initial stimuli [188].

All nine subjects completed a perceptual threshold test for our baseline DCS train of 205 μ s PW, 200 Hz PF, and 200 ms TD, with 79% thresholds of 0.47 to 3.76 mA which may differ from day to day. The differences in perceptual threshold are likely due to variability of the ECoG grid position over post-central gyrus, S1 morphological differences between subjects, and the degree of intervening cerebrospinal fluid between the electrodes and the cortex or the use of depth electrodes in Subject 8 [171,172,174,189]. Differences may also result from potential baseline cognitive differences, the subjects' levels of attentiveness [190], and their subjective experience of the stimuli. Subjects 6 and 8 also completed a JND test of their current amplitudes with estimated JNDs ranging from 120-149 μ A. We tested two static amplitudes for Subject 6 and found that the JNDs increased when the static amplitude increased, following expectations from Weber's law which describes how JNDs are proportional to the intensity of the stimulus [188]. However, the proportionality constant was not consistent, as it was 0.1 for the lower static amplitude (125 μ A/1250 μ A) and 0.07 for the higher static amplitude (149 μ A/2000 μ A). This could be due to errors in the estimate of the true JND given just 50 trials per psychometric curve.

Five subjects completed additional perceptual threshold tests with varied PW or PF. As has been reported previously, we found that the current required to elicit a sensation decreases with increasing PF or PW [138,181]. We also found that the charge required to reach threshold, as measured by charge per pulse (Figure 5-6), increased for increasing PW, but decreased with increasing PF. This relationship between threshold charge and PW or PF is consistent with psychophysical studies using ICMS of S1 in non-human primates [181], ICMS of barrel cortex in rats [191] and retinal microstimulation in humans [192]. The increase in required charge for longer PWs is thought to be due to an increase in sodium channel inactivation with increasing PWs resulting in an increasing charge to reach threshold [164]. Alternatively with increased PFs, successive pulses of higher PFs may produce augmented inhibitory currents thereby improving

signal-to-noise ratios of elicited neural activity and requiring less charge to reach threshold [191]. Verifying that this relationship between PW or PF and the threshold charge holds in S1 DCS is an important finding as it suggests that we can use this relationship to develop efficient stimulation waveforms which will elicit a conscious percept with as minimal charge delivery as possible.

Although greater current amplitudes were associated with higher rates of perception, subjects' perception was not dependent on S1 DCS amplitude alone. Previous studies of DCS with high-density ECoG grids have similarly found that perception is not simply based on exceeding a necessary current amplitude or charge threshold [138,139]. Subject 5's inability to perceive DCS trains with 82 μ s PW despite increasing the amplitude to 6 mA is in line with results from Lee et al. in which most subjects required at least 200 μ s PWs to perceive the stimulus [139]. However, Subject 6 could feel DCS trains with PWs of 164 μ s during the charge discrimination experiment. Subject 8 reported perceiving PWs of 82 μ s, though for this subject DCS was delivered via depth electrodes rather than subdural ECoG electrodes, and the current spread and resultant perception of charge delivered subcortically is expected to behave differently than in the other seven subjects with subdural electrodes. Like amplitude, increasing PW to an extent may increase the likelihood of perceiving the DCS, but absolute values remain subject-dependent. Similarly, Subjects 2 and 3 were unable to consistently respond to DCS trains of 100 ms in duration during a response timing task (Chapter 6), in line with previous results demonstrating that increasing the TD decreases the amplitude threshold, but only through approximately 250 ms [113].

We also considered several measures of charge and how they may correspond to subject perception of S1 DCS. Previous ICMS work in non-human primates revealed that threshold charge per phase depends on the PW and PF and therefore cannot predict subject perception alone [181]. Similarly, a high-density ECoG study by Muller et al. found that charge per time (defined as PF x current amplitude) could not predict perception and that in some cases trains with equal charge per time had different perceptual outcomes [138]. We found that like charge per phase, charge exchange per train, in isolation, could not predict subject perception. In some cases subjects responded to DCS trains with low charge exchange per train and high charge per phase, but did not respond to trains with a higher charge exchange per train and lower charge per phase. Figure 5-7 illustrates how the charge per phase of the first pulse and charge exchange per train both affect subject perception and neither can explain perception alone. Taken together, charge per phase and charge exchange per train encompass four DCS variables: amplitude, PW, PF, and TD. Charge per phase accounts for the amplitude and PW of the first pulse directly, while charge exchange per train (i.e., total charge) includes amplitude, PW, PF, and the TD (as $PF \cdot TD =$ the number of pulses). Given the mutual dependence of these charge measures on the amplitude and PW, there will always be a correlation between the two charge measures. Rather than implying a relationship between charge per phase and charge exchange per train, we reveal in Figure 5-7 that there is sometimes a separation between the perceived and not perceived S1 DCS trains when visualized this way, whereas this separation is not always apparent when considering other measures of charge.

While measures of charge may help elucidate whether or not subjects will perceive a S1 DCS train, S1 DCS percepts are not solely dependent on the charge delivered. In the charge discrimination study, Subject 6 could perceive a difference in intensity between three of the six sets of conserved-charge trains at rates above those expected by chance: \uparrow Amp + \downarrow PW, \uparrow Amp + \downarrow PF, and \uparrow PF + \downarrow Amp (Figure 5-9). Interestingly, when asked which train was more intense, this subject identified the trains with a higher amplitude over those with a greater PW or PF even when both trains had an equal total charge delivered. This result suggests that current amplitude may be the predominant parameter in the subjective experience of the perception of intensity evoked by S1 DCS. However, we did not control for JNDs in this experiment, nor did we measure the PW or PF JNDs for Subject 6. It is possible that rather than being indicative of a predominance of amplitude in the perception of intensity, this observation is due to a more noticeable change in the amplitude parameter over the changes in the PW and PF parameters based on their relative JNDs. That is, with a JND of between 125 and 149 μ A for an initial intensity of 1.25 mA, the change in amplitude used in the discrimination task from 1.25 to 1.5625 mA spanned approximately 2 to 2.5 discriminable steps based on the amplitude JND. If, for example, the PW JND was 35 μ s, then the change from 205 to 246 μ s for the discrimination task would only span approximately 1.2 steps in the PW JND. Thus, even though both the amplitude and the PW were increased by 20-25% and those increases alone were discriminable above chance, the change in amplitude could be more noticeable due to a relatively smaller JND and more discriminable steps between the tested amplitudes, than the steps between the tested PWs.

During the charge discrimination task, Subject 6 could identify a more intense train at rates higher than those expected by chance when the current amplitude or PW were increased alone. However, when the PF was increased alone, Subject 6 only identified the comparison train as more intense in 8 out of 10 trials, which is not significant given a binomial distribution ($p=0.11$). Prior work from our group found that using S1 DCS via macro-scale ECoG subjects could generally discriminate between frequencies of 75 and 100 Hz or 50 and 75 Hz [110]. However, according to Weber's law the approximate PF JND is likely larger for the higher baseline PF of 200 Hz. Indeed, in Subject 9 we found a 79% PF JND threshold of 161 Hz with a static PF of 200 Hz (Figure 5-8). Additionally, prior work from Hiremath et al. in one subject with a high-density ECoG grid found that although there was a linear relationship between PF and intensity, the perceived intensity began to plateau after approximately 200 Hz [111]. This supports the idea that the change from 200 to 249 Hz for Subject 6 was not large enough or alternatively it used a baseline PF that was too high to elicit a substantial change in perceived intensity. Nonetheless, the observation that Subject 6 can discriminate between DCS trains of equal charge in three out of six sets holds.

Interestingly, there seems to be a lack of agreement between Subject 6's responses to the intensity question and the same-different question in that at times the subject does not report a noticeable difference in the trains that were perceived as more intense (Figure 5-9). From our data we cannot determine the reason for this discrepancy, but there are a number of possibilities. For instance, the same-different question followed the intensity question so the subject could have forgotten the perceptual experience of the DCS stimuli by that point. It is

conceivable that she could have decided to only respond that the trains were ‘different’ if there was a difference besides intensity or she may have been able to perceive and identify changes in intensity even when she was not aware of a difference in the percept [193].

For all of the S1 DCS trains tested, subjects’ percept descriptions were similar to those reported in earlier studies with DCS, such as “pulsing” and “buzzing” [109–111,139], and generally described abstract, artificial sensations. However, Subject 6 surprisingly reported that DCS with a 50 Hz frequency felt “moderately” or “quite natural” (scores of 4 and 5 out of 7 on our naturalness scale), descriptors that have been thought to only be accessible to electrical stimulation via the more spatially-focused ICMS (e.g., [130,131]) or the earlier-stage peripheral nerve stimulation (e.g., [69,103]). The same subject rated the baseline DCS with a 200 Hz pulse frequency as a 2 or 3 (“hardly” or “partly” natural). Thus, she ascribed the full range of naturalness ratings to the percepts she experienced suggesting that low-frequency S1 DCS is perceived as a more natural stimulation. Clearly, more subjects and a natural haptic percept control (such as that used in Flesher et al. [130]), are necessary to support this hypothesis. Future work should explore the possibility that certain DCS stimulation parameters may yield more natural sensations than others.

Further, two recent studies with high-density ECoG grids reported the qualitative results of changing the PW. Hiremath et al. reported that their high-density ECoG subject perceived DCS trains with 200 μ s PWs as an “electrical buzz”, whereas he perceived DCS with 400 μ s PWs as “tingling” [111]. In contrast, Lee et al. reported that in nine high-density ECoG subjects an increase in PW produced an increase in the perceived strength of the sensation more often than a different percept quality [139]. In just 15% of their responses, an increase in PW changed the receptive field of sensation. In this current macro-ECoG study, we find that a change in PW most often changed the receptive field. In two of our subjects (Subjects 5 and 8), changes in the PW produced a change in the location of the perceived sensation (Figure 5-3). In one subject (Subject 4), an increased PW increased the size of the receptive field. Subject 8 also described a decreasing strength of sensation as the PW changed, but in an inconsistent manner (Table 5-3, decreased strength for 410 and 82 μ s relative to 205 μ s).

Overall, our subjects reported localized percept areas ranging from single fingertips to large areas of the palm, similar to the sensation fields reported by Lee et al. [139], and sometimes smaller than those reported by Hiremath et al. [111] (smallest area reported was the entirety of the fifth digit). Although both studies used high-density ECoG arrays (3 mm and 4.5 mm center-to-center spacing for Lee et al. [139] and Hiremath et al. [111], respectively), Hiremath et al. used monopolar stimulation as compared to our and Lee et al.’s use of bipolar stimulation. The expected additional current spread from monopolar stimulation versus bipolar stimulation could explain the trend towards larger sensory receptive fields [172,194]. Lee et al., also reported that in one subject as the amplitude increased the subject’s receptive field moved from the palm and fifth finger to several fingertips [139]. Similarly, we found that changes in DCS parameters could cause the location of the perceived sensation to expand or move (Subjects 4, 5, 7, and 8) when the PW or PF changed. Future studies could consider whether we can use electrode choice and DCS parameters to localize percepts to different areas.

Compared to macro-ECoG stimulation, ICMS and high-density ECoG stimulation offer a higher spatial resolution due to their smaller electrode surface areas. Additionally, recent research using ICMS of somatosensory cortex suggests that ICMS may more frequently elicit more natural sensations than subdural ECoG grids [130,131]. However, we have demonstrated that the psychophysics of macro-scale ECoG stimulation has similarities to both high-density DCS and ICMS. Therefore, the principles underlying all cortical stimulation methods may be applied across modalities as we expand our understanding of the psychophysics of cortical stimulation for sensory feedback. Of particular interest, is our finding that the relationship between the charge required to elicit a conscious percept and the PW and PF which has been found previously in other studies of microstimulation [181,191,192] holds with macro-scale S1 DCS in humans. This suggests that we can design efficient S1 DCS stimulation waveforms with low PWs and higher PFs to elicit a perception with as little charge as possible. In the future, we can consider modeling this relationship to select the most effective combinations of DCS parameters as has been done for human retinal stimulation [192].

6 Response Timing

As we have argued, DCS of S1 could help restore sensation and provide task-relevant feedback in a neuroprosthesis, but to do so we must understand the timing of DCS perception. However, the response time to S1 DCS in humans has not been studied or compared to the response time to cutaneous haptic stimulation. Here we compared the response times to DCS of hand S1 to haptic stimuli delivered to the hand in four subjects. We found that subjects responded significantly slower to S1 DCS than to natural, haptic stimuli for a range of DCS train durations. Median response times for haptic stimulation varied from 198 ms to 313 ms, while median responses to reliably perceived DCS ranged from 254 ms for one subject, all the way to 528 ms for another. We discerned no significant impact of learning or habituation through the analysis of blocked trials, and found no significant impact of cortical stimulation train duration on response times. Our results provide a realistic set of expectations for latencies with somatosensory DCS feedback for future neuroprosthetic applications and motivate the study of neural mechanisms underlying human perception of somatosensation via DCS.

The work presented in this chapter was completed jointly by another graduate student, David Caldwell, and myself. We both established and programmed the experimental protocol, collected the data, and interpreted the results. The statistical analyses were conducted by David Caldwell who also created the figures in this chapter. David wrote the first draft of the manuscript and we edited it together as is presented below.

The following chapter has been submitted for publication as:

Caldwell, D. J.* , J.A. Cronin*, J. Wu, K.E. Weaver, A.L. Ko, R.P.N. Rao, and J.G. Ojemann. Direct stimulation of somatosensory cortex results in slower reaction times compared to peripheral touch in humans. *Scientific Reports*.

* These authors contributed equally

I have made slight modifications to the manuscript to fit in the framework of this document.

6.1 Introduction

Integration of somatosensory feedback into brain-computer interfaces (BCIs) has been shown to improve BCI task performance [64–66,68,122], and is also a consumer design priority for prosthetics users [8] and potential BCI end users such as individuals with paralysis [9,10]. The study of cortical stimulation for providing somatosensory task feedback has garnered increasing attention because of the realization that the absence of sensory feedback in many current BCIs may limit performance and extensibility [60]. Prior work has shown that humans can respond to direct cortical stimulation (DCS) of the surface of the primary somatosensory (S1) cortex [110–113], which engenders an artificial sensory percept organized according to standard somatotopy. Recent work has revealed that S1 DCS can be used for somatosensory feedback for closed-loop control in a motor task [109]. Furthermore, DCS has also been shown to induce prosthetic hand ownership [137] (more on this research in Chapter 7). Thus, DCS offers the potential to close the loop in human BCIs by providing a mechanism to encode sensory feedback from an end effector to a user.

While prior work suggests that the integration of somatosensory feedback into a BCI is possible and enhances performance relative to a task without somatosensory feedback, the comparison of human S1 DCS to haptic stimulation has not been well explored. Specifically, given that S1 DCS completely circumvents ascending dorsal column pathways, how human subjects' response times to DCS differ from response times to natural haptic stimulation has not been examined. This is an important consideration for effective BCI development aiming to integrate cortical stimulation as a method of sensory feedback as response latency invariably constrains feedback loop architecture.

We asked four subjects to press a button as soon as they perceived either a cutaneous haptic touch to the hand or a percept from S1 DCS via electrocorticography (ECoG) grids covering the surface of the hand somatosensory cortex (see Figure 6-1 for general overview, Figure 6-2 for subject specific experimental procedures). We initially hypothesized that direct cortical stimulation, by bypassing the ascending peripheral circuitry, would result in faster reaction times than peripheral haptic stimulation. We additionally hypothesized that subjects would become faster over multiple blocks of DCS as they learned to interpret the signal, and that subjects' response times to DCS would decrease with longer, sustained train durations relative to shorter trains with a constant stimulation current amplitude.

Remarkably, all four subjects were significantly slower to respond to the S1 DCS than to haptic touch. Additionally, with our two blocks of testing we saw no significant differences between trial types and blocks, suggesting that on a short time scale, appreciable learning was not occurring. In three subjects we tested the train duration hypothesis and found that train lengths as short as 100 ms and up to 800 ms did not significantly affect the response times to the cortical stimulation. We performed off-target testing to serve as a control for the possibility that subjects were responding to stimulation that was applied anywhere in the cortex, rather than directly in somatosensory cortex. This reinforces our testing of electrical stimulation and subsequent activation of primary somatosensory cortex compared to natural ascending peripheral pathways activated through touch, converging on S1. We also included null trials without any stimuli to control for subject suggestibility and response anticipation. Our results shed new light on human perceptual processing of S1 DCS and may direct future studies regarding the application and mechanisms of DCS for both basic neuroscience research and neural engineering applications.

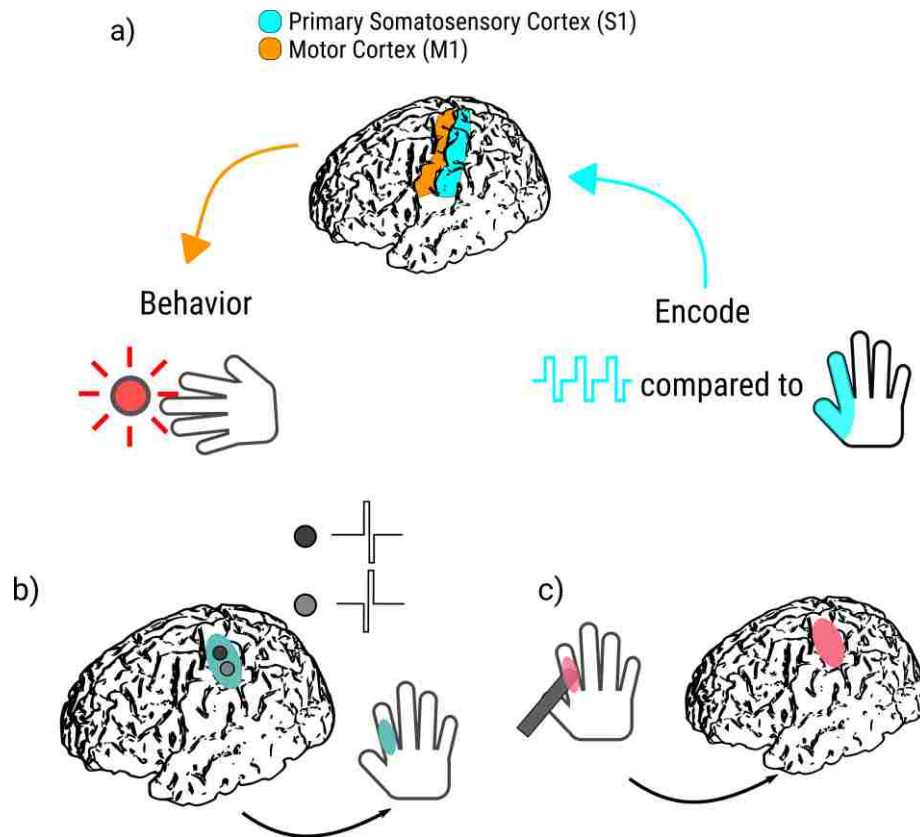


Figure 6-1. Response timing experimental protocol

a) Here, we test the impact on behavioral performance for native cortical input (haptic touch) compared to artificial feedback (bipolar direct cortical stimulation of primary somatosensory cortex via ECoG electrodes). (b-c) Schematic overview of experimental paradigm. **b)** DCS to S1 hand cortex results in a sensory percept over a specific, consistent location on the hand. **c)** An experimenter uses a digital touch probe to provide haptic feedback to the same hand location. The subject then responds in both cases as soon as he or she feels sensation in the hand region, using a button held in the opposite hand to perceived sensation.

6.2 Methods

Subjects

Human subjects (n=4) were implanted at Harborview Medical Center (Seattle, WA) with ECoG grids, following the general methods outlined in Chapter 4. Individual patient demographics can be found in Table 6-1, with their corresponding cortical reconstructions and DCS electrode positions shown in Figure 6-3. Epileptic foci are also identified in Table 6-1, to illustrate that we expected neurotypical somatosensory cortical processing for our reaction time task.

Subject	Gender	Age	Experiments	Stimulation Current	Coverage and DCS percept localization	Seizure etiology
1	Female	21	Cortical Stimulation Digital touch probe Off Target	2500 μ A	Right-sided grid; Distal phalange of digit 2	Complex partial epilepsy with multifocal ictal onset and at least 2 distinct epileptogenic areas with seizures arising from right frontal and right temporal regions. No resection / no pathology, VNS implant.
2	Male	37	Block 1: Cortical/Off Target interleaved; Digital touch probe Block 2: Cortical/Off Target interleaved; Digital touch probe	1500 μ A	Left-sided grid; All of digit 3	Focal epilepsy isolated to a left parietal calcified lesion (widespread calcifications eliciting diffuse and severe reactive changes including astrogliosis and microgliosis with unknown origin). Seizures originating from left lateral parietal cortical lesion.
3	Male	26	Block 1: Cortical/Off Target interleaved; Digital touch probe Block 2: Cortical/Off Target interleaved; Digital touch probe	2000 μ A	Right-sided grid; Distal phalanges of digits 3-5	Simple partial seizures from focal cortical dysplasia originating over the right frontoparietal region. No resection – neuropace implant.
4	Male	34	Block 1: Cortical/Off Target interleaved; Digital touch probe Block 1 again: Cortical/Off Target interleaved; Digital touch probe	1000 μ A 1200 μ A	Left lateral grid; Palmar area near base of digit 1	MRI negative, partial seizures originating from the left mesial temporal area including the anterior temporal pole and hippocampus. Pathology included mild gliosis with leptomeningeal and subpial reactive changes.

Table 6-1. Subject Demographics

This table shows the demographics for all the patients in this study, including experiments completed, stimulation currents used, and the localization of subjects' percepts, electrode locations, and seizure etiology.

Cortical Reconstructions

Cortical reconstructions and electrode localization were performed as outlined in Chapter 4.

Stimulation Waveform and Hardware

We used the stimulation hardware described in Chapter 4. DCS trains consisted of 200 Hz biphasic pulses with 200 μ s per phase, as such DCS trains were previously found to elicit percepts during S1 stimulation [109].

Cortical Stimulation

Subjects' perceptual thresholds for DCS were determined by incrementally increasing the current amplitude of a 200 ms DCS train in steps of 250 μA from a starting amplitude of 500 μA (Subjects 1 and 2), 1000 μA (Subject 3), or 200 μA (Subject 4) until the subject could perceive the stimulation as indicated by verbal report (Figure 6-2). In two subjects (Subjects 2 and 3), the first pair of DCS electrodes that we tried did not elicit a consistent perceptual experience, so we tried a different pair of electrodes and again found the perceptual threshold (Figure 6-2). Due to experimental time constraints, we only comprehensively tested one pair of stimulation electrodes. During our screening tests we swept through different electrode pairs to choose the pair and stimulation polarity that most reliably produced recognizable percepts localized to the hand. Once we found this pair of electrodes for a given polarity, we conducted all remaining experiments for the day with that bipolar configuration to maximize the number of trials we were able to acquire.

We first determined subjects' stimulation electrodes and perceptual current thresholds as described above, and then used a suprathreshold current amplitude during the experiment for all DCS conditions (Table 6-1). To ascertain a suprathreshold stimulation current amplitude, we required two subjects (Subjects 2 and 4) to correctly identify, in ten sequential two-alternative forced choice (2AFC) trials, whether one or two 200 ms DCS trains with a suprathreshold current amplitude were delivered before proceeding from the perceptual thresholding to the response timing experiment (Figure 6-2). This demonstrated that the subjects could reliably perceive the 200 ms DCS trains at that current amplitude. For the other subjects (Subjects 1 and 3), we achieved reliable discernment of stimulation with a suprathreshold amplitude (250-500 μA above their perceptual threshold) and proceeded with the response timing experiment without conducting the ten sequential 2AFC trials due to time limitations.

For Subject 2, after successfully completing the ten 2AFC trials, we attempted to match perceived intensity between the haptic feedback condition and the 200 ms DCS train condition by increasing the DCS current amplitude until the subject felt that the two stimuli were of qualitatively equal strength (Figure 6-2). We did not attempt intensity matching in Subjects 1 or 4 due to time constraints and patient fatigue. In Subject 3, we did not attempt intensity matching because DCS elicited relatively weak percepts and raising the current amplitude high enough to match its perceived intensity to that of the haptic stimuli would increase the risk of afterdischarges.

Haptic Stimulation

We applied haptic feedback with digital touch probes (Karolinska Institute) that time stamped the deflection, and touched the cutaneous region where subjects localized the DCS percepts (Figures 6-1, 6-2). An audio signal presented to the researcher via headphones but which was inaudible to the subject, cued the experimenter to apply the haptic feedback. We used the digital touch probes previously [137] in conjunction with cortical stimulation, and at the time of manufacturing they were calculated to have a touch onset with an average delay of 1.04 ± 0.48 ms (mean \pm standard deviation). To account for experimenter variability, and possible hardware changes over time, we measured them again and found them to have a touch onset with a

delay of mean 5.24 ± 3.26 ms (mean \pm standard deviation) and median 6.45 ms relative to an electrical short circuit. The small difference in registered touch onset, if added onto the digital touch probe latencies, does not change our significant effects in total.

Experimental Protocol

After determining DCS current amplitudes, we completed one (for Subject 1) or two (for Subjects 2-4) blocks of response timing trials, each separated into a DCS set and a haptic stimulation set (Figure 6-2). During the DCS set we delivered DCS train lengths of 200 ms for Subject 1, and train lengths of 100, 200, 400 and 800 ms in the subsequent three subjects (Subjects 2-4). Intertrial intervals of both DCS and haptic feedback were jittered (ranging from 2.5 to 3.5 seconds) to minimize anticipatory effects or rhythmic perception by the subjects. We broke up the DCS and haptic stimulation conditions into separate sets to allow subjects to anticipate and focus on one method of stimulation at a time. We reasoned that interleaving haptic and cortical stimulation within one block would result in a greater degree of uncertainty and error due to perceptual differences between modalities, rather than allowing a comparison between conditions where the subject was acclimated to either stimulation type.

All subjects were instructed to respond as quickly as possible by pressing a button held in their hand contralateral to sensation when they perceived the DCS or haptic sensation. The first subject was instructed not to look at the stimulated hand, while the subsequent three subjects (Subjects 2-4) were blindfolded to reduce potential confounds of visual distraction.

Off-target control stimulation

As a control, we also delivered off-target stimulation to a region outside of S1 during the DCS experimental set. This was to ensure that the responses were specific to DCS of S1, rather than a response to general, non-targeted DCS. For the off-target stimulation electrodes, we chose two electrodes that would be safe for bipolar stimulation based on prior clinical mapping and knowledge of the subjects' epileptic foci. We used a 200 ms DCS train length and the same suprathreshold current amplitude for off-target stimulation as we used for S1 stimulation. As detailed below and in Figure 6-2, Subject 1 completed a third set after the DCS and haptic sets with this off-target control stimulation. For Subjects 2-4, we interleaved off-target stimulation with the on-target, S1 stimulation during the DCS sets.

Subject 1 trial progression

In Subject 1 during the DCS set, we delivered 86 trials of 200 ms trains of stimuli with 17 trials of null stimuli (i.e., no stimulation as a control) interleaved in a random order. In the haptic set, we delivered 103 trials of haptic touch, again with 17 interleaved null trials. During the third and final set, we delivered 20 trials of off-target stimulation, interleaved with 6 null trials (Figure 6-2).

Subject Experimental Progression

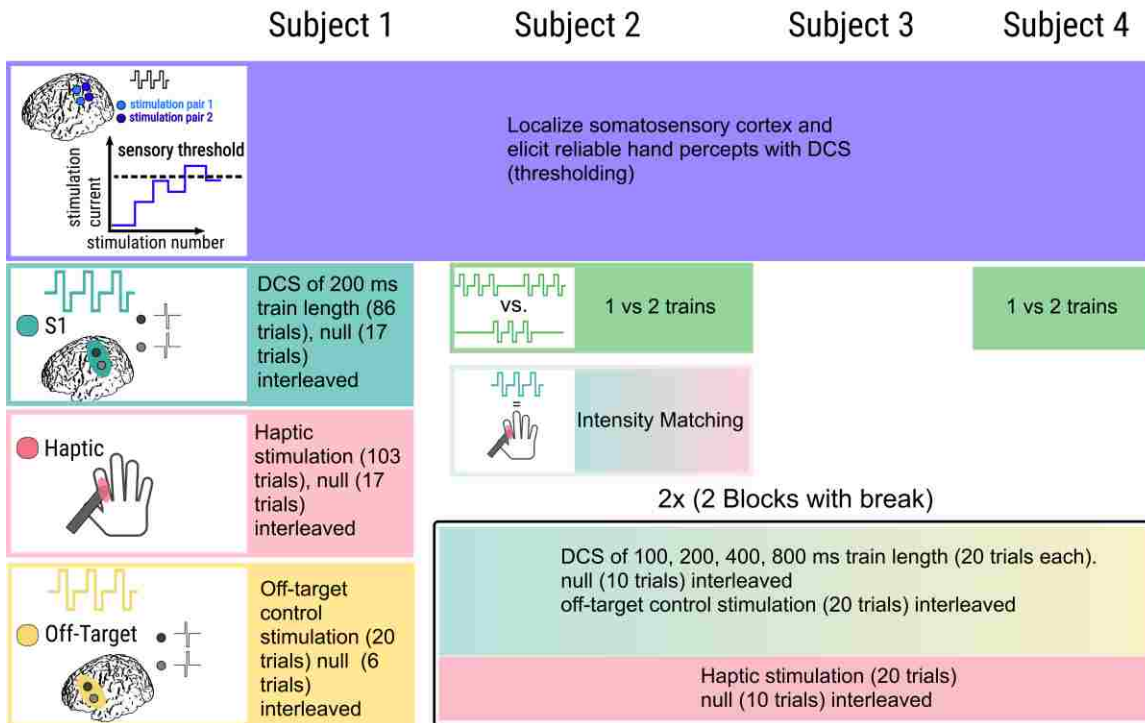


Figure 6-2. Response timing experimental progression by subject

Each column represents the experimental progression for our four subjects from top to bottom. In all subjects, we localized electrodes which elicited a reliable percept on the hand upon stimulation. We then found a threshold level of stimulation where sensations were elicited, and used stimulation currents above this to ensure reliable perception with 200 ms trains. Subjects 2 and 4 both performed a two-alternative forced choice task of discriminating between one and two trains to confirm our test amplitudes were suprathreshold. Subject 2 then performed an intensity matching experiment in which we identified stimulation levels that elicited approximately the same strength of response as the haptic touch provided by the experimenter. All subjects completed experimental trials after we established the suprathreshold current to use. Subjects 2-4 all had two blocks consisting of 100, 200, 400, and 800 ms trains, interleaved with 20 off-target and 10 null trials, followed by 20 haptic stimuli trials interleaved with 10 null trials.

Subjects 2-4 trial progression

For Subjects 2-4, we first delivered a DCS stimulation set based on stimuli timing and conditions from a pre-generated file that randomly interleaved 20 trials each of 100, 200, 400, and 800 ms train-length S1 DCS trials with 10 null trials and 20 off-target DCS trials, for a total of 80 S1 DCS trials and 30 control trials. Next during the haptic set, we provided 20 trials of haptic stimulation through the digital touch probes, with 10 null control trials randomly interleaved. After a brief rest period (5-10 minutes), we proceeded to a second block of cortical and haptic stimulation sets (Figure 6-2).

Data Analysis

We performed all data post processing and analysis in MATLAB and Python with custom scripts. To calculate the response times in the DCS conditions we took the temporal difference between the onset of the stimulation train and the subject's button press, while for response times in the haptic feedback condition, we calculated the difference between the registered timing of the deflection of the digital touch probe and the subject's button press. We identified and excluded outliers as trials with reaction times slower than 1 second and faster than 150 ms from further analysis, as faster responses are unlikely for untrained human subjects [195], and slower ones more likely represented a decrease in attention to the task rather than a true response time. Additionally, we did not consider trials where either the button did not respond appropriately to the subject's press, or the digital touch probe did not register deflection. Table 6-2 includes how many trials were analyzed for each subject and condition.

Anderson-Darling tests for normality confirmed that the data was not consistently well described by a normal distribution, therefore we proceeded with non-parametric testing. We corrected for multiple comparisons by dividing an alpha value of 0.05 by the number of conditions tested within each subject. Specifically, both conditions for Subject 1 were not normally distributed ($p = 2.725e-4$ and $1.888e-8$ for haptic and 200 ms DCS conditions, respectively). For Subject 2 the 100 ms DCS, 800 ms DCS, and haptic conditions were not normally distributed ($p = 9.631e-5$, 0.0096 , and $1.399e-16$, respectively), while the 200 and 400 ms DCS condition failed to reject the null hypothesis of being normally distributed ($p = 0.046$, 0.194 , respectively). For Subject 3 the 800 ms DCS and the haptic conditions were not normally distributed ($p = 0.006$ and $3.502e-4$, respectively), while the 200 and 400 ms DCS conditions failed to reject the null hypothesis of being normally distributed ($p = 0.235$ and 0.165 , respectively). For Subject 4 the 800 ms DCS and haptic feedback conditions were not normally distributed ($p = 0.006$ and $1.186e-6$, respectively), while the 200 and 400 ms DCS conditions failed to reject the null hypothesis of being normally distributed ($p = 0.401$ and 0.087 , respectively). Due to the presence of non-normally distributed groups, we proceeded with non-parametric testing for all subjects, using the non-parametric Wilcoxon Rank Sum and Kruskal-Wallis tests (with Dunn-Sidak corrections for post-hoc comparisons for mean ranks [196,197] to assess differences between conditions with an alpha significance level of 0.05. To assess blockwise differences, we used Rank Sum tests with Bonferroni corrections, and a base alpha critical level of 0.05.

Further, we tested for equal variances between groups using the Brown-Forsythe test [198]. For Subjects 2 and 4, testing revealed no significant differences in variances between groups, whereas for Subjects 1 and 3, there were significant differences in variances (critical value of 0.05; not significant- Subject 2: $p = 0.094$, Subject 4: $p = 0.0873$; significant- Subject 1: $p = 0.0113$; Subject 3: $p = 5.662e-4$). Thus, for Subjects 2 and 4 statistically significant differences between conditions from the Kruskal-Wallis and post-hoc tests were interpreted as differences in medians with haptic stimulation being significantly faster than cortical stimulation, while for Subjects 1 and 3, statistically significant differences were interpreted as differences in stochastic dominance of one sample over another [197].

6.3 Results

Response Times

In Subject 1, we compared haptic stimulation to 200 ms trains of S1 DCS with a suprathreshold current amplitude. Haptic feedback elicited a significantly different reaction time as compared to the 200 ms DCS trains ($p = 6.105e-16$, Figure 6-3). The median response time for the S1 DCS trains was 459 ms, while the median response time for the haptic feedback condition was 313 ms (Table 6-2), in line with classic tactile reaction time responses [195,199]. Minimum, 25% and 75% quartile ranges, and maximum response times for all subjects are reported in Table 6-2. This subject did not perceive off-target DCS, and responded to a single null stimulation trial. In light of the results from Subject 1, we subsequently chose to consider possible effects of S1 DCS train length on reaction times, acquiring and comparing haptic responses to train lengths of 100, 200, 400 and 800 ms with suprathreshold currents in Subjects 2-4

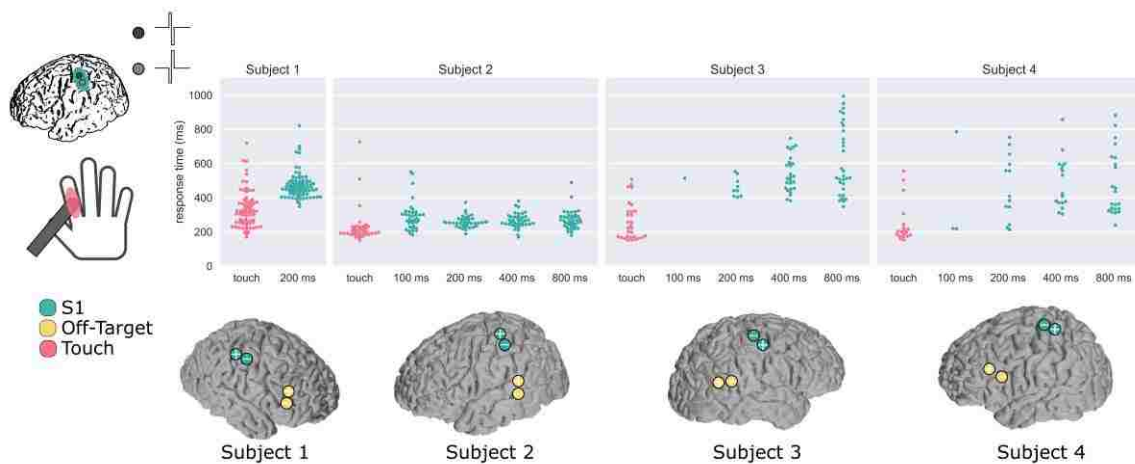


Figure 6-3. Comparison of reaction times for four subjects and their DCS electrodes

Each dot represents a response time for a given trial, colored by condition. Pink indicates the haptic test condition, while turquoise indicates S1 DCS conditions and electrodes over hand sensory cortex. Subject 1 only received the 200 ms DCS and haptic stimulation conditions, while Subjects 2, 3, and 4 had 100, 200, 400, and 800 ms trains of stimulation applied. The two separate blocks for Subjects 2, 3, and 4 were pooled together for each subject. Off-target DCS control electrodes are indicated in yellow. Electrode locations are based on cortical surface reconstructions for each subject as described in the Methods. Electrodes with a plus symbol (+) indicate anodal-first stimulation, while electrodes with a minus symbol (-) indicate cathodal-first stimulation.

In addition to testing four DCS train lengths for Subjects 2-4, we additionally inserted a rest condition in between two blocks to test for habituation or adaptation (Figure 6-4). There were no significant differences between blocks for Subjects 2-4, so we combined them for further statistical analyses. Specifically, for Subject 2, there were no significant blockwise differences between the conditions ($p = 0.811$, $p = 0.715$, $p = 0.675$, and $p = 0.0962$ for the 100, 200, 400, and 800 ms DCS train conditions, respectively; $p = 0.579$ for the haptic condition, critical threshold of $p = 0.01$). For Subject 3, we excluded the 100 ms condition from statistical analyses due to only a single response within one block. Blockwise differences were not significant for

any of the other conditions for Subject 3 ($p = 0.064$, $p = 0.087$, and $p = 0.155$ for the 200, 400, and 800 ms DCS train conditions, respectively; $p = 0.519$ for the haptic condition, critical threshold of $p = 0.0125$). Similarly, for Subject 4, we excluded the 100 ms condition because of a single response on one block, and two responses on another block. Again, blockwise differences were not significant for any of the other conditions for Subject 4 ($p = 0.035$, $p = 0.669$, and $p = 0.109$ for the 200, 400, and 800 ms DCS train conditions, respectively; $p = 0.316$ for the haptic condition, critical threshold of $p = 0.0125$).

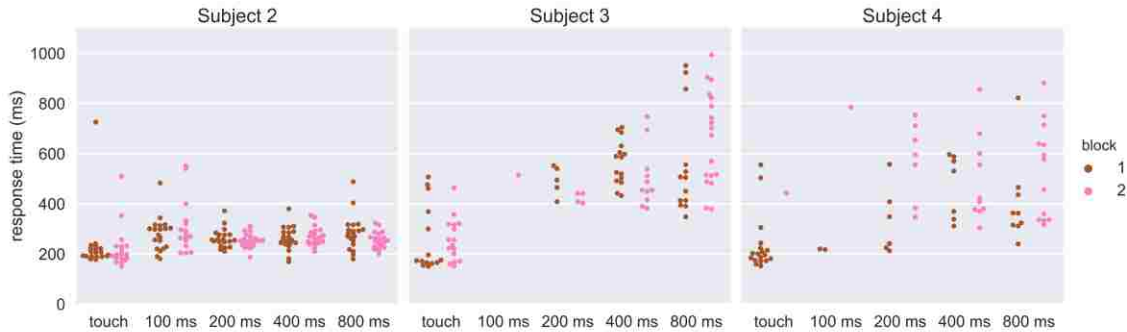


Figure 6-4. Comparison of the two blocked sessions for three subjects

Each dot represents a response time for a given trial, colored by block. Of note is the non-normality of some of the response timings for different conditions. Additionally, the paucity of responses for Subject 3 to the 100 ms and 200 ms conditions, and for Subject 4 to the 100 ms condition suggests the stimulation level was at or near their perceptual thresholds.

For Subject 2, all S1 DCS response times were found to be significantly different than the haptic response times due to statistical differences in medians ($p = 3.654e-8$ for the 100 ms, $p = 7.000e-5$ for the 200 ms, $p = 2.064e-6$ for the 400 ms, and $p = 1.866e-6$ for the 800 ms DCS train, adjusted p -value threshold = 0.05), while no S1 DCS conditions differed significantly from each other (Figure 6-3). The median response times for the 100, 200, 400, and 800 ms DCS trains were 277, 254, 261, and 265 ms, respectively, while the median response time for the haptic feedback condition was 198 ms (Table 6-2). For this subject we chose off-target stimulation electrodes that had been safely tested during clinical language mapping but used much lower current amplitudes than tested clinically (Figure 6-3, Subject 2, off-target electrodes). The subject perceived the off-target stimulation as a vague, non-tactile, and non-localized sensation, and described it as distinct from the DCS sensation. Although he could perceive the off-target DCS, he was able to volitionally not respond to these trial types and did not respond to any of the off-target stimuli within our 150-1000 ms response time window. The subject responded within our time window to a single null stimulus.

For Subject 3 the 200, 400, and 800 ms DCS response times were found to be significantly different than the haptic feedback response times, due to haptic feedback stochastically dominating the reaction times ($p = 0.029$, $p = 5.971e-8$, $p = 1.290e-10$, respectively), while no S1 DCS conditions differed significantly from each other. Subject 3 only responded in one trial with

100 ms S1 DCS trains with a response time of 514 ms, so we excluded statistical comparisons with the other conditions. Median S1 DCS response times were 442, 515, and 528 ms for the 200, 400, and 800 ms DCS trains, respectively, while the median haptic feedback response time was 222 ms (Figure 6-3, Table 6-2). This large difference in medians provides convincing evidence that the cortical stimulation resulted in significantly slower reactions than haptic stimulation. This subject responded within our 150-1000 ms response window once to off-target stimulation, although they did not report being able to perceive the off-target stimulation. The subject did not respond to the null-condition.

For Subject 4 the 200, 400, and 800 ms S1 DCS response times were found to be significantly different than the haptic response times due to a significant difference in medians ($p = 1.161e-3$, $p = 8.803e-5$, $p = 1.107e-4$, respectively), while no S1 DCS conditions differed significantly from each other. Subject 4 responded on only three trials with 100 ms S1 DCS trains with a median reaction time of 220 ms, so we excluded the 100 ms DCS condition from further statistical analysis. Median DCS response times were 408, 423, and 400 ms for the 200, 400, and 800 ms DCS trains, respectively, while the median haptic response time was 201 ms (Figure 6-3, Table 6-2). This subject did not perceive the off-target stimulation or the null stimulation.

For Subjects 1 – 3, there was no indication of adaptation, nor reported description of the stimulus intensity as weakening and changing throughout the DCS sets. After the first block with Subject 4, however, he verbally described a noticeable decrease in stimulation intensity as the trials proceeded. Therefore on the subsequent block we increased the DCS current amplitude from 1.0 mA to 1.2 mA. The subject again verbally described a decrease in perceived intensity as the trials proceeded during the second block despite the increased current amplitude. This suggests individual differences in adaptation to cortical stimulation, perhaps dependent on parameters such as the electrode location, medication status, subject attentiveness, or amount of cerebrospinal fluid underneath the electrodes.

Qualitative Assessment

The subjects described the S1 DCS as non-painful, using descriptions such as a “pins and needles” like sensation (Subject 1), a “buzz”, or the feeling of “something brushing” against the skin (Subject 2), “tingling” (Subject 3), and “pulse” or “throb” (Subject 4). These subjective descriptions are in line with previous reports for S1 DCS [110,111,139]. The subjects reliably localized the percept from S1 DCS during the experiment and across blocks (see Table 6-1 for percept localization). However, the pair of electrodes initially chosen for Subject 2 were not reliably localized, with the subject localizing the percepts from some stimuli to the proximal thumb and some to the proximal palmar area of the fifth finger. Therefore, prior to any experimentation, we selected a different pair of electrodes for Subject 2 that generated a percept which the subject reliably localized to the third finger.

For Subject 2 we attempted to match the perceived intensity of the 200 ms DCS train to that of the haptic stimulation (see Methods, Figure 6-2), and although we were able to make their intensities more similar to one another, we were not able to match them completely. As we increased the DCS current amplitude, Subject 2 felt that the percept he experienced both

increased in intensity and in the size of the localized area. As a result, during the experiment his perceived intensity of the S1 DCS was slightly less than the perceived intensity of the haptic stimulation in order to keep the localized areas of the sensation similar. Despite matching the sensation intensities as well as possible, Subject 2 described the haptic and cortical stimulation as very distinct from one another. The S1 DCS percept was initially localized to the same region as the haptic stimulation (dorsal side of third finger), but then radiated across the skin.

Subject	Experimental condition	Minimum (ms)	25% lower quartile (ms)	Median (ms)	75% upper quartile (ms)	Maximum (ms)	Number of trials responded to and within response time bounds
1	200 ms	348	422	459	495	821	81/86
	digital touch probe	169	254	313	374	719	73/103
	null simulation	N/A	N/A	724	N/A	N/A	1/40
	off-target stimulation						0/20
2	100 ms	182	232	277	314	551	36/40
	200 ms	188	235	254	276	372	40/40
	400 ms	169	244	261	288	380	40/40
	800 ms	180	234	265	291	488	40/40
	digital touch probe	151	189	198	228	726	38/40
	null simulation	N/A	N/A	449	N/A	N/A	1/40
	off-target stimulation						0/40
3	100 ms	N/A	N/A	514	N/A	N/A	1/40
	200 ms	403	409	442	494	553	9/40
	400 ms	383	455	515	603	747	26/40
	800 ms	348	466	528	806	994	31/40
	digital touch probe	151	169	222	318	507	30/40
	null simulation						0/40
	off-target stimulation	N/A	N/A	484	N/A	N/A	1/40

4	100 ms	218	219	220	503	786	3/40
	200 ms	213	347	408	595	754	13/40
	400 ms	305	371	423	588	857	17/40
	800 ms	240	334	400	624	882	22/40
	digital touch probe	153	178	201	234	556	19/40
	null simulation						0/40
	off-target stimulation						0/40

Table 6-2. Reaction times for each subject and each condition

In all subjects, cortical stimulation resulted in significantly different reaction times than haptic stimulation (assessed through non-parametric Wilcoxon Rank Sum and Kruskal-Wallis tests). Final column reports the number of trials responded to by each subject across both blocks for each of the trial types given our response time limits of 150-1000 ms, and appropriate signal detection. Response times outside of this range were considered outliers based on expected human performance (see Methods, Data Analysis for details). Blank boxes indicate trial types with no responses.

6.4 Discussion

Our study characterized the differences in reaction times between cortical and haptic stimulation in four human subjects. Our results demonstrate that response times to cortical stimulation are significantly slower than to haptic stimulation. We additionally demonstrate that cortical stimulation trains of varying lengths do not significantly affect the reaction times for suprathreshold cortical stimulation parameters.

Our results are consistent with a previous observation in non-human primates that intracortical microstimulation of area 1 in primary somatosensory cortex results in significantly slower response times than peripheral stimulation [200]. This delayed response for DCS is counterintuitive at first, as one may suspect that bypassing the ascending peripheral afferents through DCS would reduce the distance traversed by the sensory volley and consequently result in faster reaction times. However, as previously suggested [200], electrical stimulation may be exciting both inhibitory and excitatory connections in unnatural combinations, driving slower behavioral responses.

In human neocortex, approximately 20% of neurons are interneurons, many of which are inhibitory and contribute to local inhibitory neural circuits [201]. Similarly, in rodent neocortex, approximately 20-30% of neurons are interneurons [202]. This is important when considering the neural response to electrical stimulation, as microstimulation in rodents has been demonstrated to result in a spatiotemporal smear of activity, due to the evoked activity consisting of a combination of fast excitatory responses and inhibitory responses [203]. In addition to an unnatural spatial cortical activation, electrical microstimulation in rodents results

in different trends in trial-to-trial variability relative to natural sensory stimuli [204]. Thalamocortical simulations suggest that high levels of synchrony generated by electrical stimuli, which are not seen in natural stimuli, are responsible for this difference in the shape of the trial-to-trial variability curves [204].

Additionally, electrical microstimulation, as used in the intracortical microstimulation experiments, activates neurons primarily through their axons [166,205], although other regions of the cell such as the cell body and dendrites may also be activated depending on stimulus polarity and orientation. Non-human primate work using microstimulation combined with fMRI has shown that electrical stimulation may disrupt cortico-cortical signal propagation by silencing output of areas where the afferents are electrically stimulated [169]. This supports the idea that electrical stimulation results in a distinctly different activation pattern, which may explain a less optimal (and longer response time) reaction to electrical stimuli compared to natural haptic stimulation. Other hypotheses for the delayed response to S1 DCS include the possible need for downstream amplification, from a region such as the thalamus, that is initially skipped via S1 stimulation [200], or the possibility that surface stimulation is unable to directly stimulate deeper primary somatosensory areas, including area 3b where direct intracortical microstimulation has been shown to elicit similar reaction times to haptic stimulation during a discrimination task in non-human primates [128].

Early cortical stimulation work in elderly dyskinetic patients [112] suggested a 500 ms stimulation train was required for consistent perception of DCS with a liminal, or near-threshold, current amplitude. Later work in epileptic patients demonstrated that a 250 ms stimulation train could elicit conscious perception with near-threshold current amplitudes [113]. Furthermore, Ray et al. illustrated the inverse relationship between DCS train duration and the current amplitude required for perception, with current thresholds increasing as the train durations decreased¹³. We observed a similar phenomenon in Subjects 3 and 4, where for a fixed current, shorter train lengths did not elicit conscious percepts. These two subjects' inability to reliably respond to the 100 ms train duration condition, suggests that we may have been using a stimulation current amplitude that was too low to reliably discern train lengths under 200 ms (the train length used for perceptual thresholding) at a fixed amplitude. Additionally, Subject 3 perceived fewer of the 200 ms DCS trials than the 400 ms or 800 ms DCS trials, suggesting that we were stimulating close to the threshold train duration and intensity parameters.

In contrast to Subjects 3 and 4, Subject 2 reliably discerned all of the stimulation trains and had much faster reaction times. In this case we seemed to be operating far above the minimum current threshold necessary for the various DCS train lengths tested. As Subject 2 was the only subject for whom we attempted DCS/haptic stimuli intensity matching (see Methods), we used a current amplitude that was notably greater than the subject's perceptual threshold (roughly 750 μ A greater). The other subjects completed the task with current amplitudes that were only roughly 250-500 μ A above their perceptual thresholds. Stronger intensity stimuli are known to produce faster response times [199], and it is possible that, to a degree, more suprathreshold

DCS currents may lead to faster response times, but further experimentation is necessary to examine this hypothesis.

Human reaction times from one study in untrained, healthy volunteers have been found to vary between 210 and 400 ms [195], but can range down to 140-150 ms with practice for certain individuals [199]. With this as a basis for normal comparisons for our untrained subjects, we similarly find a range of different response times to cortical and haptic stimulation. This suggests that for future BCI implementation, an individual's innate response time may need to be considered in light of variable latencies. That is, if one subject requires on average 500 ms to respond to cortical stimulation, while another subject requires 300 ms, this requires design considerations on the BCI side to account for time differences in the feedback loop.

Response times are also modulated by non-somatosensory features such as visual feedback, arousal, motivation, and attention [199]. In well-practiced healthy subjects, response times based purely on visual feedback are slower than those based on tactile stimuli for a simple reaction time task (approximately 180 ms on average compared to 140 ms, respectively) [199]. The combination of haptic and visual feedback has been shown to result in faster reaction times relative to visual feedback alone for computer-based tasks in healthy human subjects²⁶. We controlled for potential effects of visual feedback by having Subjects 2-4 wear a blindfold, and asking Subject 1 to close her eyes. Subjects' attention may have also affected their response times, but we did not attempt to quantify their attentiveness. Experimenter observation suggests that Subject 2, who had the fastest response times, was the most engaged in the task and approached it with a competitive, game-like attitude. However, we cannot ascertain that Subject 2's attentiveness affected his response times, and have presented other possible explanations for his faster responses including use of a higher suprathreshold stimulation amplitude compared to those for the other three subjects. Mere observation suggests that Subject 1 was the groggier and least engaged in the task, correlating with their slowest haptic reaction times. Future studies may consider including a comparison of response times to S1 DCS and haptic stimuli with visual feedback (i.e., eyes open without a blindfold as would be likely in a future application) to understand how visual feedback may modulate response times. As we increase task complexity and move away from a simple reaction time task as performed here, the benefits from additional feedback beyond only visual feedback may become even more apparent.

An additional factor to be explored in the future is the impact of the polarity of the bipolar stimulation used. Due to experimental time constraints we were unable to comprehensively test the effect of anodic relative to cathodic first stimulation at each electrode, but due to the different cortical activation due to the polarity of stimulation, there could be an effect on reaction times and perception [206,207].

Each of our blocks lasted on the order of 10 minutes, with 5-10 minutes of rest between the blocks. The lack of a consistent, discernible habituation or learning effect suggests that either the sessions were not long enough or frequent enough to elicit learning or habituation, or that subjects were already reacting close to their fastest possible reaction times. We do not claim

that repeated training over multiple sessions and days would not show a decrease in reaction time, but rather we are unable with our acute ECoG epilepsy experiments to address this particular question.

In Subjects 1, 3, and 4, the frontal and temporal electrodes used for the off-target stimulation elicited no sensation and were only responded to once by Subject 3. However, in Subject 2 whose off-target stimulation site was over a language area, the subject perceived a vague, non-localizable, sensation of the stimulation. These off-target electrodes had been safely tested during clinical mapping and avoided possible seizure foci. We used current amplitudes much lower than those tested clinically to further avoid afterdischarges and match the suprathreshold stimulation used in the other S1 DCS conditions. Subject 2 described the off-target DCS as distinct from the S1 stimulation conditions, and had no difficulties in responding only to S1 stimulation. This suggests that humans can receive stimulation in multiple cortical regions and distinguish them within short temporal intervals.

An unknown factor in the work presented here is the extent to which DCS of S1 is also impacting ipsilateral M1, and through connections to contralateral M1, motor output. Our subjects are able to perform motor tasks with the hand being stimulated concurrently, suggesting that there is not grossly visible motor disruption on the ipsilateral or contralateral side. Our subjects also are able to perceive temporally overlapping natural haptic stimulation and DCS at the same spatial location, suggesting that there is not global inhibition or cortical jamming. However, we do acknowledge that some of the delay observed could indeed be due to some potential motor disruption from charge spread. This study does not serve to address this, but rather, presents data revealing significant delays in the timed response to S1 DCS with respect to natural touch. This effect may possibly be due to a delay in conscious perception of the DCS or in the motor output pathway, which has implications for neuroprostheses and closed loop BCI design.

Our results, while elucidating aspects of human perceptual processing of S1 DCS, demonstrate a need for further exploration of the neural mechanisms underlying the reaction time differences between S1 DCS and haptic stimulation. We found, in four human subjects, that response times to cortical stimulation are significantly different than to haptic stimulation. The fact that there appears to be a significant delay in cortical processing and subsequent response after DCS does not preclude ECoG stimulation from being a promising modality for feedback in a neuroprosthetic application. Rather, this highlights the importance of understanding variables such as human reaction time for neuroprosthetic applications and appropriately designing devices to account for these temporal delays. Our ongoing studies are aimed at understanding and potentially speeding up the temporal response to ECoG stimulation by varying stimulation parameters, regions targeted, and waveform shape.

7 Ownership of Artificial Limbs

As discussed in the Introduction, peripheral nerve stimulation in human subjects with transradial amputations can increase subjects' sense of embodiment of their personal prosthesis [68]. We desire future cortical-level BBIs with somatosensory feedback to evoke a similar sense of embodiment or ownership over the end effector the BBI is linked to, because it is expected that embodiment of the BBI will create a more positive user experience. A recent study on the home use of a sensory feedback-enabled myoelectric prosthesis that compared the users' experiences with and without the sensory feedback, found that both subjects had a generally improved experience with sensory feedback, and importantly they experienced a greater sense of embodiment and self-reported improved psychosocial measures when the sensory stimulation was on [208]. Specifically, surveys on the psychosocial impact of the sensory-enabled prosthesis demonstrated that subjects experienced a normalization of their body schema, a lessening of their perceived disability, a higher confidence, and an improved perception on their ability to use their prosthesis to interact with others when somatosensory feedback was enabled. The subjects also wore the prosthesis more, performed a greater proportion of tasks with the prosthesis, and used the prosthesis to actively touch or grasp objects more often when the sensory stimulation was enabled [208]. The BBI in this experiment used extra-neural peripheral electrodes to deliver sensations to the users' thumbs, index, and middle fingers that corresponded to the intensity measured by sensors at the fingertips of the prostheses [208].

Although prior work had demonstrated that S1 DCS could elicit sensations, prior to the study discussed here, it was unknown whether DCS would be able to elicit a sense of ownership over or embodiment of a prosthesis. Given our interest in elucidating the potential of DCS for somatosensory feedback, we conducted an experiment to probe whether DCS could evoke a sense of ownership over an artificial limb using a novel version of the rubber hand illusion (RHI).

The work presented in this chapter was completed in collaboration with another lab member, Dr. Kelly Collins, and a visiting researcher, Dr. Arvid Guterstam, a member of the Ehrsson Lab of the Karolinska Institutet and an expert on the rubber hand illusion and other body illusions. I helped them collect the following data, but Dr. Collins and Dr. Guterstam completed the analyses of the results and created the figures in this chapter.

The following work has been published as:

Collins, K. L., A. Guterstam, J.A. Cronin, J.D. Olson, H.H. Ehrsson, & J.G. Ojemann (2016). "Ownership of an artificial limb induced by electrical brain stimulation." *Proceedings of the National Academy of Sciences*, 114(1): 166-171.

I have adapted the published report substantially to present the results as they relate to the present discussion of the functionality of DCS of S1.

7.1 Introduction

The rubber hand illusion (RHI) is a visual-tactile illusion during which subjects refer tactile sensations from their own, hidden hand to a rubber hand within view, which is also being synchronously touched [5,209]. During the RHI, subjects experience a sense of ownership over

the rubber hand. The published results in two subjects suggest that DCS can induce a sense of ownership of an artificial hand. These results have important implications to the application of somatosensory stimulation in rehabilitative devices, in which one would want a user to experience a sense of ownership over the device (e.g., a prosthesis).

7.2 Methods

Subjects were positioned with their real hand (contralateral to the ECoG grid) hidden behind a screen so that they could not see it. A rubber hand matching the handedness of their contralateral hand was positioned in front of them, as depicted in Figure 7-1. The experimenter repeatedly touched the rubber hand with a digital touch probe that registered deflection and triggered 500-ms DCS trains with a 100 Hz PF to be delivered to hand S1. Experimental blocks were 60 seconds long and consisted of five different conditions (1 experimental and 4 control conditions) as outlined in Table 7-1.

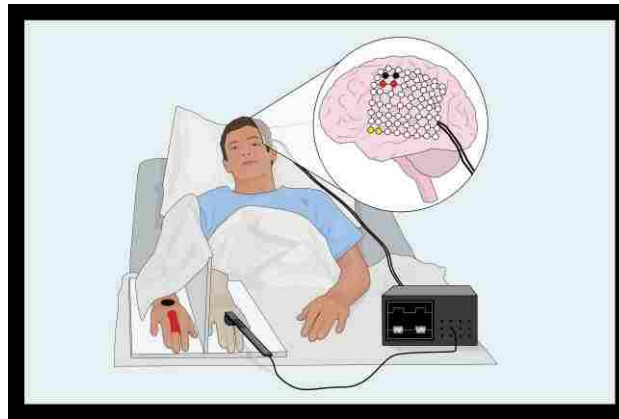


Figure 7-1. Rubber hand illusion setup

The experimenter first applied bipolar DCS over two hand S1 DCS electrodes (highlighted in red) to determine to where the subject localized the percept (illustrated as an example with red shading over the third finger). During conditions 1 and 2 (Table 7-1), the experimenter repeatedly touched the rubber hand with the digital touch probe at the location corresponding with the percept's location. The digital touch probe triggered a 500 ms DCS train, thus creating a spatially congruent experience of the DCS percept and the visual cue from the rubber hand. During condition 3, the experimenter touched the same spot on the rubber hand, but DCS of the forearm sensory cortex (electrodes highlighted in black with corresponding forearm location highlighted) was triggered, creating a spatially incongruent experience. During condition 4, the experimenter again touched the same spot on the rubber hand, but DCS to an off-target site that was not expected to elicit any conscious sensory experience (electrodes highlighted in yellow) was triggered. The purpose of each condition is provided in Table 7-1. Figure from published RHI article [137].

We asked subjects to verbally report the vividness of the illusion after a cue was presented. Subject 2 reported his experience of the illusion after each trial, whereas Subject 1, who was slower to respond, reported her experience of the illusion every 4 seconds (approximately every other trial). Both subjects were instructed to report how much they agreed with the statement, "It feels as if the rubber hand were my hand," using a scale ranging from -3, "I

completely disagree,” to +3, “I completely agree,” with 0 indicating, “I neither agree nor disagree.” Before and after each experimental block, subjects completed an intermanual reaching task while they were temporarily blindfolded and the screen blocking their real hand was removed. They were asked to point to the location of their real (contralateral) hand using their ipsilateral hand. Proprioceptive drift was calculated as the difference between the measurements before and after the block, with positive values indicating a drift towards the rubber hand. Prior research has established positive proprioceptive drift values as an indirect behavioral proxy of the feeling of limb ownership [210].

Conditions	Type/Purpose	What the digital touch probe triggered
1-SynchFinger	Illusion condition	Synchronous DCS
2-AsynchFinger	Control for temporal incongruence	DCS delayed by 1,000 ms
3-SynchWrist control	Control for spatial incongruence	DCS to forearm sensory cortex
4-SynchRemote control	Control for suggestibility	DCS to off-target electrodes outside of SI
5-Placebo	Control for suggestibility	No DCS

Table 7-1. RHI experimental conditions

Five conditions – one experimental and four controls – were used to assess subjects’ experience of artificial limb ownership during the RHI with S1 DCS. As explained in Figure 7-1, the digital touch probe was always applied to the same spot on the rubber hand. Conditions 1 and 2 created a spatially congruent experience by triggering DCS to the hand S1 electrodes which elicited a sensation that was localized to the subject’s hand and corresponded to the spot on the rubber hand that the experimenter touched. Condition 1, the experimental condition, was temporally congruent in addition to being spatially congruent, as the digital touch probe immediately triggered the S1 DCS. Condition 2, however, was temporally incongruent, as the DCS was delayed by 1,000 ms following the touch from the digital probe. Condition 3 was temporally congruent but spatially incongruent by triggering S1 DCS over the forearm electrodes (Figure 7-1). Conditions 4 and 5 both controlled for subject suggestibility by either stimulating off-target electrodes (Condition 4, Figure 7-1) or triggering no stimulation (Condition 5) as to produce no somatosensation when the rubber hand was touched.

7.3 Results

Both subjects that completed the RHI with DCS experienced the illusion in the synchronous, spatially congruent experimental condition (Condition 1, SynchFinger; Figure 7-2). Surprisingly, Subject 1 also appeared to experience the illusion under the AsynchFinger control condition (Condition 2) based on her verbally reported strength of ownership (Figure 7-2A). However, Subject 1’s proprioceptive drift was greater in the SynchFinger illusion condition than in the AsynchFinger control condition (Figure 7-2B). This suggests that Subject 1’s high verbal reports during the AsynchFinger condition may have been due in part to task compliance and stimulation order effects as the SynchFinger illusion condition came just before the AsynchFinger condition. Subject 2 only experienced the illusion under the experimental Synch Finger condition (Condition 1; Figure 7-2 C and D).

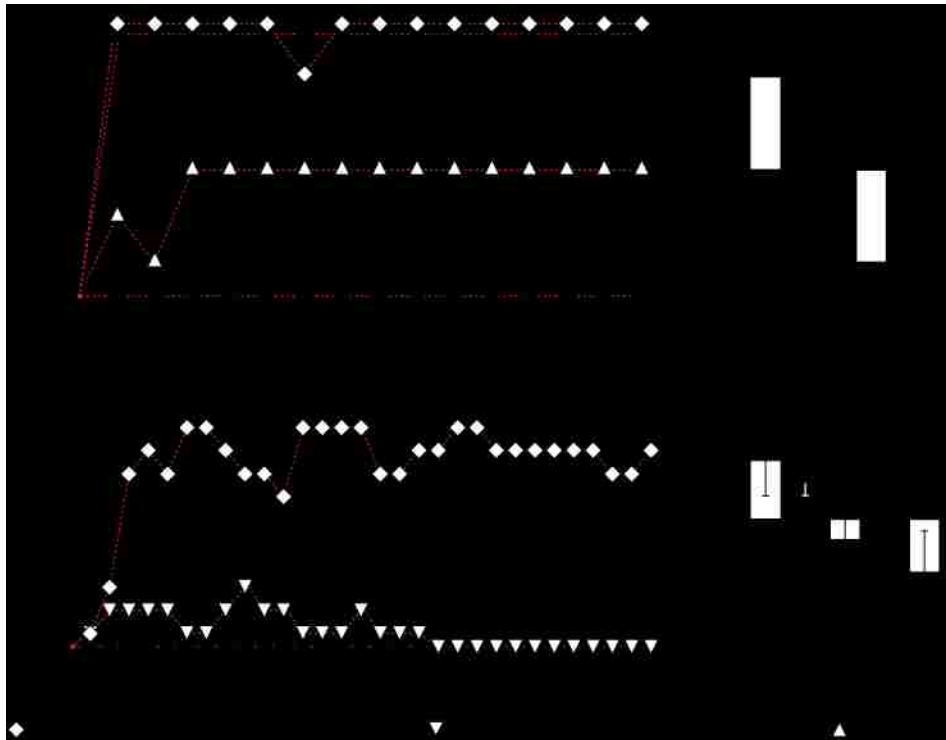


Figure 7-2. Rubber hand illusion results

Ownership ratings (Subject 1-A and Subject 2-C) and proprioceptive drift results (Subject 1-B and Subject 2-D). Subject 1 experienced the illusion and reported high ownership ratings during the SynchFinger experimental condition (Condition 1, Table 7-1) as well as the AsynchFinger condition (Condition 2), but not during the other conditions (A). Subject 1's proprioceptive drift results (B) suggest that she felt the ownership illusion most during the SynchFinger condition, and that her ownership rating responses to the AsynchFinger condition may have been due to task compliance and/or stimulation order effects (her AsynchFinger condition followed the SynchFinger condition). Subject 1 did not complete the SynchWrist control condition due to fatigue after completing the first four experimental blocks. Subject 2 experienced the illusion and reported high ownership ratings during the SynchFinger experimental condition, but not the other four control conditions (C). Subject 2's proprioceptive drift results (D) also support the finding that he experienced a sense of ownership of the rubber hand most during the SynchFinger condition. Figure from published RHI article [137].

7.4 Discussion

Previous research on body ownership and prostheses demonstrated that upper limb amputees can experience a sense of ownership of a prosthesis during the RHI. However, this research required tactile stimulation of the residual limb [211,212] or reinnervated skin regions from TMR [213]. The RHI research presented here from two subjects was the first demonstration that the RHI could be induced without peripheral stimulation, using DCS of S1 instead. This is significant, as it suggests that cortical stimulation will be able to create a sense of ownership over a neural rehabilitative device. For those lacking afferent input from, for example, a paralyzed limb, restoring sensorimotor function will have to involve bypassing the injured afferent nerves, and stimulation at the central nervous system level is one such method. The

results of Subject 2 indicate that the illusion is dependent on a certain degree of spatial and temporal congruence. This suggests that S1 DCS and visual cues can be integrated into a coherent representation, so long as rules governing spatiotemporal congruence of normal perception are met [209].

8 DCS for Task-based Feedback

We have thus far established some of the relationships between S1 DCS parameters and human subjects' perceptual thresholds, subjects' response times to S1 DCS as compared to haptic stimuli, and that S1 DCS can evoke a sense of ownership over an artificial limb. However, we have not yet discussed whether subjects will be able to use DCS in a functional manner. At the time of this experiment, prior work had demonstrated that peripheral stimulation methods could be used to perform a task [68,69,106], but the functionality of S1 DCS had not been explored in this manner. Thus, in this work we evaluated human subjects' ability to continuously modulate their motor behavior based on feedback from S1 DCS. Subjects wore a dataglove that measured their hand aperture position and received one of three stimuli over the hand sensory cortex based on their current hand position as compared to a target aperture position. Using DCS somatosensory feedback, subjects adjusted their hand aperture to move towards the target aperture region. One subject was able to achieve accuracies and R^2 values well above chance (best performance: $R^2 = 0.93$; accuracy = 0.76/1). Performance dropped during the catch trial (same stimulus independent of the position) to below chance levels, suggesting that the subject had been using the varied S1 DCS feedback to modulate their motor behavior. To our knowledge, this study represented one of the first demonstrations of using direct cortical surface stimulation of the human sensory cortex to perform a motor task, and is a first step towards developing closed-loop human sensorimotor BCI.

The following chapter has been published as:

Cronin, J.A, J. Wu, K. Collins, D. Sarma, R.P.N. Rao, J.G. Ojemann, and J.D. Olson. (2016). "Task-Specific Somatosensory Feedback via Cortical Stimulation in Humans." *IEEE Transactions on Haptics*, 9(4): 515-522.

I have made slight modifications to the manuscript to fit in the framework of this document.

8.1 Introduction

Previous research has demonstrated that human subjects can discriminate the intensity of abstract percepts from electrocorticography (ECoG)-based stimulation (i.e., electrical stimulation of the brain surface) with either varied frequency or varied amplitude [110]. Building upon this work, we tested how subjects can utilize abstract sensory feedback in a motor task. We hypothesized that human subjects could use cortical sensory stimulation feedback to continuously modulate their motor behavior to find and follow an unknown target hand position. Three stimulation states (no stimulation, a low-intensity stimulation, and a higher-intensity stimulation) corresponded to three hand aperture states (position of the hand relative to a target position). Our results show that one subject was able to successfully adjust his hand position in response to the ECoG stimulation feedback in order to follow the moving target position with above-chance performance. Two other subjects attempted the task but were unable to complete it; their results are presented primarily in Appendix 2.

8.2 Methods

Subjects

Human subjects (n=3) were implanted at Harborview Medical Center (Seattle, WA) with ECoG grids, following the general methods outlined in Chapter 4.

Cortical Reconstructions

Cortical reconstructions and electrode localization were performed as outlined in Chapter 4.

Stimulation Protocol

We used the stimulation hardware described in Chapter 4. DCS trains consisted of biphasic square pulses with 200 μs phase widths. The inter-pulse interval (IPI) was 4600 μs , yielding a pulse frequency of 200 Hz. Each train duration was 200 ms and was followed by an inter-train interval (ITI) of 400-800 ms. We determined the rough perceptual threshold for stimulation by incrementally increasing the current amplitude in steps of 250-500 μA up to no more than 5000 μA . We defined a low-intensity stimulation waveform (Stim 1) with a PW of 200 μs , PF of 200 Hz, TD of 200 ms and a current amplitude slightly above the perceptual threshold. We then defined a higher-intensity stimulation waveform (Stim 2) with the same parameters, but with a current amplitude above that of Stim 1, such that the subject, as self-reported, could clearly discriminate the two stimuli at rest. Stimulation current amplitudes and the ITI were slightly modified during the task for two subjects based on their feedback and are detailed in the Results, Section 8.3. The catch trial used an amplitude that was between that of Stim 1 and Stim 2.

Experimental Protocol

Three subjects wore a 22 degree-of-freedom dataglove (Cyberglove II, CyberGlove Systems, San Jose, CA) to measure the position of their hand, which we sampled every 50 ms with a custom MATLAB script. To begin the task, subjects opened and closed their hand (in a palmar grasp [214], as if grasping a cylindrical object) with the dataglove for approximately 20 seconds. We took the first vector of the singular value decomposition of these movements as the primary trajectory of aperture motion. During the task, every new glove sample was projected onto the primary trajectory, and the magnitude of the resulting vector was taken as the non-normalized aperture value. We then calculated the normalized aperture value ranging from 0 to 1 based on the subject's minimum (closed) and maximum (open) hand positions. We instructed subjects that they would be asked to open and close their hand to find and follow a target aperture path. Cortical electrical stimulation using the waveforms described above provided feedback to the subjects on their current state. The subjects could be in one of three states (Table 8-1, Cases A-C). We instructed all subjects to open their hand before the trial and stimulation began so that they would start in the state without cortical stimulation (Case A, Table 8-1).

We describe below the specific methods and results for one subject (Subject 2) who performed above chance and completed a catch trial. Two other subjects participated in the task but were unable to complete the task with a catch trial due to poor performance (see Results, Section 8.4 and Appendix 2). To help learn the relationship between the stimulation pattern and his hand position relative to the target position, Subject 2 was trained with concurrent visual feedback for three trials before receiving stimulation feedback solely. His single catch trial delivered the same stimulation regardless of the subject's state. (Catch, Table 8-1).

Case	Hand Position	Aperture Value	Stimulation
A	Too open	< target	None (Stim 0)
B	Within target	Within target	Low (Stim 1)
C	Too closed	> target	Higher (Stim 2)
Catch	All positions	All values	Catch stim

Table 8-1. Possible aperture hand states or cases

The aperture value was calculated from the subject's current hand position, and stimulation was dependent upon the aperture value.

Target Paths

We set Subject 2's target path width to span 15% of his own aperture range from opened (aperture value = 1) to closed (aperture value = 0). Two types of paths were created: a training path and several evaluation paths, for use in training and evaluation trials, respectively. The training path was a simple sine wave with a frequency of approximately 0.02 Hz. For each of the evaluation trials the subject used a different evaluation path that we created by summing four sinusoids with randomly selected frequencies that were no greater than 0.02 Hz. Figure 8-1 shows example evaluation paths with the subject's hand aperture values overlaid. Figures 8-2 and 8-3 illustrate the order of Subject 2's trial path types.

Accuracy

We defined accuracy as the fraction of time spent inside the target region and calculated it as: $(\text{samples inside target range})/(\text{total samples})$ over the entire trial. To determine chance accuracy, we simulated 1,000 random walks, calculated the accuracy of each, and then took the mean. Each random walk was created by drawing with replacement from that trial's set of position changes and cumulatively adding these position changes to a starting position. If the random walk started at the first sample position, when the subject's hand was too open, it may have never entered the target region. Thus, we defined the starting position as the first point that the subject's hand entered the target region. We then calculated the chance accuracy only over the period beginning with the starting position to ensure that the random walk always started within the target range and thus calculate a more robust measurement of chance. We computed the resultant chance accuracy as: $(\text{samples inside target range})/(\text{last sample} - \text{first sample that subject enters target range})$. We measured the subject's performance from the beginning of the trial rather than when they first entered the target region, because during some trials subjects did not enter the target region quickly; therefore, calculating the accuracy from when they first entered the target region would result in an inflated value.

Line Fit: R^2

As another measure of performance, we calculated the R^2 values for each trial by fitting a least-squares linear model of the subject's recorded hand aperture motions to the optimal path - the path through the center of the target region. The R^2 value was defined as: $R^2 = SS_{reg}/SS_{tot}$, where

$SS_{reg} = \text{Sum of squares of the regression} = \sum_i (f_i - \bar{y})^2$,

$SS_{tot} = \text{Total sum of squares} = \sum_i (y_i - \bar{y})^2$,

and y is the recorded aperture data while f is the linear model.

The interpretation of this R^2 value is similar to a traditional goodness of fit of a model to experimental data. In this case we are interested in assessing the goodness of fit between our recorded aperture data and the optimal path, as compared to random walk. We used the 1,000 random walks created in the accuracy calculation to determine the chance R^2 value for each trial by again calculating the R^2 value of each random walk, and then taking the mean.

8.3 Results

Three subjects who had grid coverage over their hand sensory area participated in this task. For each subject, cortical stimulation over the chosen electrodes (Figure 4-1 for Subject 2) elicited an abstract sensation in their hand. None of the subjects thought that the stimulation felt normal. We asked them to describe the sensation to us without any guiding questions, and their percept descriptions are provided in Table 5-3 (Subjects A-C in the table correspond to Subjects 1-3 in this study). To maintain two differentiable stimuli we had to increase the amplitude of cortical stimulation several times during the experiment for Subjects 2 and 3 (Table 8-2).

As mentioned above, only Subject 2 consistently performed above chance levels and completed a catch trial. Subject 1's and Subject 3's results are detailed in Appendix 2 and discussed briefly after Subject 2. Their level of engagement was much less than that of Subject 2 and likely contributed to their poor performances [215].

Subject 2 wore the dataglove on his right hand, the hand contralateral to the implanted ECoG grid, and therefore perceived a sensation from the stimulation on the same hand that he had to move. He used these perceived sensations as feedback on his current hand position relative to the target aperture position and responded by adjusting his hand position. Subject 2 learned to respond properly to the cortical stimulation and follow the unknown target aperture path (Figure 8-1a).

Subject	Trials	Stim 1		Stim 2	
		Amplitude (mA)	ITI (ms)	Amplitude (mA)	ITI (ms)
1	All (1-3)	2.50	800	3.50	800
2	1	1.75	800	2.00	800
	2-3	2.00	800	2.25	800
	4-12	2.00	800	2.40	800
	13-14	2.00	800	2.40	400
3	1-3	1.75	800	2.25	400
	4-7	2.00	800	2.50	400
	8-11	2.00	800	2.75	400

Table 8-2. Current amplitude and inter-train interval values for Stim 1 and Stim 2

To maintain discriminable stimuli, the amplitude values had to be increased several times during the experiment for Subjects 2 and 3. The inter-train interval (ITI) was also changed during Subject 2's trials.

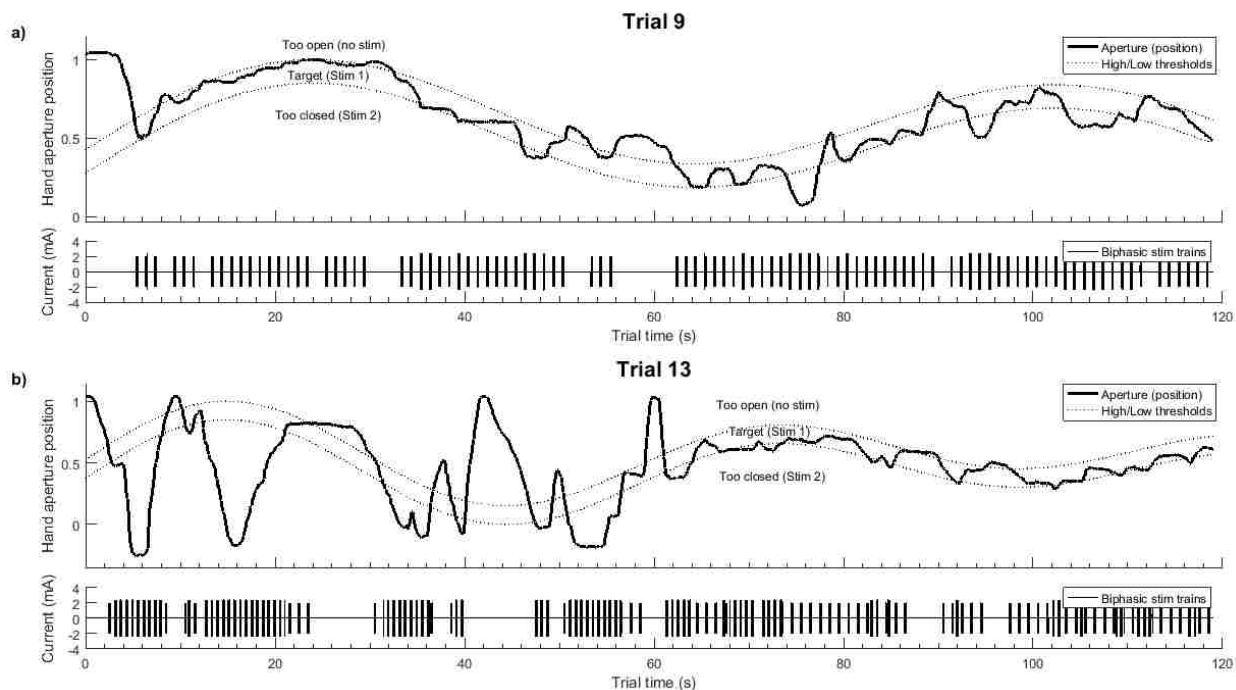


Figure 8-1. Sample traces of hand position and DCS waveforms from aperture task

Traces of Subject 2's hand aperture position relative to the aperture target thresholds with corresponding stimulation current amplitudes (a: Trial 9, b: Trial 13). Stimulation pulses were biphasic, but due to the time scale only the 200 ms stimulation trains are visible not the individual pulses (Stim 1 = 2.0 mA, Stim 2 = 2.4 mA, ITI Trial 9 = 800/800 and ITI Trial 13 = 800/400 for Stim 1/Stim 2, Table 8-2). Subjects' aperture values could move outside of the 0 to 1 range if they made hand movements that were outside of the range used during the normalization period (Section 2.4). Subjects were instructed to start each run with their hand open in order to begin in the no-stimulation region (Table 8-1, Case A). Subject 2 sometimes overshoot the target boundaries, but responded to error feedback (Case A, no stimulation; or, Case C, higher-intensity stimulation) by changing his direction of motion. a) Subject 2 was able to follow the target pathway and stay in the target boundaries with a high performance of: accuracy = 0.6145, $R^2 = 0.8194$. b) Subject 2 had trouble finding the target region at the beginning of the trial, resulting in lower performance values of: accuracy = 0.4023, $R^2 = 0.1001$.

Subject 2 completed 14 total trials: a set-up trial, 6 training trials, 6 evaluation trials, and a catch trial (Figures 8-2 and 8-3). During the first three training trials he received visual feedback concurrent with the cortical stimulation feedback and used it to explore the state space and understand the stimulation feedback. During the following three training trials he received only cortical stimulation feedback. The first two trials lasted for 45 seconds each, while the remaining trials lasted for two minutes each, as the subject thought that 45 seconds was too short. We started with amplitudes of 1.75 mA and 2.0 mA, respectively for Stim 1 and Stim 2 for Subject 2 based on his own qualitative report that they were discriminable. During the task we increased the stimulation amplitudes twice based on the subject's feedback to maintain discriminable stimuli (Table 8-2). In one case, Subject 2 also noticed a beat or rhythm to the

stimulation sensation and wondered if we could change the rhythm of one of the waveforms to make them more easily discriminable. We believe he was noticing the ITI and therefore decreased the ITI of Stim 2, the more intense stimulation, from 800 ms to 400 ms while maintaining its increased amplitude over Stim 1 (trials 13 and 14, Table 8-2). We notified the subject of this change before he began Trial 13.

We defined the fraction of time spent inside the target region as the subject’s accuracy level. In 11 of the 13 non-catch trials Subject 2 performed above chance level in accuracy (Figure 8-2), the two lower performances being the first two trials. During the catch trial, which used the same stimulation feedback regardless of the state, the subject’s accuracy dropped to below chance. In quantifying the subject’s path we also considered the R^2 value as a measure of the goodness of fit of the subject’s hand motions to the ideal path. Similar to the accuracy levels, the subject’s R^2 values generally increased during the training trials and fell below chance levels during the catch trial (Figure 8-3). During trial 13 Subject 2’s R^2 value dropped to just over chance, as he had trouble finding the target region for the first half of the trial and made large deviations out of the target region during that time (Figures 8-1b and 8-3).

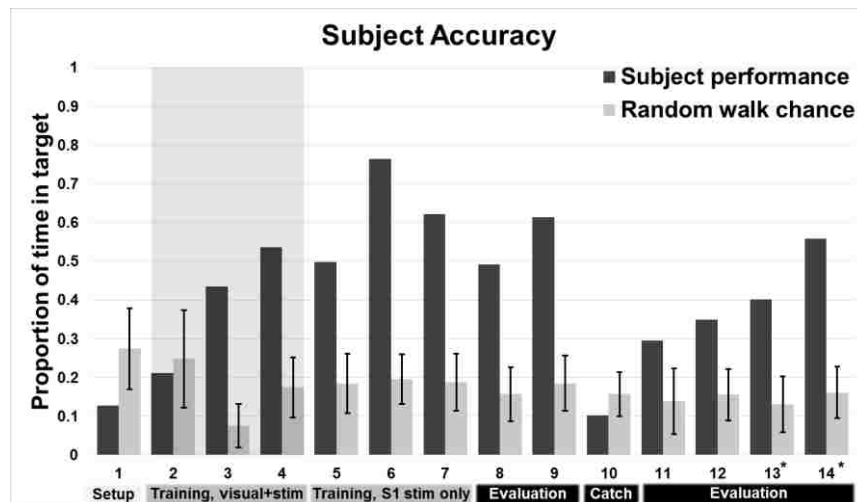


Figure 8-2. Subject 2’s accuracy levels as a measure of performance

Accuracy was calculated as $(\text{samples inside target range})/(\text{total samples})$ while chance levels were determined with 1,000 simulated random walks. Mean chance accuracy values with error bars for the standard deviation are displayed. The subject’s accuracy is above chance level for 11 of the 13 non-catch trials. During the setup trial the subject had trouble mapping the cortical stimulation to the necessary motor response, but used the following 3 training trials with concurrent visual and stimulation feedback (shaded, trials 2-4) to explore the state space and learn to use the feedback. His accuracy dropped to below chance levels during the catch trial (same stimulation feedback regardless of the state) suggesting that he was relying on the cortical stimulation to achieve a high performance. Table 8-2 lists the stimulation amplitudes and ITIs for each trial. *Trials 13 and 14 used a shorter ITI for Stim 2 than the previous trials.

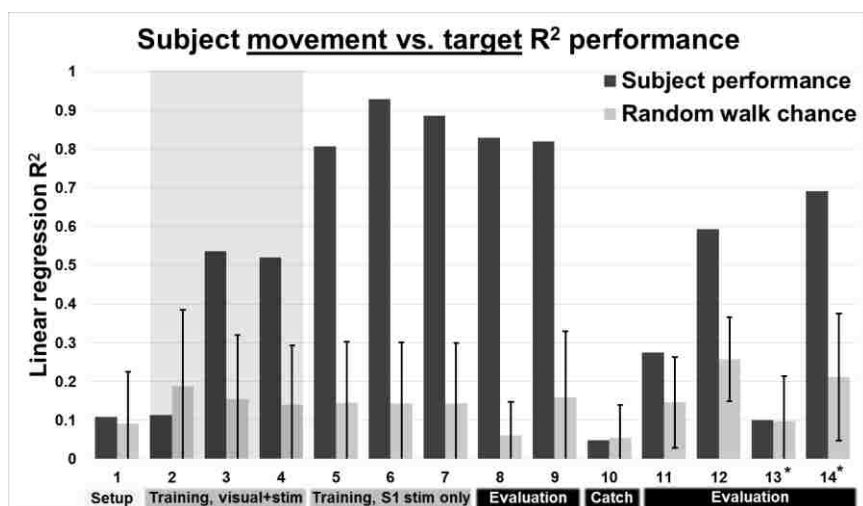


Figure 8-3. Subject 2's R² values as a measure of performance

Shaded trials 2-4 used concurrent visual and cortical stimulation feedback. Chance values were simulated with the random walks used for the accuracy chance calculations. Mean chance R² values with error bars for the standard deviation are displayed. The R² values follow a trend similar to the accuracy values (Figure 8-2), and considered together the accuracy values and the R² values can illustrate the subject's overall performance. In trials with high accuracies and high R² values, the subject slowly opened and closed his hand and remained relatively close to the target region even when he exited it. In trial 13, with a low R² value and higher accuracy, the subject deviated largely from the target region while searching for it (Figure 8-1b), and then eventually found and followed the path increasing his accuracy but not his R² value. Again, Table 8-2 lists the stimulation amplitudes and ITIs for each trial. *Trials 13 and 14 used a shorter ITI for Stim 2 than the previous trials.

The two other subjects that participated in this task had poor performances as measured by accuracy and R² values. Subject 1's and Subject 3's accuracies ranged from 0.1133 to 0.6446 and 0.0945 to 0.6533, respectively (Figures 11- 1 and 11-4). Their R² values ranged from 0.0442 to 0.1505 and 0.0006 to 0.7927, respectively (Figures 11-2 and 11-5). For Subject 3 these values include trials with visual feedback, and for both subjects their performance was often near chance for trials without visual feedback. Their complete results are included in the Appendix 2.

8.4 Discussion

Using feedback from cortical sensory stimulation alone, one of our subjects (Subject 2) was able to continuously modulate his motor output to follow the aperture target path and perform well above chance. Two other subjects (Subjects 1 and 3) were behaviorally unable to achieve high performances in the task, and we were not able to complete enough trials with them to comment on learning.

Subject 2

Subject 2's performance, as measured by accuracy and R² values, had a generally increasing trend during the training trials. The first two training trials, which included concurrent visual and

cortical stimulation feedback, may seem to have surprisingly low performances; however, the subject used these trials to explore the aperture space and stimulation states rather than trying to follow the exact path. This subject's first two evaluation trials have lower performances than the max training performance, likely due to the use of new and unknown target paths for each evaluation trial. During the catch trial, when the subject received the same stimulation in all states, the performance levels dropped to below the chance values suggesting that the subject had been relying on the varied cortical sensory stimulation to complete the task. In the non-catch trials, the subject must have been able to discriminate between the two stimuli in order to find and follow the target path and achieve a high performance. The discriminability of stimulation waveforms was demonstrated in previous work that varied the current amplitude and the pulse frequency [110]. The subject's performance in the post-catch trials did not jump back up to pre-catch levels, because as Subject 2 expressed, the catch trial confused him and he was attempting new methods of completing the task.

Subjects 1 and 3

Working with human subjects who have recently undergone neurosurgery presents various challenges, including transiently reduced attention levels and cognitive abilities. Additionally, our stimulation studies require that subjects be back on their anti-epileptic medications before participating, which limits the amount of available study time. We did not have time to test many stimulation patterns or stimulation to aperture state mappings with these subjects, so we cannot say whether the task was simply too challenging, or whether both Subjects 1 and 3 would have struggled with any tasks during that period of time. Additionally, both subjects became fatigued during this task so we were unable to determine whether the subjects would have learned the task with more time.

It is clear that this task requires complex attention, is not completely intuitive, and is sensitive to fatigue. These limitations are lessons for future somatosensory stimulation experiments. More research will also need to be conducted to determine how subjects can best learn to use cortical stimulation feedback. We also see the need for a method to assess task comprehension and attention. Such a validity measure would allow us to only proceed with a task if the subject was attentive enough to warrant participation.

Performance Measures

Taken together the two measures of performance, accuracy and R^2 , can highlight different behavioral responses. Accuracy levels reflect the percent of time that the subject remains within the target region, but do not capture how large the subject's deviations are when they leave the target region. In contrast, R^2 values take the size of the subject's deviations into account, but do not directly measure whether the subject was inside the target region. One explanation for high R^2 values with low accuracy levels (e.g., the subject follows the target path, but often remains just outside of the target region) is that the subject has substantial knowledge and expectations of the pattern of the target path, but does not completely understand how to use the stimulation feedback to re-enter the target region. We do not see such a relationship between the accuracy levels and the R^2 values in Subject 2's results. In fact, we see the opposite relationship (high accuracy relative to the R^2 value) in trial 13 (Figure 8-1b).

In this instance, the subject started losing the ability to discriminate Stim 1 and Stim 2 and thus had trouble finding the target region. For the first half of the trial he opened and closed his hand in large motions throughout the entire aperture range ‘feeling’ for the target region. When he eventually found that region, he was able to follow the path for the remainder of the trial. This increased his accuracy level, but due to the large deviations from the ideal path made at the beginning of the trial, his R^2 value remained low.

Adaptation

During our work with these subjects, we noticed that there appeared to be an element of adaptation or habituation to the stimulation signal over time, consistent with previous observations in cutaneous vibrotactile stimulation in humans in which the perceived stimulation intensity on the subjects’ fingertips decreased over time [216]. All three subjects, at various points in the experiment, expressed that the two stimulation sensations were becoming hard to discriminate, thus making the task more difficult. In response, we increased one or both current amplitudes and the difference between the two amplitudes for Subjects 2 and 3 (Table 8-2). The differences in stimulation amplitude that we used are similar to those reported in previous work which demonstrated that human subjects can qualitatively recognize differences in ECoG stimulation current amplitudes as small as 0.4 mA [110]. However, this prior work used different stimulation parameters (e.g., phase widths, pulse frequency, train duration, and ITI) than we did, so the results cannot be directly compared.

As in some cutaneous vibrotactile studies, one may be able to exploit adaptation to enhance subjects’ discrimination between two similar stimuli [217,218]. Specific experiments to study the timing and nature of this adaptation and the just noticeable differences of stimuli will need to be considered. Due to our time limitations we chose to have subjects self-report discriminability, but future experiments could use established psychometric tests [219–222] to quantitatively measure discriminability and assess changes over time and how the degree of discriminability affects task performance.

Pulsed Feedback

We chose pulsed feedback with an inter-train interval of 400-800 ms (Table 8-2) for two primary reasons. First, we wanted to minimize the risk of stimulation-induced seizures, and felt that continuous stimulation increased that risk. Secondly, we chose to use a sufficiently long ITI in order to potentially pull out ECoG recording data between stimulations. This time-division multiplexing (TDM) of the stimulation and recording periods could be used in a closed-loop BCI to allow for tactile feedback without obscuring all neural recordings of motor intention with a stimulation artifact [223]. After removing the stimulation artifact from the ECoG recording we believe that our ITI still leaves enough time for meaningful motor decoding based on our previous experiments which generally use 200 ms windows for decoding. We will test whether these ITIs are sufficient for quality motor decoding in future experiments.

Closed-loop BCI Application

Along with the use of TDM, we developed this task to resemble the tactile feedback that one could receive in a closed-loop BCI. For example, a prosthetic hand could have three states that

signaled: Case A) when the subject was not touching an object (no stimulation, Stim 0); Case B) when the subject was grasping the object with enough force (Stim 1); and Case C) when the subject was grasping the object too tightly (Stim 2). Ideally, more positions or grasp states would be encoded, but they could follow this pattern of increasing stimulation intensity as the tactile input became more intense, as in tightening one's grasp on an object. This paradigm represents a simplified feedback strategy and provides a framework for the development of future approaches.

Stimulation Percepts

Recently there has been a discussion of whether tactile feedback for BCIs will need to be biomimetic [60]. One argument holds that BCI applications may be able to use sensory substitution and thereby elicit abstract sensations that the user will substitute for normal tactile sensations. Users may map the abstract sensation to a normal sensation and no longer perceive it as abstract [122]. Alternatively, another argument holds that only biomimetic feedback will allow subjects to regain the sort of dexterous movement and tactile sensations that normally occur [121,224]. The basis for this argument is that naturally occurring tactile and proprioceptive sensations are so varied that the only way to encode all of them in a meaningful way will be to create biomimetic sensations through stimulation so that users don't have to create a new representation and mapping of abnormal sensations. With just three subjects, this study does not allow us to speculate on whether sensory substitution will suffice, but we did find that Subject 2 was able to use the abstract sensation to achieve performances well above chance with three defined states. Similar tasks using cortical sensory stimulation on human subjects will provide more insight into users' needs and a better understanding of the number of states that may be encoded with abstract sensations before biomimicry is required.

To our knowledge, the results presented here represent one of the first demonstrations of using cortical surface (ECoG) stimulation of the human sensory cortex to perform a motor task. We believe ECoG stimulation will offer new avenues for investigating haptic feedback, as ECoG electrodes allow us to directly stimulate the somatosensory cortex of awake human subjects who can describe the sensation and any differences between two stimuli. Our study demonstrates that subjects can react to cortical sensory stimulation, and while it may require increased attention or cognitive abilities, one subject was able to continuously modulate his motor behavior in response to the stimulation feedback. Although this task was not optimized, the subject was able to use the abstract feedback from cortical stimulation and map it to a new task demonstrating a proof of concept for the use of ECoG somatosensory stimulation for motor task feedback. Future experiments will explore the relationship between stimulation parameters and humans' perceptions of the stimulation to begin to establish a basis for cortical stimulation waveform development. Ideally such research will compile psychophysical data for human responses to ECoG stimulation just as has been done in non-human primates with ICMS stimulation [181]. Our results demonstrate how ECoG stimulation may be used as a tool to further understand tactile and proprioceptive encoding for closed-loop BCIs in humans.

9 Conclusion

9.1 Review of Findings

Early work from our lab on DCS of the somatosensory cortex demonstrated that humans can differentiate S1 DCS with either varied frequency or varied amplitude [110]. Building on this work we have: i) examined the psychophysics of DCS including subjects' perceptual thresholds and just-noticeable differences; ii) revealed that subjects' response times to S1 DCS are slower than those for haptic stimuli; iii) demonstrated that S1 DCS can evoke a sense of ownership over an artificial limb; and, iv) evaluated subjects' ability to use S1 DCS as feedback in a motor-based task.

Beginning with our study on the psychophysics of S1 DCS we confirmed prior reports from ICMS and high-density ECoG studies that neither amplitude, PW, PF, nor charge delivered can predict near-threshold perception alone [138,139,181]. However there is a relationship between the charge per pulse required to reach subjects' perceptual thresholds and the PW and PF, which suggests that we can design efficient stimulation waveforms to elicit a conscious percept with as little charge as possible. Specifically, lower pulse widths and higher pulse frequencies were found to require less charge per pulse to elicit a conscious percept during S1 DCS. This relationship between decreasing PW or increasing PF, and decreasing perceptual charge thresholds has been reported previously in psychophysical studies of ICMS of S1 in non-human primates [181], ICMS of barrel cortex in rats [191], and retinal microstimulation in humans [192], but to our knowledge had not been confirmed in human S1 DCS studies.

In the same study of S1 DCS psychophysics, we also demonstrated that although the charge delivered affects subjects' perceptions of DCS, DCS percepts are not solely dependent on charge and subjects can discriminate between S1 DCS trains with the same total charge, especially when the amplitude is changed. Our results from one subject also suggest that amplitude may be the predominant parameter in the subjective experience of intensity. We only completed the charge discrimination study in two subjects, and for one of those subjects our results suggest that we did not use large enough changes in the DCS parameters to create any DCS trains with substantial perceptual differences. Thus, this experiment should be conducted on more subjects to build a better understanding of the effects of total charge delivered in a DCS train on subjects' perceptual experiences. In the future, knowledge of how charge delivered affects subjects' percepts will guide our design of stimulation waveforms that can elicit unique percepts.

Next, during our study of human response times to S1 DCS, we found that subjects respond significantly slower to S1 DCS stimuli with varied train durations than they do to haptic stimuli applied to the hand. As humans generally respond faster to tactile feedback than to visual feedback [200], and as we desire somatosensory feedback in neuroprostheses to improve the function of BCIs over visual feedback alone, this increase in the response time to S1 DCS is both interesting and somewhat concerning for the future of DCS in BBCIs. At a minimum, our findings have implications for how we develop BBCIs in the future as we will need to consider the latency between measuring a sensory event (e.g., applied pressure on the fingertip of a

prosthesis) and a subject perceiving that sensory event following stimulation. Moreover, our results suggest that further research on the perception of S1 DCS and how DCS activates the underlying neural tissue is required to design stimulation waveforms that will elicit conscious perception as quickly as possible.

After our discussion of the psychophysics of S1 DCS and response times to DCS, which established that humans can perceive DCS of the hand somatosensory cortex, we demonstrated that S1 DCS can also evoke a sense of ownership over an artificial limb [137]. This is a promising result, as evoking a sense of ownership over a prosthesis will likely improve users' experience of a BCI and may also have psychosocial benefits such as improving users' confidence in using their prosthesis to interact with their environment and others [208].

Finally, in an experiment designed to test subjects' ability to use S1 DCS as feedback (the aperture task) we demonstrated that subjects can react to DCS of somatosensory cortex, and one subject could successfully use it as feedback in a motor task. However, the fact that two of the three subjects were unable to complete the full study suggests that it may require increased attention or cognitive abilities and that DCS may not be a trivial feedback signal to learn. We cannot say whether the task design or the DCS itself made this task difficult to complete, but do know that subjects thought certain changes to the stimulation waveform (i.e., increasing the current amplitude and changing the ITI) made the task easier. Importantly, we did not test subjects' just-noticeable differences prior to completing the aperture task, so it is possible that the subject who performed best had a smaller amplitude JND than the other two subjects and was thus able to notice a more substantial perceptual difference in the stimulation trains. This demonstrates the need to conduct basic psychophysical tests before conducting more complicated tasks with S1 DCS.

Although our results from the aperture task suggest that DCS may be a nontrivial signal to learn, there is evidence from other studies that sensory feedback can be learned. In humans, cochlear implant users improve their performance on speech perception tests over time (ranging from three months to two years) as they get better at interpreting the signal [95,97]. In S1 ICMS studies in rodents and non-human primates, subjects have learned to use somatosensory feedback to interpret novel patterns and their performance can improve with practice [122–124]. Studies have also demonstrated that humans and non-human primates alike can learn and adapt to using a motor-based BCI [29]. Subjects' ability to learn to control a BCI and improve their performance suggest that in the future we may be similarly able to improve a subject's performance with S1 DCS-based feedback. Due to our experimental time constraints we were unable to test subjects' ability to improve their performance on the aperture task over a substantial length of time, but future research with humans with chronic ECoG implants could enable such studies.

The results from the rubber hand illusion experiment and the aperture task are especially interesting when viewed in light of the abstract nature of the S1 DCS via macro-ECoG electrodes. As explained previously (Chapter 5), DCS of somatosensory cortex using our clinical macro-ECoG grids, elicits percepts that subjects often describe as “hardly”, “partly”, or

“moderately natural.” How useful such abstract sensations can be in future BBCI applications that require seamless integration into everyday tasks is still unknown, but it is promising that these abstract sensations were able to elicit a sense of ownership (two subjects) and be used as feedback in a task (one subject).

Researchers in the field of BCI sensory feedback discuss two general approaches to generating useful sensory feedback: biomimicry and adaptation [60]. The argument for biomimicry holds that only biomimetic feedback will allow subjects to regain the sort of dexterous movement and tactile sensations that normally occur [121,224]. The basis for this argument is that naturally occurring tactile and proprioceptive sensations are so varied that the only way to encode all of them in a meaningful way will be to use stimulation methods and parameters that cause neural activity as similar as possible to the natural neural response to a given stimulus. The adaptation approach holds that applications may be able to use sensory substitution and elicit abstract sensations that the user will substitute for normal tactile sensations over time. Users may map the abstract sensation to a normal sensation and no longer perceive it as abstract [122]. DCS via ECoG electrodes will fall into the adaptation category of sensory feedback approaches, as the stimulation does not activate normal neural pathways of sensory information flow. The ability to induce a feeling of artificial limb ownership during the RHI experiment and use of S1 DCS to perform a motor-task supports the idea that subjects will be able to learn to interpret and use the abstract sensations elicited by S1 DCS even though DCS, especially via macro-ECoG electrodes, does not evoke a biomimetic neural response.

9.2 Limitations

Working with human ECoG subjects has a number of advantages that we have discussed. Namely, humans’ capacity to tell us exactly what they feel or perceive following S1 DCS and our ability to work with subjects who have a clinical need for acute ECoG giving us access to more human subjects than we could have for research purposes alone. However, there are also several limitations of working with clinical macro-ECoG subjects including the fact that future BBCI devices are unlikely to use the low-density, clinical ECoG arrays used in the experiments presented here. Rather, future devices will more likely use high-density electrodes, perhaps even higher-density than what is currently available for human studies. Higher-density electrodes could potentially target a more focused tissue volume and create percepts with a smaller and more controllable receptive field. To do so however, researchers will need to engineer a device that can output enough current to generate a percept without causing damage by creating too high of a current density across a small electrode surface area [180]. New developments in intracortical microelectrodes could also feasibly overcome the obstacle of initiating an inflammatory response and allow for long-term intracortical recording and stimulation capabilities. Due to the physics and physiology surrounding cortical electrical stimulation (see Introduction, Stimulation Physiology), it is more likely that penetrating microelectrodes will be able to target the deeper proprioceptive areas (e.g., area 3a in S1) than surface electrodes. New developments in high-density electrodes or intracortical electrodes without an inflammatory response could make DCS via macro-ECoG arrays obsolete in the field of BBCIs.

This raises the question as to whether or not research on DCS using macro-ECOG arrays is still beneficial. We reason that because certain aspects of cortical electrical stimulation seem to be maintained across modalities (e.g., the relationship between perceptual charge thresholds and pulse frequency or pulse width), it is probable that other aspects of macro-ECOG DCS will be similar across modalities as well. Thus, we argue that studying the principles underlying human perception of electrical stimulation in a modality that is widely available holds importance.

Another limitation of working with clinical epilepsy patients is that they have a neurological disorder that is not what we are primarily interested in studying. All of the subjects who participated in these studies underwent acute monitoring with ECOG arrays because they had medically intractable epilepsy. We expect that all of our subjects had neurotypical somatosensory processing because their epileptic foci were not in the somatosensory cortex, but we cannot rule out the possibility that their epilepsy or a comorbidity affected our results. Indeed, the fact that we expect our subjects to have neurotypical somatosensory processing sets them apart from the group of individuals with sensorimotor deficits that we hope to help with a somatosensory-enabled BBCI. We therefore cannot guarantee that the findings presented here will translate directly to people with sensorimotor disorders; however, recent results in S1 stimulation in several people with tetraplegia suggest that cortical electrical stimulation does and will work in those with a sensorimotor disorder or impairment [130,131]. Related to subjects' clinical care, subjects' perceptual experiences of S1 DCS may be affected by the medications that they are taking including pain and anti-epileptic medications and/or their relative level of arousal. Based on our observations during psychophysics experiments with several subjects, we suspect that subjects' level of arousal and their pain medication affected their perceptual thresholds. However, it is not clear whether neurological changes directly affected their ability to perceive S1 DCS, or if arousal and medication effects simply changed their level of attentiveness and engagement with the task, affecting their performance.

9.3 Future Work

The results presented here demonstrate that DCS and other forms of cortical electrical stimulation (e.g., ICMS) can be used to create somatosensory percepts that could be beneficial as feedback in a BBCI. However, none of the devices or methods used in the studies that we have discussed here are ready for non-research, home use as part of someone's standard of care or daily life. Significant future work remains to be done to develop a BBCI that can function in an uncontrolled, variable, and noisy environment.

Future work could include continued exploration of DCS parameters and their effects on perception, consideration of how to provide multiple channels of feedback, and experiments with chronic implants to investigate how subjects' S1 DCS perception may change over time. Researchers should also consider how S1 DCS is integrated with other sensory cues including visual cues, to better understand how a BBCI may perform in a non-controlled setting. Throughout continued experiments, researchers should consider how subjects' neural signals recorded from the somatosensory cortex and other cortical areas may relate to DCS perception. These future research ideas are briefly outlined below. Another question we must consider regarding the development of rehabilitative BBCI devices, and one that will be discussed more

in the Ethical Considerations section of this chapter, is: at what point will the performance and benefits of a BBCI as compared to the standard of care outweigh the risks associated with implanting and using a BBCI? Some of the research ideas outlined below could help the scientific community address these questions and develop a BBCI with substantial benefits over the inherent risks of implanting a device.

Further DCS Parameter Exploration

Here we presented human psychophysical results which focused on manipulating the current amplitude, pulse width, and pulse frequency of S1 DCS trains. We did not exhaust the space of parameter combinations that could be tested, nor did we consider the psychophysical effects of certain stimulation parameters, including the train duration. With more data on the effects of stimulation parameters on subjects' perceptual experiences, we may be able to model this relationship as has been done for human retinal stimulation [192].

Train Duration

In the psychophysical studies presented in Chapter 5 all of the DCS trains had a duration of approximately 200 ms. Surprisingly, Libet et al. [112] found that the average minimum train duration for a perceptual response was about 500 ms when using liminal or near-liminal current amplitudes. This is of course in contrast to our observation that 200 ms DCS trains often elicit a tactile sensation and at times 100 ms trains can as well (Chapter 6, Response Timing). Ray et al. have also found that using ECoG grids, bipolar stimulation trains can be as short as 250 ms, and that shorter trains require a higher current amplitude for perception [113]. There are several possible reasons for these differences. Libet et al. did not use ECoG grids, and used primarily monopolar, monophasic stimulation rather than bipolar, biphasic stimulation. Their choices of pulse width and pulse frequency, often longer and slower, respectively, than what we typically use, could also contribute to the observed differences.

Prior work has also considered the relationship between train duration and pulse frequency. Kim et al. observed a decrease in the train duration necessary for perception of ICMS in non-human primates when pulse frequency was increased and other parameters were held constant [181]. Libet et al. also found that in humans within the range of pulse frequencies tested (between 15 Hz and 240 Hz), utilization train durations tended to decrease as frequencies increased [112]. It is possible that just as we and others [181,191,192] have found that the threshold charge per pulse decreases with increasing frequency, the threshold charge exchange (total charge delivered in the train) may also decrease allowing for a shorter train duration with higher pulse frequencies. Continuing to consider how train duration and the number of pulses affects perceptual responses could provide a more complete picture of the psychophysics of S1 DCS and direct the design of more efficient stimulation waveforms.

Pulse Width

Thus far in our work we have manipulated the pulse width of S1 DCS waveforms to assess the resultant perceptual current thresholds, but we have not fully explored how PWs may influence a subject's percept. The single subject in a micro-ECoG S1 stimulation study by Hiremath et al. reported two distinct sensations for 200 and 400 μ s pulse widths [111]. In contrast, Lee et al.

reported that in nine subjects an increase in PW produced an increase in the perceived strength of the sensation more often than a different percept quality [139]. Models of retinal microstimulation suggest that different pulse widths and temporal stimulation patterns may stimulate different subpopulations of neurons thereby creating different percepts [192]. Continued study of the effect of PW on human perception of DCS could elucidate how we can manipulate stimulation parameters to create a range of discernable percepts.

More Complex Waveforms

Given the physics of cortical electrical stimulation and the location of proprioceptive locations (e.g., area 3b within the central sulcus), it will be difficult to target proprioceptive areas with DCS, as it is difficult to get enough current into deeper regions of the gray matter without activating more superficial layers. We have an ongoing collaboration with other research groups to model macro-ECOG DCS with the goal of selecting a set of electrodes for multipolar stimulation that will target a specific region of interest, such as area 3b.

In addition to potentially targeting specific cortical areas, more complex DCS patterns could alter subjects' perceptual experience of the waveform and possibly elicit more natural sensations. For example, we have begun testing subjects' response times to DCS waveforms with two pulses that are 1.5-2.5x the perceptual threshold followed by thirty-eight pulses (to create a 200 ms train duration) at a lower but still suprathreshold amplitude. Preliminary results suggest that subjects can respond faster to these high-low DCS trains than to constant-amplitude DCS trains that have an equal total charge. A DCS train could also model the stimulation patterns used by Tan et al. [69] when they elicited pressure and tapping sensations in two subjects via peripheral nerve cuff electrodes. In that work they used stimulation pulses whose pulse width varied based on a sine wave envelope [69].

Multiple somatosensory feedback channels

Considering rehabilitative BCI development with a wide lens, we need to ask how S1 DCS - or any type of cortical somatosensory feedback - will function in a future device. The work presented here and in other somatosensory stimulation studies in humans [109–111,130,131,137–139] has generally used a single channel of feedback (with one or two electrodes for monopolar or bipolar stimulation, respectively). While a single channel or axis of feedback could be helpful to some, one can imagine why multiple channels or axes of somatosensory feedback would be more useful. Consider trying to grasp a coffee cup. Typically, someone with an intact sensorimotor system would reach for and grasp the cup with an expectation of the tactile and proprioceptive sensations that will arise during this action. If the cup is unexpectedly light (perhaps someone drank all of your coffee), your sensorimotor system will register any slip or strain occurring at your fingertips and the sudden rising of your arm as you applied more force than necessary to lift the lightweight cup. Your body can respond to this unexpected result by comparing an efference copy of your expected sensations to the afferent input representing the sensations that actually occurred [75,225]. Usually mismatches between predicted and actual somatosensory signals can be responded to by adjusting load or grip forces about 100 ms after contact [52]. Stimulating cortical somatosensory areas may not enable this correction process, especially considering the S1 DCS response times of 254 ms to

528 ms that we reported here. Even if we accept the slow response times and determined exactly what stimulation parameters could elicit a wide range of uniquely discernable percepts, we would still need to determine how to map tactile events to stimulation trains in a way that users can interpret or learn. The information relayed from afferents in our fingertips is not simply reflective of a two-dimensional grid of mechanoreceptors which are either making contact or not with an object. Incorporated in that signal are responses from more remote points of contact that are due to skin stretch and strain that provide the user with a complete picture of their interaction with an object [52]. Thus, although a single channel of somatosensory feedback such as those studied here could be useful in conveying a single axis of information (e.g., total grasp force applied to an object), more channels will be needed to convey additional spatial information about contact location and varying forces [72].

Chronic implant experiments

As discussed, a limitation with our research is the short period of time over which we can run stimulation studies with patients implanted with ECoG arrays for clinical treatment of epilepsy. Recently, a study with S1 DCS via high-density ECoG arrays was conducted in a subject with a brachial plexus injury for research purposes [111]. Although this study was limited to 28 days, it demonstrates the potential for conducting longer-term S1 DCS studies in humans. Longer-term studies could allow researchers to study how subjects adapt to DCS over time, including if subjects experience a change in their perceptual thresholds or just-noticeable differences. This is critical information for creating a functional BBCI as any changes in perception would have to be accounted for perhaps with a calibration process.

Longer-term studies could also provide the opportunity to evaluate how attention and noisier, more natural environments will affect S1 DCS perception. It is possible that the perceptual thresholds that we and others have measured during relatively well-controlled experiments, will not translate directly to daily use in a noisier environment. A study of ICMS in the barrel cortex of freely behaving rats reported that perceptual thresholds may increase in behaving animals as compared to studies with head-restrained animals [226].

Multisensory considerations

During the review of the relevant somatosensory physiology in the Introduction, I mentioned that higher-level cortical areas integrate somatosensory information with that from other sensory receptors to form our perception of incoming stimuli [72,86,209,227]. The rubber hand illusion experiment (Chapter 7) demonstrated that DCS can integrate with visual cues to form a cohesive perceptual experience and evoke a sense of ownership over the artificial limb [137]. Besides that experiment, however, our other results were obtained without congruent visual information. During the blindfolded response timing experiment (Chapter 6) subjects did not have any visual information, and during the psychophysics experiments (Chapter 5) subjects had incongruent visual and tactile information. They felt a percept on their hand due to the S1 DCS without seeing the congruent visual cues one would expect with tactile perception. Previous research on multisensory integration suggests that such incongruent cross-modal sensations may impair performance [228,229].

Researchers could conduct experiments to probe how visual cues affect subjects' perception and performance on tasks with S1 DCS feedback. During our RHI experiment, one subject noted that his perception of the tactile sensation changed when the experimenter pressed straight down on the rubber hand rather than stroking the rubber hand, suggesting that visual cues can indeed affect S1 DCS percepts, but we have not explored this further. A better understanding of the interaction between S1 DCS, visual cues, and performance is essential to the development of BBCLs, as real-world applications will most likely involve the integration of intact vision and restored somatosensation.

DCS Perception and Cortical Signals

There is a vast literature on the conscious perception of sensory stimuli, but exactly how tactile stimuli are consciously perceived – even when arriving naturally from peripheral afferents – is not fully understood. A number of studies agree that low alpha power (8-14 Hz) in local, task-relevant areas (e.g., somatosensory cortex) precedes correctly perceived stimuli. This observation is often explained with the idea that strong alpha power reflects functional inhibition which would impede conscious perception of a stimulus [230]. Studies have also demonstrated alpha-band suppression following spatial attention cuing prior to a tactile stimulus [231]. van Ede et al. demonstrated alpha- and beta-band suppression in subjects' contralateral sensorimotor areas after spatially orienting to an upcoming tactile stimulus on either the left or right hand [232]. This study also found that beta-band suppression over the contralateral sensorimotor cortex was associated with faster response times to a tactile stimulus, but not to trial accuracy [232]. The authors speculate that the observed alpha- and beta-band suppression may represent a neural desynchronization that could enable selective gating between S1 and S2 (the primary and secondary somatosensory areas) [232]. However, there is also evidence that alpha-band phase synchrony increases in task-relevant regions in attention tasks with concurrent local amplitude suppression [233].

Prior work in ECoG found that modulations in high-gamma activity (60-150 Hz) were correlated with the subjects' attentional states. Specifically, high-gamma activity was greater over somatosensory cortex when subjects were attending to vibrotactile stimuli [234]. Similarly, Bauer et al. found an increase in gamma-band (60-95 Hz) activity over contralateral somatosensory cortex when attention was cued to the left or right hand, but this increase in gamma-band activity appeared approximately 100 ms after the tactile stimulus onset [235]. Similarly, Muller et al. demonstrated that high gamma activity following S1 DCS via high-density ECoG arrays in humans was well correlated to conscious perception of the DCS stimuli. Continued study of the relationship between cortical signals and DCS perception could reveal a brain state that is more conducive to stimulation than others and generate a method of timing the delivery of S1 DCS to increase the likelihood of conscious perception.

9.4 Ethical Considerations

Before closing we will review some of the ethical considerations that should be reflected on as we research and develop cortical stimulation devices and BBCLs. A more thorough discussion on neuroethics and the current state of research in this field can be found in [236–239]. As mentioned earlier, as we develop BBCLs and the technologies that will enable them, we must

consider how the benefits of such devices will compare to the risks associated with implantation [238] or other neurophysiological and/or psychological consequences [237]. Psychological consequences could include anxiety, depression, and changes to self-perception, or other adverse reactions that we are not currently aware of [238–240]. Importantly, we must also consider how the benefit-risk ratio will differ by individuals for any number of reasons including their degree of impairment or perceived impairment. For example, a 2015 survey of people with tetraplegia demonstrated that their interest in different BCI control types varied depending on the level of their injury [241].

Neuroethics research has identified several other areas of concern or issues that must be considered in addition to the notion of the benefit-risk trade off. First, there is concern of how BCIs may affect a user's sense of self and their autonomy [237,239]. Drawing from the more extensive research and experience with DBS for treating neurological disorders, a small proportion of patients can develop unwanted side effects that affect their identity including changes to their personality and unhappiness [238]. In a study of people undergoing clinical trials using DBS for treatment of depression and obsessive-compulsive disorder, one participant's report points to concerns of identity and agency when using a BCI [242]:

"I've begun to wonder what's me and what's the depression, and what's the stimulator. I mean, for example, I can be fine, and then all of a sudden... and, and I might realize it later, I do something socially or interpersonally, just not right. I'll say something that is insensitive or just misread a person entirely, say something that either makes ME look like a fool, or, hurts them, or, something along that line. I can't really tell the difference. There are three things—there's me, as I was, or think I was; and there's the depression, and then there's depression AND the device and, it, it blurs to the point where I'm not sure, frankly, who I am" [242].

BBCIs for sensorimotor rehabilitation could create similar questions of autonomy and identity.

If we consider the general design of a BCI which records neural signals, decodes a user's intention from those signals, and then sends a command to an end effector to execute the user's intended action we can think of a situation in which some of the user's autonomy may be lost. Specifically, if a user decides to perform an action and a computer decodes that intention but then the user changes their mind, can the BCI refrain from executing on the initial intention or thought [237]? If not, then the user's prosthesis or end effector may perform an unintended action, and if the user has incorporated their end effector into their self image, they could feel that they themselves have unintentionally acted. There is concern that psychological challenges may arise if a user begins to doubt their own ability to intentionally control their (or their prosthesis') behavior or actions [237]. Along the same line, exactly when a person becomes consciously aware of their intent or desire to move is not fully understood. This leads to a debate as to who or what is really controlling the movement of a BCI end effector - is the user in control of the BCI even if it is decoding motor-related signals that arise before conscious awareness, or is the BCI in control, and how does this affect a BCI user's autonomy [237]?

Another neuroethics consideration deals with users' privacy and security when using a BCI. Breaches in privacy or security could be intentional and malicious or unintentional, such as

interference from external sources that disrupts a wireless BCI system [237]. A 2014 report outlined the potential threat posed to BCI platforms, including how a previous study used a commercially available, noninvasive BCI system to analyze users' brain signals and try to detect their 4-digit PINs, bank information, birth months, locations of residence, and their recognition of faces [243]. Besides the illicit behavior of trying to capture BCI users' private information, a BCI platform could also be hacked with the intention of interfering with the processing system to disrupt a users' intended actions, or create wholly unintended actions of the end effector [237].

As research into BBCIs continues, we must also consider the ethical implications of the consent process and the study design itself. When an individual with a neurological impairment or disorder is considering participating in research, we must take care to appropriately set expectations in line with the potential research outcomes. Prior work has reported that nearly two thirds of patients undergoing a trial testing the use of DBS for depression thought that they were receiving therapeutic treatment not participating in a clinical trial [238,244]. There are also questions of how to consent certain participants, if all people who could benefit from a BBCI have the capacity to consent to research, and how caregivers should be involved in the consent process [238]. For example, how should researchers approach people with locked-in syndrome for consent to research or therapeutic implantation if they cannot currently communicate with others? Furthermore, for certain studies caregivers may be highly involved with the research process, and the results of the research could have the potential to significantly alter the relationship between the caregiver and the BCI user by decreasing dependency [238]. Due to the complexities of the consent process and the time-varying nature of research and one's understanding or conception of the research, prior work has recommended viewing consent as a process rather than a single step and as such considering if re-consent is needed [238].

During BBCI development we must also consider how to deliver equal access to future devices, recognizing that such rehabilitative devices could be prohibitively expensive and possibly unattainable under our current healthcare system. During the research and clinical trial process itself, we must also address the fact that the financial incentives of device manufacturers may not lead to equal access by prioritizing certain neurological disorders for research (i.e., those that may have higher returns on investment), or inadvertently precluding people with the condition who cannot afford to participate in the clinical trial [237].

Finally, we have to consider what happens to users when a research study ends, a clinical trial is cancelled, or a neurotechnology company drops support of a device, especially if users have been implanted with a device. Consider, for example, the approximately 250 people who had experienced rehabilitative benefits from an implanted device by NeuroControl. The NeuroControl Freehand System was approved by the FDA in 1997 and used functional electrical stimulation of forearm and hand muscles to restore hand grasp function in people with tetraplegia (C5 and C6 level spinal cord injuries) [245–247]. Users controlled their grasp using movement of their opposite shoulder, so the device was only available to those with remaining shoulder control [245,248]. In 2001, the company decided to end production of the device to

focus on other technologies for larger markets, but went out of business several years later, leaving all of the users without device support or the option to replace failing parts or remove the device altogether [237,247,248]. Although this was legal, it was arguably unethical as it caused users undo stress, frustration, and possibly more significant psychological trauma. As John Mumford, a Freehand System user for over a decade, explained in a 2015 MIT Technology Review article, “To all of a sudden have that taken away—it’s incredibly frustrating. There’s not a day where I don’t miss it” [248]. Another Freehand user on an online users’ support group (set up by a researcher from the original project) wrote in 2017 that, “I’m still using my Freehand system every single day and can’t imagine how awful life would be without it. Such a shame they overstretched and went bust. Hope the original professor gets his patent back and gets an updated system back for the good of everyone who could benefit” [249]. Presumably that user has been using stockpiled parts to repair their device, as others have reported doing [248]. Former Freehand users have also reported concerns about whether or not the inactive device needs to be surgically removed [248,249]. As one online user wrote, “Been thinking about getting the device removed but was basically told the risk outweighed the benefits” [249]. This experience also calls into question the consent process and whether or not users need to be specifically informed of the potential for companies to fold and withdraw device support. One former Freehand user expressed that had he known that there was a chance that NeuroControl could go out of business he would not have gotten the implant [248].

Other recent clinical trials and research studies have raised similar concerns around how to ethically terminate studies that involve implanted neural devices. A study that began in the mid-2000s to address treatment-resistant depression using deep brain stimulation – the BROADEN trial – ended participant recruitment early after a double-blind, sham-controlled phase of the study failed to demonstrate a statistically significant difference between groups of patients [250]. However, 77 participants went on to complete a follow-up, long-term stage of the study, which was meant to last for four years but was also terminated early [250]. Of the 77 participants that completed the long-term phase, 48% had an antidepressant response within 2 years of active DBS stimulation and 25% achieved remission during that time. The authors defined “antidepressant response” as a 40% or greater reduction in score on the Montgomery-Asberg Depression Rating Scale (MADRS) [250]. Although the trial has ended, a reported 44 patients want to keep the implanted device [251]. Before beginning the study, the study sponsor, St. Jude Medical (acquired by Abbott Laboratories), had agreed to pay for either the cost of removing the implanted device or to supply rechargeable batteries at the end of the trial for those who wanted to keep the device. Yet, those 44 patients would still be responsible for costs associated with maintaining the device – possibly including additional surgeries which could cost tens of thousands of dollars [251]. Researchers and ethicists involved with or following this clinical trial worry that the cost of maintaining such a device could significantly burden patients and argue that moral responsibilities or obligations necessitate providing care beyond the length of a study [251,252].

Another recent report illustrates the possible emotional strain of ending a research study even at the planned time. As Graczyk et al. report, at the end of their study a participant who had been using a sensory-enabled prosthesis at home expressed his concern about losing the

sensation that he had become accustomed to: “Tonight’s my last night with it, when I come back, I gotta wear it another 3 weeks, but that’ll be without sensation. **That’s like losing your hand all over again!** [our emphasis]” [208]. The field will need to address how to ethically end research studies, perhaps developing guidelines or regulations; to begin, researchers could develop plans for enabling post-study access and explain those plans to potential study participants during the consent process [252].

10 Appendix 1 - S1 DCS Psychophysics

Additional perceptual threshold and psychometric curve figures

Additional figures are included here to illustrate the method of fitting psychometric curves to subjects' perceptual thresholding data and estimating a 79% perceptual threshold based on the best-fit Weibull function as explained in Chapter 5.

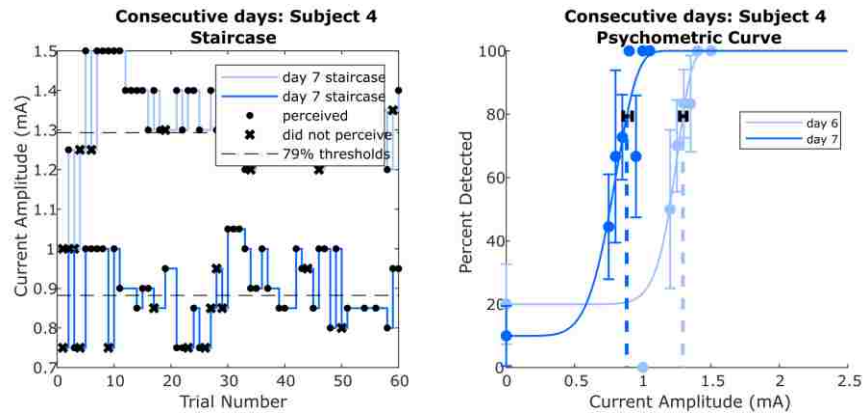


Figure 10-1. Another sample of perceptual thresholding staircases

Left: Subject 4 completed perceptual thresholding staircases with the baseline staircase (205 μ s PW, 200 Hz PF, 200 ms TD) two days in a row. Subject 4 had a significantly lower perceptual threshold on the second day of testing than on the first day ($p=9.999e-5$, permutation test). As in Figure 5-4, the double-interleaved 3-down 1-up staircases are merged together for each of the tested parameter sets for visualization. **Right:** Subjects' staircase results were fit with a Weibull function as described in Chapter 5 and Figure 5-4. Vertical error bars represent the standard deviation of the sample of yes/no responses. Black horizontal error bars represent the 68% BC_a confidence intervals around the estimated amplitude threshold (these are also provided in Table 5-3).

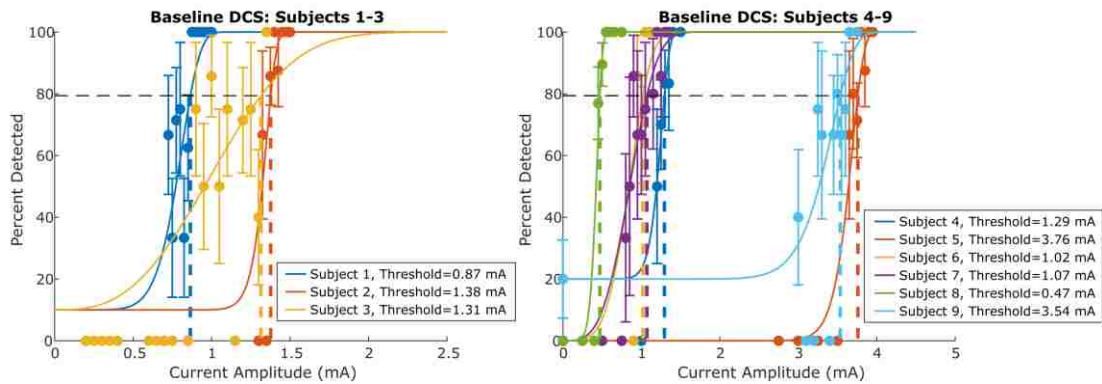


Figure 10-2. All subjects' psychometric curves for the baseline DCS train

Subjects' staircase results were fit with a Weibull function parameterized with a slope and threshold using a maximum likelihood approach to estimate their psychometric curves. Subjects 1-3 completed single staircases without any catch trials so we set the lower bound of the psychometric functions to an estimated false positive rate of 10%. Subjects 4-9 used a double-interleaved staircase consisting of two separate and interleaved 3-down 1-up staircases (as in Figure 5-1) with 5 catch trials each. We used subjects' catch trial results to set the lower bound of the psychometric functions to their false positive rate. Error bars represent the standard deviation of the sample of yes/no responses. Subjects' estimated thresholds and their 68% BC_a confidence intervals are provided in Table 5-3 and Figure 5-5.

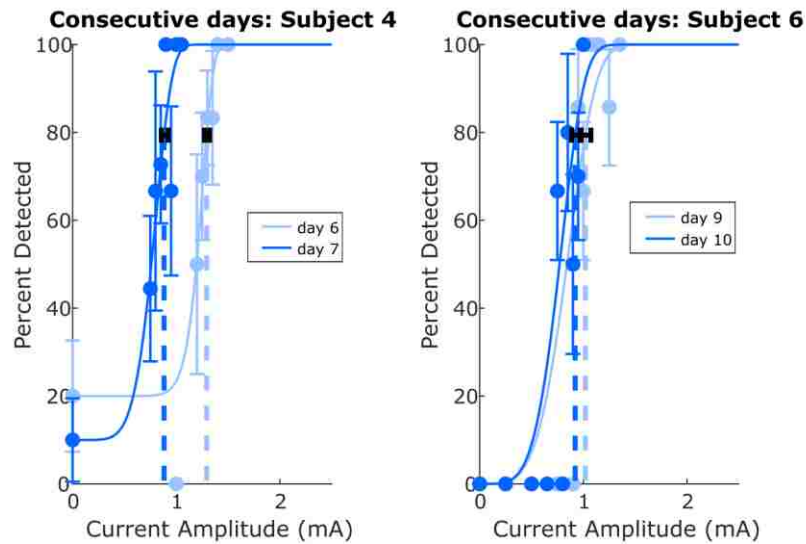


Figure 10-3. Perceptual thresholds for baseline DCS trains on consecutive days

Subjects 4's and 6's performances on two baseline perceptual thresholding staircases on consecutive days. Both subjects' perceptual amplitude thresholds decreased significantly from the first to the second day of stimulation. Horizontal error bars in black represent the 68% BC_a confidence intervals for the threshold parameter as estimated using a parametric bootstrap method. Vertical error bars represent the standard deviation. **Left:** Subject 4's 79% perceptual threshold decreased from 1.29 to 0.88 mA from days 6 to 7 post implant. **Right:** Subject 6's 79% perceptual threshold decreased from 1.02 to 0.92 mA from days 9 to 10 post implant.

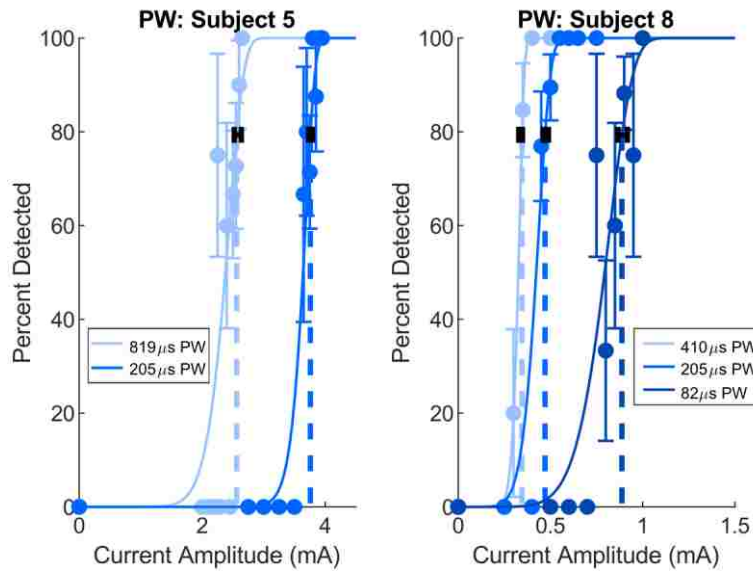


Figure 10-4. Perceptual thresholds for DCS trains with varied PW

Subjects 5's and 8's performances on two perceptual thresholding staircases with varied PW. Both subjects' perceptual amplitude thresholds increased as the PW decreased. **Left:** Subject 5's 79% threshold increased from 2.56 to 3.76 mA with a decreasing PW of 819 μs to 205 μs . **Right:** Subject 8's 79% threshold increased from 0.35 to 0.47 to 0.89 mA with a decreasing PW of 410 μs to 205 μs to 82 μs .

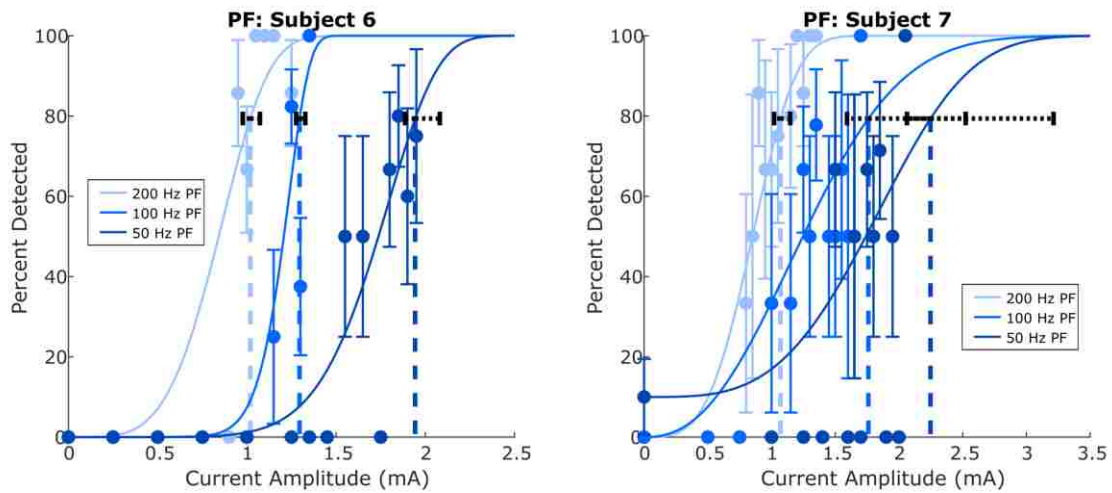


Figure 10-5. Perceptual thresholds for DCS trains with varied PF

Subjects 6's and 7's performances on perceptual thresholding staircases with varied PF. Both subjects' perceptual amplitude thresholds increased with decreasing PF. **Left:** Subject 6's 79% threshold increased from 1.02, to 1.30, to 1.94 mA for PFs of 200, 100, and 50 Hz, respectively. **Right:** Subject 7's 79% threshold increased from 1.07, to 1.76, to 2.25 mA for PFs of 200, 100, and 50 Hz, respectively.

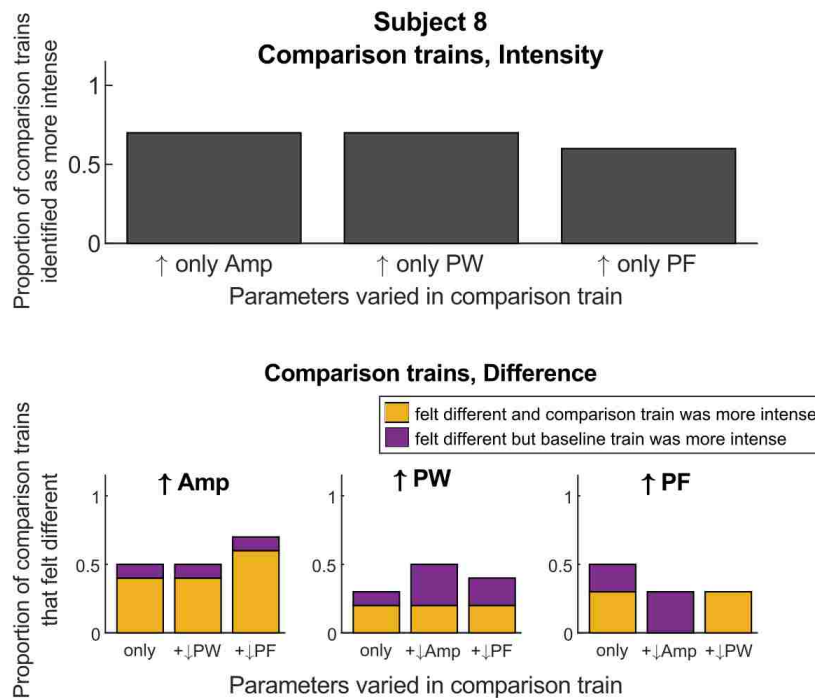


Figure 10-6. Charge discrimination results for Subject 8

The top row illustrates the subject's responses to the question of intensity (i.e., "Which train felt more intense?"). A higher proportion indicates that the subject frequently responded that the comparison train was more intense than the baseline train. The top row illustrates just the three baseline-comparison DCS train pairs in which only one parameter was altered and the charge was not conserved. The bottom row illustrates the subject's responses to the question of different (i.e., "Did the stimulation feel the same or different?"). Subplots are separated based on the parameter which was increased, with each bar representing either that parameter increased alone, or along with a decrease in one of the other two parameters. Yellow bars indicate the proportion of baseline-comparison train pairs which felt different from one another and the comparison train was identified as more intense, whereas purple bars indicate the proportion trains that felt different but in which the baseline train was more intense. Subject 8 did not respond with above chance levels to any of the questions, so we suspect that he was unable to reliably feel a difference in any of the stimulus trains.

Goodness of Fit

We used a previously described method to assess the goodness of fit of the Weibull function to our data [186]. Briefly, we fit our data to the Weibull cumulative distribution function defined as:

$$F(x; \alpha, \beta) = 1 - \exp \left[- \left(\frac{kx}{\alpha} \right)^\beta \right] \quad (1)$$

with

$$k = \left[-\log \left(\frac{1-t}{1-g} \right) \right]^{\frac{1}{\beta}} \quad (2)$$

where α is the threshold value, β is the slope value, t is the performance level at threshold (e.g., 79%), and g is the subject's false positive rate. The psychometric function was then defined as:

$$\psi(x; \alpha, \beta, \gamma) = \gamma + (1 - \gamma)F(x; \alpha, \beta) \quad (3)$$

After fitting the data to this function using a maximum likelihood estimation approach [186], we simulated a distribution of expected parameters with 10,000 Monte Carlo simulations using the best-fit function as the generating function. For the purposes of assessing goodness of fit, we considered the log-likelihood ratio, or deviance, between the model and simulated or empirical data. The resultant distribution of Monte Carlo-simulated deviances represents the deviances one can expect from an observer whose responses are binomially distributed according to the best-fit for Equation 3. An empirical deviance value that is greater than the 97.5th percentile of deviances would indicate overdispersion and a poor fit between the data and best-fitting psychometric function [186]. We also considered the correlation coefficient between deviance residuals and the probabilities predicted by the best-fit function which could indicate a linear relationship between the two. An empirical correlation coefficient outside of the 95% confidence interval for the distribution expected by chance could suggest that the functional model (i.e., F , Equation 1) is inappropriate for our data. Using these measures, all of our subject data was well fit by a psychometric Weibull function of the form in Equation 3 (see Figure 10-7 for representative data and Table 10-1 for values).

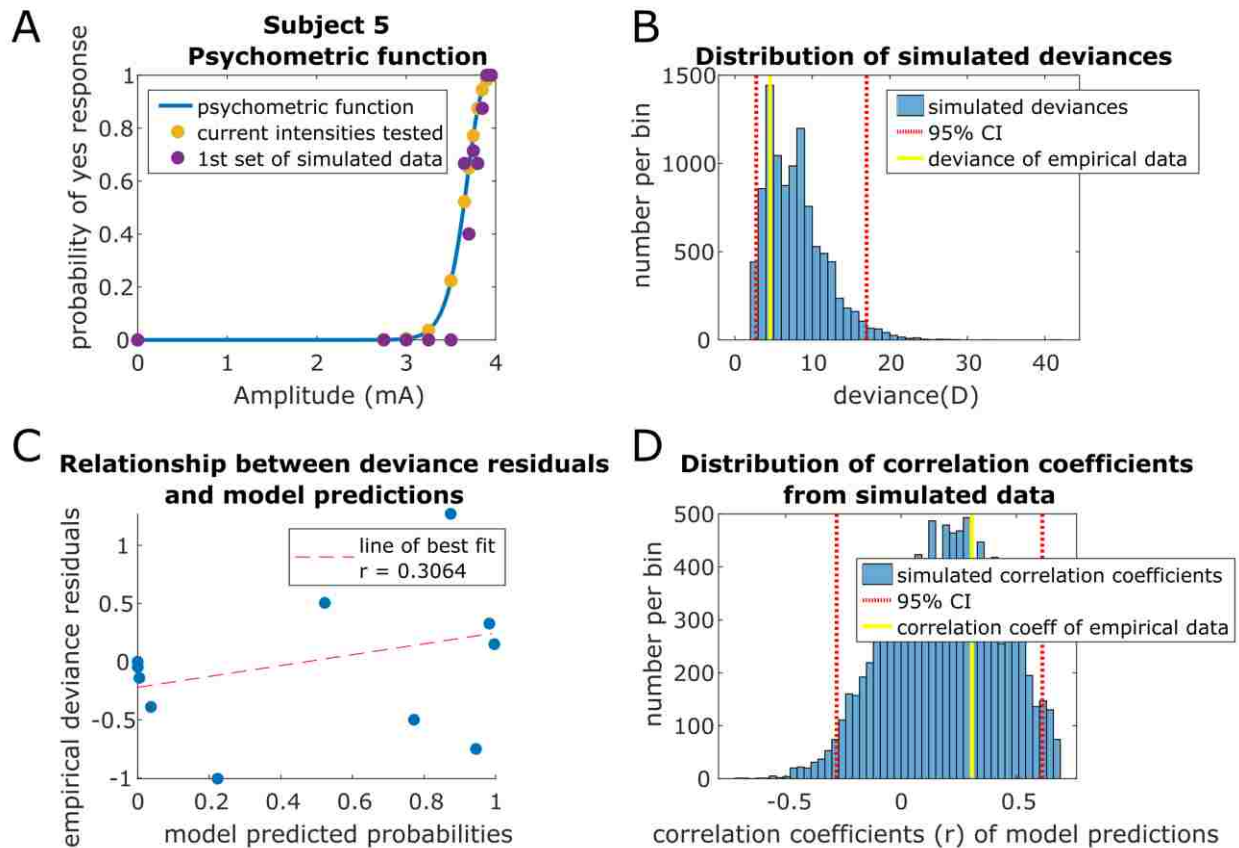


Figure 10-7. Example of goodness of fit assessment for Subject 4

A) Illustration of using the best-fit psychometric function as the generating function for the parametric bootstrap. The red points indicate the amplitude levels and their corresponding probabilities which are used to generate the simulated data. Green points illustrate a single simulation of new data using the best-fit generating function. Distributions of deviances (B) and correlation coefficients (D) are produced via 10,000 Monte Carlo simulations and compared to empirical measurements of deviance and correlation (yellow lines on the histograms). C) Depiction of the relationship between the empirical deviance residuals and the model-predicted probabilities, with the corresponding empirical correlation coefficient.

Subject	DCS Parameters	Deviance			Correlation coefficients of deviance residuals		
		empirical	2.5th percentile	97.5th percentile	empirical	2.5th percentile	97.5th percentile
1	baseline	12.66	3.38	22.99	0.18	-0.43	0.64
2	baseline	9.05	2.69	14.76	0.29	-0.68	0.77
3	baseline	20.73	11.56	34.32	0.22	-0.28	0.57
4	baseline, 1st day	2.09	2.66	15.88	0.39	-0.58	0.81
	baseline, 2nd day	6.14	2.58	16.92	0.10	-0.58	0.79
5	baseline	4.54	2.76	17.00	0.31	-0.28	0.61
	819 μ s PW	8.43	5.52	21.59	0.16	-0.39	0.62
6	baseline, 1st day	12.03	4.30	18.48	0.25	-0.28	0.59
	100 Hz PF, 1st day	12.28	0.85	13.35	0.07	-0.69	0.83
	50 Hz PF, 1st day	8.68	4.04	21.46	0.00	-0.45	0.63
	baseline, 2nd day	10.70	3.43	18.04	0.11	-0.44	0.65
7	baseline	6.77	5.96	23.91	0.28	-0.29	0.55
	100 Hz PF	8.58	8.23	28.21	0.10	-0.33	0.51
	50 Hz PF	27.10	9.76	29.69	0.05	-0.42	0.58
8	baseline	2.62	0.42	10.95	0.26	-0.26	0.41
	410 μ s PW	0.07	0.07	8.32	0.37	-0.37	0.48
	82 μ s PW	6.30	2.76	17.54	0.09	-0.41	0.75
9	baseline	8.35	7.69	25.37	0.13	-0.42	0.63

Table 10-1. Goodness-of-fit test results for fit of Weibull function to perceptual staircase results

Values from goodness-of-fit test considering the deviance between the model and data, and the correlation coefficient between deviance residuals and the probabilities predicted by the best-fit function. Empirical deviance values less than the 97.5th deviance percentile and empirical correlation coefficients within the 2.5-97.5th percentiles for correlation coefficients would suggest a good fit between the model function and the data. Using these measures, all subject data was well fit by a by a psychometric Weibull function.

Bridging Assumption

From the 10,000 Monte Carlo simulations, we also obtained distributions of the threshold parameter for each threshold test and used them to estimate the 95% bias-corrected and accelerated (BC_a) confidence intervals around the best-fit threshold value. Acknowledging that the best-fit parameter values are very likely to deviate somewhat from the true, underlying, and unknown parameters, we tested the validity of applying our estimates of variability (i.e., the confidence intervals) from the bootstrap data to the true, underlying function (i.e., the bridging assumption). Again following a method previously described by Wichmann and Hill [187], we calculated the BC_a confidence intervals which would result from eight new generating functions spaced along the 68% confidence intervals (for threshold and slope) for the original generating function (Figure 10-8). If the variability was relatively stable within that range, then the widths of the confidence intervals (WCIs) at the eight new generating functions should be the same order of magnitude as the original confidence interval width. This would suggest that the variability estimates would not change considerably with small changes in the generating function and we could accept the estimate of the confidence intervals as valid for the unknown, underlying parameters [187]. Table 10-1 provides the range of the WCIs for the 68% and 95% confidence intervals for the threshold and slope parameters. Large values, such as the threshold WCI for Subject 4's 2nd day baseline, suggest that the variability is not particularly stable around the best-fit generating function. However, most of the trials have a narrow WCI range suggesting stability, and the permutation tests described in the main text provide another measure of considering significant differences among threshold values without relying purely on the confidence interval width.

Although Wichman and Hill [187] suggest reporting the largest-width confidence interval from the nine simulated sets of data as the expected confidence interval for the best-fit parameters, here we report the original BC_a confidence intervals (Appendix 1 and Chapter 5) as they are calculated from the same distributions which were used in a permutation test to consider the significance of different threshold values. We have included our assessment of the bridging assumption for full disclosure of our considerations of the threshold confidence intervals.

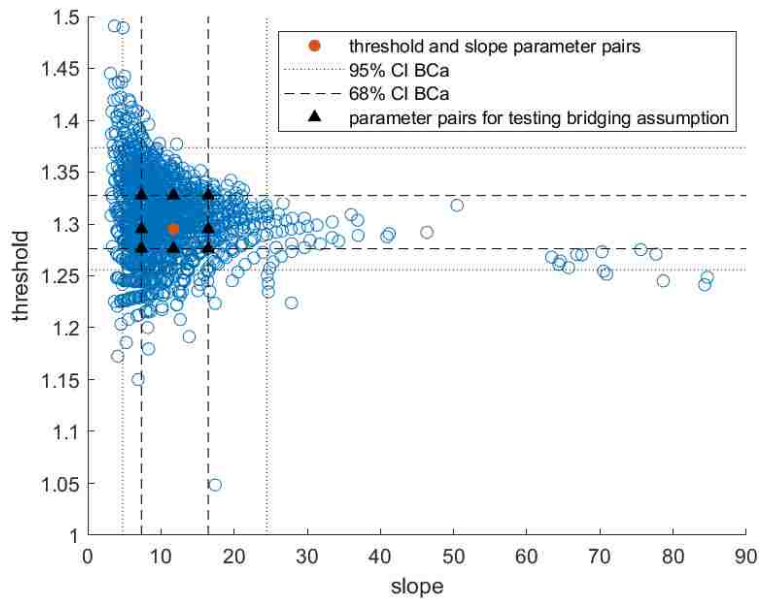


Figure 10-8. Example of bridging assumption assessment for Subject 6

The best-fit threshold and slope parameters are displayed in red with the 68% and 95% BC_a confidence intervals marked with dashed lines (see legend). Eight new pairs of threshold-slope parameters were chosen along the 68% confidence interval values (black triangles), and new parametric bootstrap simulations were performed at each one. The width of each new slope and threshold confidence intervals were compared to one another and the range across the nine total generating functions (the original best-fit and the eight selected values) are provided in Table 10-2.

Subject	DCS Parameters	Threshold CI		Threshold WCI ranges		Slope WCI ranges	
		68%	95%	68%	95%	68%	95%
1	baseline	(0.84, 0.91)	(0.82, 1.04)	0.06	0.27	3.25	8.10
2	baseline	(1.36,1.39)	(1.34, 1.40)	0.08	1.10	27.69	805.09
3	baseline	(1.22,1.55)	(1.16, 2.63)	0.62	47.30	3.28	8.02
4	baseline, 1st day	(1.27,1.32)	(1.24, 1.35)	0.10	0.73	15.59	42.82
	baseline, 2nd day	(0.86 ,0.92)	(0.82, 0.97)	0.09	9.04E+03	2.75	8.59
5	baseline	(3.73 ,3.80)	(3.70, 3.83)	0.04	0.10	22.28	60.78
	819 μ s PW	(2.52 ,2.64)	(2.48, 2.82)	0.14	0.89	5.22	10.57
6	baseline, 1st day	(0.98 ,1.07)	(0.93, 1.13)	0.14	0.35	4.29	11.02
	100 Hz PF, 1st day	(1.28,1.33)	(1.26, 1.37)	0.04	0.14	6.21	43.91
	50 Hz PF, 1st day	(1.89 ,2.08)	(1.84, 2.37)	0.31	1.00	5.87	12.42
	baseline, 2nd day	(0.89,0.97)	(0.85, 1.05)	0.05	0.15	2.06	4.06
7	baseline	(1.02,1.15)	(0.97, 1.25)	0.13	0.73	1.45	3.84
	100 Hz PF	(1.59,2.52)	(1.49, 205.43)	47.36	6.02E+10	4.64	9.66
	50 Hz PF	(2.06 ,3.21)	(1.96, 6.03e4)	1.93E+07	3.43E+10	15.09	71.83
8	baseline	(0.46 ,0.49)	(0.45, 0.50)	0.01	0.04	35.55	39.90
	410 μ s PW	(0.33 ,0.35)	(0.31, 0.36)	0.03	0.04	14.43	33.55
	82 μ s PW	(0.87 ,0.92)	(0.84, 0.95)	0.04	0.13	3.02	6.17
9	baseline	(3.48, 3.61)	(3.42, 3.81)	0.23	7.04E+4	17.12	63.56

Table 10-2. Results from testing the bridging assumption for all subjects, all trials

The 68% and 95% BC_a confidence intervals (CI) from the original best-fit generating function are provided in the 3rd and 4th columns. The 95% CIs are also reported in the main text. The final four columns provide the threshold and slope confidence interval width (WCI) ranges from the nine total generating functions used in the parametric bootstrap. The generating function parameters are illustrated in Figure 10-8. Large WCI ranges suggest that the confidence interval estimates may vary substantially around the generating function and may not be valid estimates of the variability of the true, underlying, and unknown values.

11 Appendix 2 - Aperture Task: Subjects 1 and 3

The following was published as the Supplemental Material in:

Cronin, J.A, J. Wu, K. Collins, D. Sarma, R.P.N. Rao, J.G. Ojemann, and J.D. Olson. (2016). "Task-Specific Somatosensory Feedback via Cortical Stimulation in Humans." *IEEE Transactions on Haptics*, 9(4): 515-522.

Supplemental Material

The results from the two subjects (Subjects 1 and 3, based on participation date) that were excluded from the primary discussion in Chapter 8, DCS for task-based feedback, are presented here for full disclosure of our findings. The y-axes on all figures are the same as those for Subject 2's figures in the main text for comparison. Like Subject 2, both Subject 1 and Subject 3 wore the dataglove on the hand contralateral to the implanted ECoG grid (right hemisphere grids for both Subject 1 and Subject 3), and therefore perceived a sensation from the stimulation on the same hand that they had to move. The same methods as presented in the Methods section of Chapter 8 were used for Subjects 1 and 3 except for some specifics of target path shape, concurrent visual feedback, and stimulation parameters. Those are presented below.

Subject 1: Specific Methods and Results

Subject 1 completed three trials without any visual feedback that each used a simple sine wave as a target path with a frequency of approximately 0.04 Hz for the first two trials and a frequency of approximately 0.02 Hz for the third trial. Each trial used an ITI of 800 ms and current amplitudes of 2.50 mA and 3.50 mA for Stim 1 and Stim 2, respectively (Table 8-2). For this subject's first two trials, the target area spanned 15% of her own aperture range. She expressed difficulty completing the task so we increased the target area range to 45% for the last trial (Figures 11-1 and 11-2). An example of one of her trials, trial 3, is displayed in Figure 11-3. After the third trial this subject was too sleepy to continue and asked to stop research.

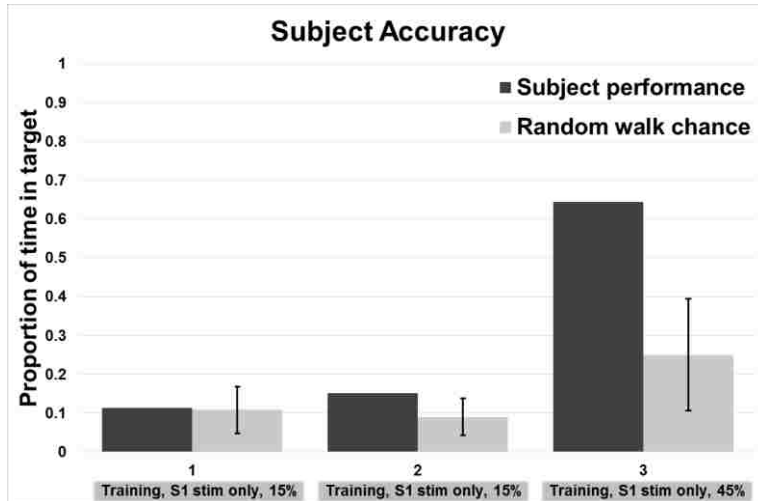


Figure 11-1. Subject 1's accuracy levels as a measure of performance

Subject 1's performance and chance performance values are provided with error bars for the standard deviation in chance performance. None of the trials included concurrent visual feedback. Trial 1 was 1 minute in length, while trials 2 and 3 were both 3 minutes in length because we thought additional time would aid performance. The labels below the trial numbers give the percentage of the subject's aperture space that the target region occupied. The target region was enlarged during the last trial because the subject was having difficulty with the task, at least in part due to fatigue.

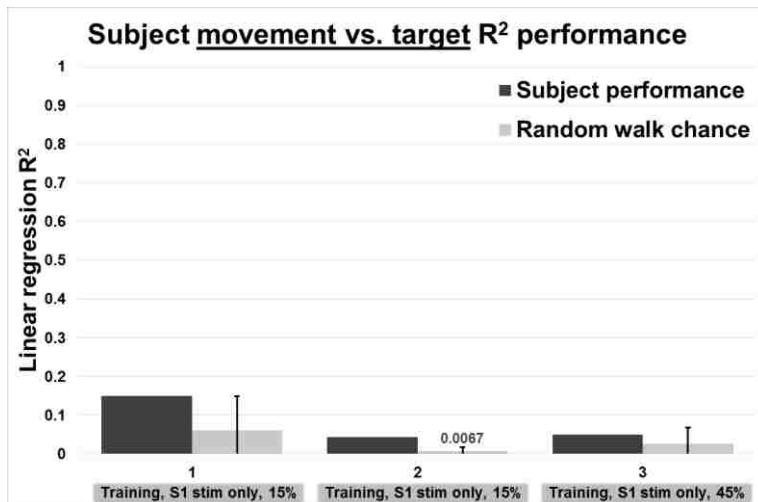


Figure 11-2. Subject 1's R² levels as a measure of performance

Subject 1's performance and chance performance values are provided with error bars for the standard deviation in chance performance. The trial types and lengths are described in Figure 11-1. The chance value for trial 2 is included over its bar so that it's clearly visible.

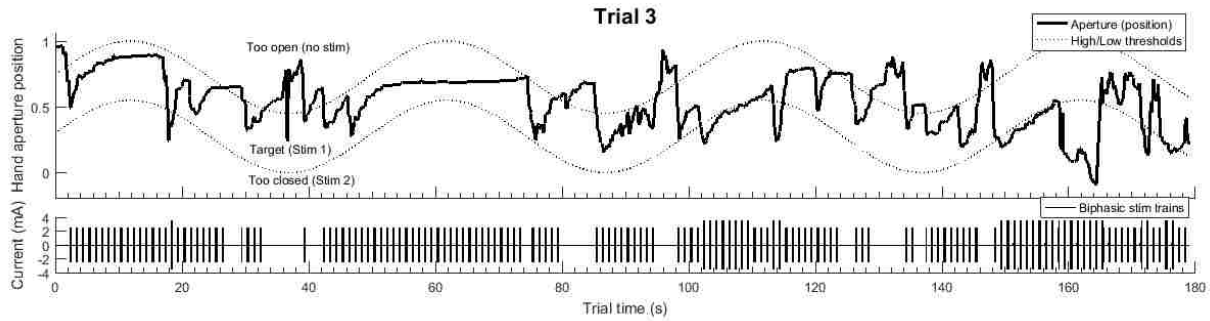


Figure 11-3. Sample trace of Subject 1's hand aperture position and DCS waveforms

Subject 1's hand aperture position relative to the aperture target thresholds with corresponding stimulation current amplitudes for trial 3. Stimulation pulses were biphasic, but due to time scale only the 200 ms stimulation trains are visible not the individual pulses (Stim 1 = 2.5 mA, Stim 2 = 3.5mA, Table 8-2). Subjects' aperture values could move outside of the 0 to 1 range if they made hand movements that were outside of the range used during the normalization period (Chapter 8, Methods). Subjects were instructed to start each run with their hand open in order to begin in the no-stimulation region (Table 8-1, Case A). Trial 3 had performance values of: accuracy = 0.6446, $R^2 = 0.0508$.

Subject 3: Specific Methods and Results

Subject 3 completed 11 trials with four different types of target paths: one practice path and three evaluation paths. The practice trial path used concurrent visual feedback and consisted of a constant target position for half of the trial duration and then a simple sine wave for the remainder of the trial. The three evaluation trial paths (Eval 1-3, Figures 11-4 and 11-5) used stimulation feedback alone, and each had its own target path created as described in the Methods section with the same frequency as Subject 2, approximately 0.02 Hz. Subject 3 also used the same ITIs for Stim 1 (800 ms) and Stim 2 (400 ms) as Subject 2 used during his last two trials (trial 13 and 14, Table 8-2) in an effort to improve stimuli discrimination. As with Subject 2, we had to increase the current amplitudes of Stim 1 and Stim 2 several times based on the subject's feedback to maintain discriminable stimuli (Table 8-2). An example of one of her trials, trial 4, is displayed in Figure 11-6. We planned to use one practice trial to begin the task and then each evaluation trial four times for a total of 13 trials. Using repeated evaluation paths in a randomized order could have allowed us to consider the effects of path learning. However this subject had trouble completing the trials without concurrent visual feedback, so we included four additional practice trials with visual feedback (trials 7-10, shaded in Figures 11-4 and 11-5) to try to help her understand the task. Even with the concurrent visual and cortical stimulation feedback, this subject did not perform well above chance and in trial 9 her accuracy was below the mean + standard deviation chance value. We believe that her performance in these practice trials with concurrent visual feedback suggests that she was not attentive enough or did not comprehend the task well enough to participate. A validity measure as described in the Discussion section of Chapter 8 could have allowed us to exclude her from participation early on in the task.

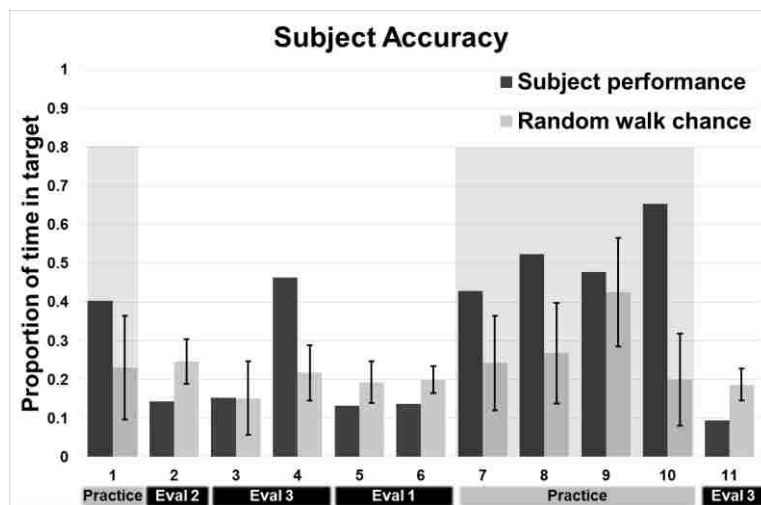


Figure 11-4. Subject 3's accuracy levels as a measure of performance

Subject 3's performance and chance performance values are provided with error bars for the standard deviation in chance performance. The practice trials included concurrent visual and cortical stimulation feedback (shaded trials) and consisted of approximately 1 minute of a constant target aperture position for the subject to explore the space, followed by approximately 1 minute of a simple sine wave. Evaluation trials 1, 2, and 3 each had their own, more complex target aperture path that was just over two minutes in length and created by summing four sinusoids together as explained in the Methods section, Chapter 8. The evaluation trials used cortical stimulation alone.

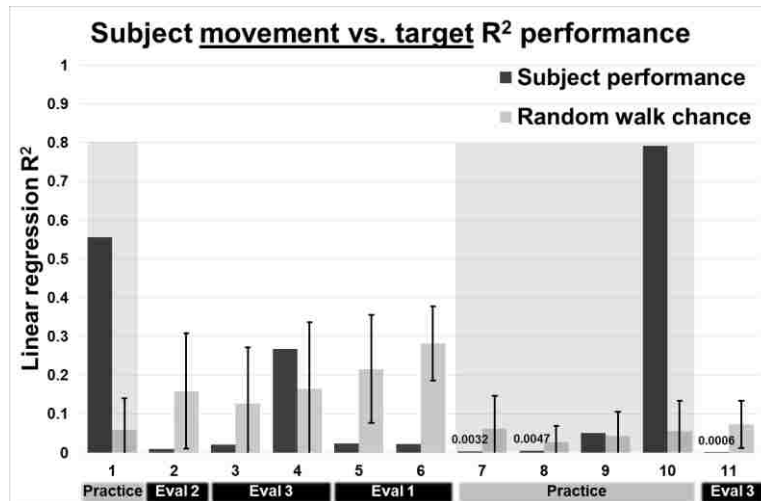


Figure 11-5. Subject 3's R² levels as a measure of performance

Subject 3's performance and chance performance values are provided with error bars for the standard deviation in chance performance. The trial types are described in Figure 11-4; shaded trials use concurrent visual and cortical stimulation feedback. The performance values for trials 7, 8, and 11 are included over their bars since they are so close to zero.

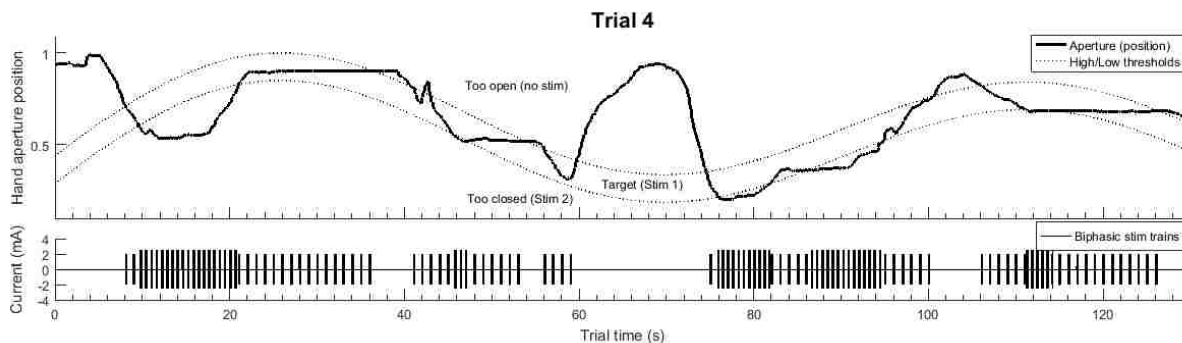


Figure 11-6. Sample trace of Subject 3's hand aperture position and DCS waveforms

Subject 3's hand aperture position relative to the aperture target thresholds with corresponding stimulation current amplitudes for trial 4. See Figure 11-3 for more figure details. For Trial 4: Stim 1=2.0 mA, Stim 2=2.5 mA (Table 8-2). Performance values of: accuracy = 0.4630, R² = 0.2673.

12 References

1. Monzée, J., Lamarre, Y. & Smith, A. M. The Effects of Digital Anesthesia on Force Control Using a Precision Grip. *J. Neurophysiol.* 89, 672–83 (2003).
2. Augurelle, A. S. Importance of Cutaneous Feedback in Maintaining a Secure Grip during Manipulation of Hand-Held Objects. *J. Neurophysiol.* 89, 665–671 (2002).
3. Brochier, T., Boudreau, M. J., Paré, M. & Smith, A. M. The Effects of Muscimol Inactivation of Small Regions of Motor and Somatosensory Cortex on Independent Finger Movements and Force Control in the Precision Grip. *Exp. Brain Res.* 128, 31–40 (1999).
4. Robles-De-La-Torre, G. The Importance of the Sense of Touch in Virtual and Real Environments. *IEEE Multimed.* 13, 24–30 (2006).
5. Botvinick, M. & Cohen, J. Rubber Hands ‘feel’ Touch That Eyes See. *Nature* 391, 756 (1998).
6. Serino, A. & Haggard, P. Touch and the Body. *Neurosci. Biobehav. Rev.* 34, 224–236 (2010).
7. Morrison, I., Löken, L. S. & Olsson, H. The Skin as a Social Organ. *Exp. Brain Res.* 204, 305–314 (2010).
8. Biddiss, E., Beaton, D. & Chau, T. Consumer Design Priorities for Upper Limb Prosthetics. *Disabil. Rehabil. Assist. Technol.* 2, 346–357 (2007).
9. Anderson, K. D. Targeting Recovery: Priorities of the Spinal Cord-Injured Population. *J. Neurotrauma* 21, 1371–1383 (2004).
10. Collinger, J. L. *et al.* Functional Priorities, Assistive Technology, and Brain-Computer Interfaces after Spinal Cord Injury. *J. Rehabil. Res. Dev.* 50, 145–60 (2013).
11. Wander, J. D. & Rao, R. P. N. Brain-Computer Interfaces: A Powerful Tool for Scientific Inquiry. *Curr. Opin. Neurobiol.* 25, 70–75 (2014).
12. Peckham, P. H. & Kilgore, K. L. Challenges and Opportunities in Restoring Function after Paralysis. *IEEE Trans. Biomed. Eng.* 60, 602–609 (2013).
13. Armour, B. S., Courtney-Long, E. A., Fox, M. H., Fredine, H. & Cahill, A. Prevalence and Causes of Paralysis—United States, 2013. *Am. J. Public Health* 106, 1855–1857 (2016).
14. Ziegler-Graham, K., MacKenzie, E. J., Ephraim, P. L., Travison, T. G. & Brookmeyer, R. Estimating the Prevalence of Limb Loss in the United States: 2005 to 2050. *Arch. Phys. Med. Rehabil.* 89, 422–429 (2008).
15. Craig, A., Tran, Y. & Middleton, J. Psychological Morbidity and Spinal Cord Injury: A Systematic Review. *Spinal Cord* 47, 108–114 (2009).
16. Hannah, S. D. Psychosocial Issues after a Traumatic Hand Injury: Facilitating Adjustment. *J. Hand Ther.* 24, 95–103 (2011).
17. DeVivo, M., Chen, Y., Mennemeyer, S. & Deutsch, A. Costs of Care Following Spinal Cord Injury. *Top. Spinal Cord Inj. Rehabil.* 16, 1–9 (2011).
18. Cao, Y., Chen, Y. & DeVivo, M. J. Lifetime Direct Costs After Spinal Cord Injury. *Top. Spinal Cord Inj. Rehabil.* 16, 10–16 (2011).
19. National Spinal Cord Injury Statistical Center. *Spinal cord injury facts and figures at a glance. University of Alabama at Birmingham* (2015). doi:10.1179/204577212X13237783484262
20. Krause, J. S., Edles, P. & Charlifue, S. Changes in Employment Status and Earnings After Spinal Cord Injury: A Pilot Comparison From Pre to Post Injury. *Top. Spinal Cord Inj. Rehabil.* 16, 74–79 (2011).
21. Foundation, C. and D. R. Policy Data Brief: Paralysis in the US. 46–49 (2012).
22. Creasey, G. H. *et al.* Reduction of Costs of Disability Using Neuroprostheses. *Assist. Technol.* 12, 67–75 (2000).
23. Roy, H. A., Green, A. L. & Aziz, T. Z. State of the Art: Novel Applications for Deep Brain Stimulation. *Neuromodulation Technol. Neural Interface* 21, 126–134 (2018).
24. Edwardson, M. A., Lucas, T. H., Carey, J. R. & Fetz, E. E. New Modalities of Brain Stimulation for Stroke Rehabilitation. *Exp. Brain Res.* 224, 335–58 (2013).
25. Lewis, P. M., Ackland, H. M., Lowery, A. J. & Rosenfeld, J. V. Restoration of Vision in Blind Individuals Using Bionic Devices: A Review with a Focus on Cortical Visual Prostheses. *Brain Res.* 1595, 51–73 (2015).
26. Moran, D. Evolution of Brain-Computer Interface: Action Potentials, Local Field Potentials and Electroencephalograms. *Curr. Opin. Neurobiol.* 20, 741–745 (2010).
27. Leuthardt, E. C., Schalk, G., Roland, J., Rouse, A. & Moran, D. W. Evolution of Brain-Computer Interfaces: Going beyond Classic Motor Physiology. *Neurosurg. Focus* 27, E4 (2009).

28. Wolpaw, J., Birbaumer, N., McFarland, D. J., Pfurtscheller, G. & Vaughan, T. M. Brain Computer Interfaces for Communication and Control. *Clin. Neurophysiol.* 113, 767–791 (2002).
29. Green, A. M. & Kalaska, J. F. Learning to Move Machines with the Mind. *Trends Neurosci.* 34, 61–75 (2011).
30. Rao, R. P. N. *Brain-Computer Interfacing: An Introduction.* (Cambridge University Press, 2013).
31. Wolpaw, J. R. & Wolpaw, E. W. *Brain-computer interfaces principles and practice.* (Oxford, 2012).
32. Schwartz, A. B., Cui, X. T., Weber, D. & Moran, D. W. Brain-Controlled Interfaces: Movement Restoration with Neural Prosthetics. *Neuron* 52, 205–220 (2006).
33. Fetz, E. E. Operant Conditioning of Cortical Unit Activity. *Science* 163, 955–958 (1969).
34. Kennedy, P. R. & Bakay, R. A. E. Restoration of Neural Output from a Paralyzed Patient by a Direct Brain Connection. *Neuroreport* 9, 1707–1711 (1998).
35. Vidal, J. J. Toward Direct Brain-Computer Communication. *Annu. Rev. Biophys. Bioeng.* 2, 157–180 (1973).
36. Hochberg, L. R. *et al.* Neuronal Ensemble Control of Prosthetic Devices by a Human with Tetraplegia. *Nature* 442, 164–171 (2006).
37. Simeral, J. D., Kim, S.-P., Black, M. J., Donoghue, J. P. & Hochberg, L. R. Neural Control of Cursor Trajectory and Click by a Human with Tetraplegia 1000 Days after Implant of an Intracortical Microelectrode Array. *J. Neural Eng.* 8, 025027 (2011).
38. Rezeika, A. *et al.* Brain-Computer Interface Spellers: A Review. *Brain Sci.* 8, (2018).
39. Birbaumer, N. *et al.* A Spelling Device for the Paralyzed. *Nature* 398, 297–298 (1999).
40. Moritz, C. T., Perlmutter, S. I. & Fetz, E. E. Direct Control of Paralyzed Muscles by Cortical Neurons. *Nature* 456, 639–642 (2008).
41. Bouton, C. E. *et al.* Restoring Cortical Control of Functional Movement in a Human with Quadriplegia. *Nature* 533, 247–250 (2016).
42. Hochberg, L. R. *et al.* Reach and Grasp by People with Tetraplegia Using a Neurally Controlled Robotic Arm. *Nature* 485, 372–375 (2012).
43. Hotson, G. *et al.* Individual Finger Control of a Modular Prosthetic Limb Using High-Density Electroencephalography in a Human Subject. *J. Neural Eng.* 13, 026017 (2016).
44. Collinger, J. L. *et al.* High-Performance Neuroprosthetic Control by an Individual with Tetraplegia. *Lancet* 381, 557–564 (2013).
45. Kübler, A. *et al.* Patients with ALS Can Use Sensorimotor Rhythms to Operate a Brain-Computer Interface. *Neurology* 64, 1775–1777 (2005).
46. Kennedy, P. *et al.* Using Human Extra-Cortical Local Field Potentials to Control a Switch. *J. Neural Eng.* 1, 72–77 (2004).
47. Vansteensel, M. J. *et al.* Brain-Computer Interfacing Based on Cognitive Control. *Ann. Neurol.* 67, (2010).
48. Ramsey, N. F., Heuvel, M. P. Van De, Kho, K. H. & Leijten, F. S. S. Towards Human BCI Applications Based on Cognitive Brain Systems: An Investigation of Neural Signals Recorded From the Dorsolateral Prefrontal Cortex. *IEEE Trans. Neural Syst. Rehabil. Eng.* 214–217 (2006).
49. del R Millan, J. *et al.* A Local Neural Classifier for the Recognition of EEG Patterns Associated to Mental Tasks. *IEEE Trans. Neural Networks* 13, 678–686 (2002).
50. Felton, E. A., Wilson, J. A., Williams, J. C. & Garell, P. C. Electroencephalographically Controlled Brain-computer Interfaces Using Motor and Sensory Imagery in Patients with Temporary Subdural Electrode Implants. *J. Neurosurg.* 106, 495–500 (2007).
51. Aflalo, T. *et al.* Decoding Motor Imagery from the Posterior Parietal Cortex of a Tetraplegic Human. *Science* 348, 906–910 (2015).
52. Johansson, R. S. & Flanagan, J. R. Coding and Use of Tactile Signals from the Fingertips in Object Manipulation Tasks. *Nat. Rev. Neurosci.* 10, 345–59 (2009).
53. Pavlides, C., Miyashita, E. & Asanuma, H. Projection from the Sensory to the Motor Cortex Is Important in Learning Motor Skills in the Monkey. *J. Neurophysiol.* 70, 733–41 (1993).
54. Abbott, A. Neuroprosthetics: In Search of the Sixth Sense. *Nature* 442, 125–127 (2006).
55. Dunbar, R. I. M. The Social Role of Touch in Humans and Primates: Behavioural Function and Neurobiological Mechanisms. *Neurosci. Biobehav. Rev.* 34, 260–268 (2010).
56. Hertenstein, M. J., Holmes, R., McCullough, M. & Keltner, D. The Communication of Emotion via Touch. *Emotion* 9, 566–573 (2009).
57. Barbero, A. & Grosse-Wentrup, M. Biased Feedback in Brain-Computer Interfaces. *J. Neuroeng. Rehabil.* 7,

- 34 (2010).
58. Nijboer, F. *et al.* An Auditory Brain-Computer Interface (BCI). *J. Neurosci. Methods* 167, 43–50 (2008).
 59. Hinterberger, T. *et al.* A Multimodal Brain-Based Feedback and Communication System. *Exp. Brain Res.* 154, 521–526 (2004).
 60. Bensmaia, S. J. & Miller, L. E. Restoring Sensorimotor Function through Intracortical Interfaces: Progress and Looming Challenges. *Nat. Rev. Neurosci.* 15, 313–325 (2014).
 61. Taylor, D. M., Tillery, S. I. H. & Schwartz, A. B. Direct Cortical Control of 3D Neuroprosthetic Devices. *Science* 296, 1829–32 (2002).
 62. Sanes, J. N., Mauritz, K.-H., Evars, E. V, Dalakast, M. C. & Chut, A. Motor Deficits in Patients with Large-Fiber Sensory Neuropathy. *Psychology* 81, 979–982 (1984).
 63. Sainburg, R. L., Poizner, H. & Ghez, C. Loss of Proprioception Produces Deficits in Interjoint Coordination. *J. Neurophysiol.* 70, 2136–2147 (1993).
 64. Suminski, A. J., Tkach, D. C., Fagg, A. H. & Hatsopoulos, N. G. Incorporating Feedback from Multiple Sensory Modalities Enhances Brain-Machine Interface Control. *J. Neurosci.* 30, 16777–16787 (2010).
 65. Klaes, C. *et al.* A Cognitive Neuroprosthetic That Uses Cortical Stimulation for Somatosensory Feedback. *J. Neural Eng.* 11, 056024 (2014).
 66. Pistohl, T., Joshi, D., Ganesh, G., Jackson, A. & Nazarpour, K. Artificial Proprioceptive Feedback for Myoelectric Control. *IEEE Trans. Neural Syst. Rehabil. Eng.* 23, 498–507 (2015).
 67. Ramos-Murguialday, A. *et al.* Proprioceptive Feedback and Brain Computer Interface (BCI) Based Neuroprostheses. *PLoS One* 7, e47048 (2012).
 68. Schiefer, M., Tan, D., Sidek, S. M. & Tyler, D. J. Sensory Feedback by Peripheral Nerve Stimulation Improves Task Performance in Individuals with Upper Limb Loss Using a Myoelectric Prosthesis. *J. Neural Eng.* 13, 016001 (2016).
 69. Tan, D. W. *et al.* A Neural Interface Provides Long-Term Stable Natural Touch Perception. *Sci. Transl. Med.* 6, 257ra138 (2014).
 70. Tomlinson, T. & Miller, L. E. Toward a Proprioceptive Neural Interface That Mimics Natural Cortical Activity. *Adv. Exp. Med. Biol.* 957, 367–388 (2016).
 71. Saal, H. P. & Bensmaia, S. J. Touch Is a Team Effort: Interplay of Submodalities in Cutaneous Sensibility. *Trends Neurosci.* 37, 689–697 (2014).
 72. Weber, D. J., Friesen, R. & Miller, L. E. Interfacing the Somatosensory System to Restore Touch and Proprioception: Essential Considerations. *J. Mot. Behav.* 44, 403–18 (2012).
 73. Saal, H. P. & Bensmaia, S. J. Biomimetic Approaches to Bionic Touch through a Peripheral Nerve Interface. *Neuropsychologia* 79, 344–353 (2015).
 74. Navarro, X. *et al.* A Critical Review of Interfaces with the Peripheral Nervous System for the Control of Neuroprostheses and Hybrid Bionic Systems. *J. Peripher. Nerv. Syst.* 10, 229–258 (2005).
 75. Borich, M. R., Brodie, S. M., Gray, W. A., Ionta, S. & Boyd, L. A. Understanding the Role of the Primary Somatosensory Cortex: Opportunities for Rehabilitation. *Neuropsychologia* 79, 246–255 (2015).
 76. Disbrow, E., Roberts, T. & Krubitzer, L. Somatotopic Organization of Cortical Fields in the Lateral Sulcus of Homo Sapiens: Evidence for SII and PV. *J. Comp. Neurol.* 418, 1–21 (2000).
 77. Creutzfeldt, O. D. *Cortex Cerebri.* (Springer-Verlag, 1993).
 78. Pleger, B. & Villringer, A. The Human Somatosensory System: From Perception to Decision Making. *Prog. Neurobiol.* 103, 76–97 (2013).
 79. Woolsey, C. N., Erickson, T. C. & Gilson, W. E. Localization in Somatic Sensory and Motor Areas of Human Cerebral Cortex as Determined by Direct Recording of Evoked Potentials and Electrical Stimulation. *J. Neurosurg.* 51, 476–506 (1979).
 80. Aukstulewicz, R., Spitzer, B. & Blankenburg, F. Recurrent Neural Processing and Somatosensory Awareness. *J. Neurosci.* 32, 799–805 (2012).
 81. Sathian, K. Analysis of Haptic Information in the Cerebral Cortex. *J. Neurophysiol.* jn.00546.2015 (2016). doi:10.1152/jn.00546.2015
 82. Karhu, J. & Tesche, C. D. Simultaneous Early Processing of Sensory Input in Human Primary (SI) and Secondary (SII) Somatosensory Cortices. *J. Neurophysiol.* 81, 2017–2025 (1999).
 83. Chen, T. L. *et al.* Human Secondary Somatosensory Cortex Is Involved in the Processing of Somatosensory Rare Stimuli: An fMRI Study. *Neuroimage* 40, 1765–1771 (2008).

84. Reed, C. L., Shoham, S. & Halgren, E. Neural Substrates of Tactile Object Recognition: An fMRI Study. *Hum. Brain Mapp.* 21, 236–246 (2004).
85. Gallace, A. & Spence, C. The Cognitive and Neural Correlates of “Tactile Consciousness”: A Multisensory Perspective. *Conscious. Cogn.* 17, 370–407 (2008).
86. Stein, B. E. & Stanford, T. R. Multisensory Integration: Current Issues from the Perspective of the Single Neuron. *Nat. Rev. Neurosci.* 9, 255–266 (2008).
87. Driver, J. & Noesselt, T. Multisensory Interplay Reveals Crossmodal Influences on ‘sensory-Specific’ Brain Regions, Neural Responses, and Judgments. *Neuron* 57, 11–23 (2008).
88. Graziano, M. S., Hu, X. T. & Gross, C. G. Visuospatial Properties of Ventral Premotor Cortex. *J. Neurophysiol.* 77, 2268–2292 (1997).
89. Guterstam, A., Gentile, G. & Ehrsson, H. H. The Invisible Hand Illusion: Multisensory Integration Leads to the Embodiment of a Discrete Volume of Empty Space. *J. Cogn. Neurosci.* 25, 1078–99 (2013).
90. Ehrsson, H. H., Spence, C. & Passingham, R. E. That’s My Hand! Activity in Premotor Cortex Reflects Feeling of Ownership of a Limb. *Science* 305, 875–877 (2004).
91. Cardini, F. *et al.* Viewing One’s Own Face Being Touched Modulates Tactile Perception: An fMRI Study. *J. Cogn. Neurosci.* 23, 503–513 (2011).
92. Nakashita, S. *et al.* Tactile-Visual Integration in the Posterior Parietal Cortex: A Functional Magnetic Resonance Imaging Study. *Brain Res. Bull.* 75, 513–525 (2008).
93. Sereno, M. I. & Huang, R.-S. A Human Parietal Face Area Contains Aligned Head-Centered Visual and Tactile Maps. *Nat. Neurosci.* 9, 1337–43 (2006).
94. Beauchamp, M. S., Yasar, N. E., Frye, R. E. & Ro, T. Touch, Sound and Vision in Human Superior Temporal Sulcus. *Neuroimage* 41, 1011–20 (2008).
95. Wilson, B. S. & Dorman, M. F. Cochlear Implants: A Remarkable Past and a Brilliant Future. *Hear. Res.* 242, 3–21 (2008).
96. Eshraghi, A. A. *et al.* The Cochlear Implant: Historical Aspects and Future Prospects. *Anat. Rec.* 295, 1967–80 (2012).
97. Fryauf-Bertschy, H., Tyler, R. S., Kelsay, D. M. & Gantz, B. J. Performance Over Time of Congenitally Deaf and Postlingually Deafened Children Using a Multichannel Cochlear Implant. *J. Speech Lang. Hear. Res.* 35, 913 (1992).
98. Rauschecker, J. P. & Shannon, R. V. Sending Sound to the Brain. *Science* 295, 1025–9 (2002).
99. Otto, K. J., Rousche, P. J. & Kipke, D. R. Microstimulation in Auditory Cortex Provides a Substrate for Detailed Behaviors. *Hear. Res.* 210, 112–117 (2005).
100. Javaheri, M., Hahn, D. S., Lakhampal, R. R., Weiland, J. D. & Humayun, M. S. Retinal Prostheses for the Blind. *Ann Acad Med Singapore* 35, 137–44 (2006).
101. Shkel, A. M. & Zeng, F.-G. An Electronic Prosthesis Mimicking the Dynamic Vestibular Function. *Audiol. Neurootol.* 11, 113–22 (2006).
102. Perruchoud, D., Pisotta, I., Carda, S., Murray, M. M. & Ionta, S. Biomimetic Rehabilitation Engineering: The Importance of Somatosensory Feedback for Brain–Machine Interfaces. *J. Neural Eng.* 13, 041001 (2016).
103. Raspopovic, S. *et al.* Restoring Natural Sensory Feedback in Real-Time Bidirectional Hand Prostheses. *Sci. Transl. Med.* 6, (2014).
104. Dhillon, G. S. & Horch, K. W. Direct Neural Sensory Feedback and Control of a Prosthetic Arm. *IEEE Trans. Neural Syst. Rehabil. Eng.* 13, 468–472 (2005).
105. Kuiken, T. A., Marasco, P. D., Lock, B. A., Harden, R. N. & Dewald, J. P. A. Redirection of Cutaneous Sensation from the Hand to the Chest Skin of Human Amputees with Targeted Reinnervation. *Proc. Natl. Acad. Sci. U. S. A.* 104, 20061–20066 (2007).
106. Hebert, J. S. *et al.* Novel Targeted Sensory Reinnervation Technique to Restore Functional Hand Sensation after Transhumeral Amputation. *IEEE Trans. Neural Syst. Rehabil. Eng.* 22, 765–773 (2014).
107. Berg, J. A. *et al.* Behavioral Demonstration of a Somatosensory Neuroprosthesis. *IEEE Trans. Neural Syst. Rehabil. Eng.* 21, 500–507 (2013).
108. O’Doherty, J. E. *et al.* Active Tactile Exploration Using a Brain-Machine-Brain Interface. *Nature* 479, 228–31 (2011).
109. Cronin, J. A. *et al.* Task-Specific Somatosensory Feedback via Cortical Stimulation in Humans. *IEEE Trans. Haptics* 9, 515–522 (2016).

110. Johnson, L. A. *et al.* Direct Electrical Stimulation of the Somatosensory Cortex in Humans Using Electrocorticography Electrodes: A Qualitative and Quantitative Report. *J. Neural Eng.* 10, 036021 (2013).
111. Hiremath, S. V. *et al.* Human Perception of Electrical Stimulation on the Surface of Somatosensory Cortex. *PLoS One* 12, e0176020 (2017).
112. Libet, B. *et al.* Production of Threshold Levels of Conscious Sensation by Electrical Stimulation of Human Somatosensory Cortex. *J. Neurophysiol.* 27, 546–578 (1964).
113. Ray, P. G. *et al.* Physiology of Perception: Cortical Stimulation and Recording in Humans. *Neurology* 52, 1044–1049 (1999).
114. Tyler, D. J. Neural Interfaces for Somatosensory Feedback: Bringing Life to a Prosthesis. *Curr. Opin. Neurol.* 28, 574–581 (2015).
115. Tan, D., Schiefer, M., Keith, M. W., Anderson, R. & Tyler, D. J. Stability and Selectivity of a Chronic, Multi-Contact Cuff Electrode for Sensory Stimulation in a Human Amputee. in *International IEEE/EMBS Conference on Neural Engineering* 859–862 (2013). doi:10.1109/NER.2013.6696070
116. Davis, T. S. *et al.* Restoring Motor Control and Sensory Feedback in People with Upper Extremity Amputations Using Arrays of 96 Microelectrodes Implanted in the Median and Ulnar Nerves. *J. Neural Eng.* 13, 036001 (2016).
117. Dhillon, G. S., Lawrence, S. M., Hutchinson, D. T. & Horch, K. W. Residual Function in Peripheral Nerve Stumps of Amputees: Implications for Neural Control of Artificial Limbs. *J. Hand Surg. Am.* 29, 605–615 (2004).
118. Hebert, J. S., Elzinga, K., Chan, K. M., Olson, J. & Morhart, M. Updates in Targeted Sensory Reinnervation for Upper Limb Amputation. *Curr. Surg. Reports* 2, 45 (2014).
119. Marasco, P. D., Schultz, A. E. & Kuiken, T. A. Sensory Capacity of Reinnervated Skin after Redirection of Amputated Upper Limb Nerves to the Chest. *Brain* 132, 1441–8 (2009).
120. Kuiken, T. A. *et al.* Targeted Muscle Reinnervation for Real-Time Myoelectric Control of Multifunction Artificial Arms. *Yearb. Orthop.* 2010, 91–93 (2010).
121. Tabot, G. A. *et al.* Restoring the Sense of Touch with a Prosthetic Hand through a Brain Interface. *Proc. Natl. Acad. Sci. U. S. A.* 110, 18279–84 (2013).
122. Dadarlat, M. C., O’Doherty, J. E. & Sabes, P. N. A Learning-Based Approach to Artificial Sensory Feedback Leads to Optimal Integration. *Nat. Neurosci.* 18, 138–144 (2014).
123. O’Doherty, J. E., Lebedev, M. A., Hanson, T. L., Fitzsimmons, N. A. & Nicolelis, M. A. L. A Brain-Machine Interface Instructed by Direct Intracortical Microstimulation. *Front Integr Neurosci* 3, (2009).
124. Thomson, E. E., Carra, R. & Nicolelis, M. A. L. Perceiving Invisible Light through a Somatosensory Cortical Prosthesis. *Nat. Commun.* 4, 1482 (2013).
125. O’Doherty, J. E., Lebedev, M. A., Li, Z. & Nicolelis, M. A. L. Virtual Active Touch Using Randomly Patterned Intracortical Microstimulation. *IEEE Trans. Neural Syst. Rehabil. Eng.* 20, 85–93 (2012).
126. Fitzsimmons, N. A., Drake, W., Hanson, T. L., Lebedev, M. A. & Nicolelis, M. A. L. Primate Reaching Cued by Multichannel Spatiotemporal Cortical Microstimulation. *J. Neurosci.* 27, 5593–5602 (2007).
127. Romo, R., Hernández, A., Zainos, A. & Salinas, E. Somatosensory Discrimination Based on Cortical Microstimulation. *Nature* 392, 387–90 (1998).
128. Romo, R., Hernández, A., Zainos, A., Brody, C. D. & Lemus, L. Sensing without Touching: Psychophysical Performance Based on Cortical Microstimulation. *Neuron* 26, 273–278 (2000).
129. London, B. M., Jordan, L. R., Jackson, C. R. & Miller, L. E. Electrical Stimulation of the Proprioceptive Cortex (Area 3a) Used to Instruct a Behaving Monkey. *IEEE Trans. Neural Syst. Rehabil. Eng.* 16, 32–36 (2008).
130. Flesher, S. N. *et al.* Intracortical Microstimulation of Human Somatosensory Cortex. *Sci Transl Med* 8, 361ra141 (2016).
131. Armenta Salas, M. *et al.* Proprioceptive and Cutaneous Sensations in Humans Elicited by Intracortical Microstimulation. *eLife* 7, e32904 (2018).
132. Borchers, S., Himmelbach, M., Logothetis, N. & Karnath, H.-O. Direct Electrical Stimulation of Human Cortex — the Gold Standard for Mapping Brain Functions? *Nat. Rev. Neurosci.* 13, 63–70 (2012).
133. Cushing, H. A Note upon the Faradaic Stimulation of the Postcentral Gyrus in Conscious Patients. *Brain* 32, 44–53 (1909).
134. Brindley, G. S. & Lewin, W. S. The Sensations Produced by Electrical Stimulation of the Visual Cortex. *J. Physiol.* 196, 479–93 (1968).

135. Dobbelle, W. H. & Mladejovsky, M. G. Phosphenes Produced by Electrical Stimulation of Human Occipital Cortex, and Their Application to the Development of a Prosthesis for the Blind. *J. Physiol.* 243, 553–576 (1974).
136. Penfield, W. & Boldrey, E. Somatic Motor and Sensory Representation in the Cerebral Cortex of Man as Studied by Electrical Stimulation. *Brain A J. Neurol.* 60, 389–443 (1937).
137. Collins, K. L. *et al.* Ownership of an Artificial Limb Induced by Electrical Brain Stimulation. *Proc. Natl. Acad. Sci. U. S. A.* 114, 166–171 (2017).
138. Muller, L. *et al.* Direct Electrical Stimulation of Human Cortex Evokes High Gamma Activity That Predicts Conscious Somatosensory Perception. *J. Neural Eng.* 15, 026015 (2017).
139. Lee, B. *et al.* Engineering Artificial Somatosensation Through Cortical Stimulation in Humans. *Front. Syst. Neurosci.* 12, 24 (2018).
140. Collins, C. E., Airey, D. C., Young, N. A., Leitch, D. B. & Kaas, J. H. Neuron Densities Vary across and within Cortical Areas in Primates. *Proc. Natl. Acad. Sci.* 107, 15927–15932 (2010).
141. Heming, E., Sanden, A. & Kiss, Z. H. T. Designing a Somatosensory Neural Prosthesis: Percepts Evoked by Different Patterns of Thalamic Stimulation. *J. Neural Eng.* 7, 064001 (2010).
142. Heming, E. A., Choo, R., Davies, J. N. & Kiss, Z. H. T. Designing a Thalamic Somatosensory Neural Prosthesis: Consistency and Persistence of Percepts Evoked by Electrical Stimulation. *IEEE Trans. Neural Syst. Rehabil. Eng.* 19, 477–482 (2011).
143. Gaunt, R. A., Prochazka, A., Mushahwar, V. K., Guevremont, L. & Ellaway, P. H. Intraspinal Microstimulation Excites Multisegmental Sensory Afferents at Lower Stimulus Levels Than Local α -Motoneuron Responses. *J. Neurophysiol.* 96, 2995–3005 (2006).
144. Gaunt, R. A., Hokanson, J. A. & Weber, D. J. Microstimulation of Primary Afferent Neurons in the L7 Dorsal Root Ganglia Using Multielectrode Arrays in Anesthetized Cats: Thresholds and Recruitment Properties. *J. Neural Eng.* 6, 055009 (2009).
145. Inanici, F. *et al.* Transcutaneous Electrical Spinal Stimulation Promotes Long-Term Recovery of Upper Extremity Function in Chronic Tetraplegia. *IEEE Trans. Neural Syst. Rehabil. Eng.* 26, 1272–1278 (2018).
146. Yizhar, O., Fenno, L. E., Davidson, T. J., Mogri, M. & Deisseroth, K. Optogenetics in Neural Systems. *Neuron* 71, 9–34 (2011).
147. Fenno, L., Yizhar, O. & Deisseroth, K. The Development and Application of Optogenetics. *Annu. Rev. Neurosci.* 34, 389–412 (2011).
148. Diester, I. *et al.* An Optogenetic Toolbox Designed for Primates. *Nat. Neurosci.* 14, 387–397 (2011).
149. Canales, A. *et al.* Multifunctional Fibers for Simultaneous Optical, Electrical and Chemical Interrogation of Neural Circuits in Vivo. *Nat. Biotechnol.* 33, 277–284 (2015).
150. Lee, W. *et al.* Image-Guided Transcranial Focused Ultrasound Stimulates Human Primary Somatosensory Cortex. *Sci. Rep.* 5, 8743 (2015).
151. Naor, O., Krupa, S. & Shoham, S. Ultrasonic Neuromodulation. *J. Neural Eng.* 13, 031003 (2016).
152. Legon, W. *et al.* Transcranial Focused Ultrasound Modulates the Activity of Primary Somatosensory Cortex in Humans. *Nat. Neurosci.* 17, 322–329 (2014).
153. Grossman, N. *et al.* Noninvasive Deep Brain Stimulation via Temporally Interfering Electric Fields. *Cell* 169, 1029–1041.e16 (2017).
154. Chen, R., Romero, G., Christiansen, M. G., Mohr, A. & Anikeeva, P. Wireless Magnetothermal Deep Brain Stimulation. *Science* 347, 1477–80 (2015).
155. Grill, W. M., Norman, S. E. & Bellamkonda, R. V. Implanted Neural Interfaces: Biochallenges and Engineered Solutions. *Annu Rev Biomed Eng* 11, 1–24 (2009).
156. Barrese, J. C. *et al.* Failure Mode Analysis of Silicon-Based Intracortical Microelectrode Arrays in Non-Human Primates. *J. Neural Eng.* 10, 066014 (2013).
157. Chestek, C. A. *et al.* Long-Term Stability of Neural Prosthetic Control Signals from Silicon Cortical Arrays in Rhesus Macaque Motor Cortex. *J. Neural Eng.* 8, 045005 (2011).
158. Downey, J. E., Schwed, N., Chase, S. M., Schwartz, A. B. & Collinger, J. L. Intracortical Recording Stability in Human Brain–computer Interface Users. *J. Neural Eng.* 15, 046016 (2018).
159. Callier, T. *et al.* Long-Term Stability of Sensitivity to Intracortical Microstimulation of Somatosensory Cortex. *J. Neural Eng.* 12, 056010 (2015).
160. Bartlett, J. R. *et al.* Psychophysics of Electrical Stimulation of Striate Cortex in Macaques. *J. Neurophysiol.*

- 94, 3430–3442 (2005).
161. Davis, T. S. *et al.* Spatial and Temporal Characteristics of V1 Microstimulation during Chronic Implantation of a Microelectrode Array in a Behaving Macaque. *J. Neural Eng.* 9, 065003 (2012).
 162. Nurse, E. S. *et al.* Consistency of Long-Term Subdural Electrocorticography in Humans. *IEEE Trans. Biomed. Eng.* 65, 344–352 (2018).
 163. Kombos, T. & Süss, O. Neurophysiological Basis of Direct Cortical Stimulation and Applied Neuroanatomy of the Motor Cortex: A Review. *Neurosurg. Focus* 27, E3 (2009).
 164. Merrill, D. R., Bikson, M. & Jefferys, J. G. R. Electrical Stimulation of Excitable Tissue: Design of Efficacious and Safe Protocols. *J. Neurosci. Methods* 141, 171–198 (2005).
 165. Rattay, F. & Wenger, C. Which Elements of the Mammalian Central Nervous System Are Excited by Low Current Stimulation with Microelectrodes? *Neuroscience* 170, 399–407 (2010).
 166. Ranck, J. B. Which Elements Are Excited in Electrical Stimulation of Mammalian Central Nervous System: A Review. *Brain Res.* 98, 417–440 (1975).
 167. Kudela, P. & Anderson, W. S. Computational Modeling of Subdural Cortical Stimulation: A Quantitative Spatiotemporal Analysis of Action Potential Initiation in a High-Density Multicompartment Model. *Neuromodulation* 18, 552–64 (2015).
 168. Histed, M. H., Bonin, V. & Reid, R. C. Direct Activation of Sparse, Distributed Populations of Cortical Neurons by Electrical Microstimulation. *Neuron* 63, 508–522 (2009).
 169. Logothetis, N. K. *et al.* The Effects of Electrical Microstimulation on Cortical Signal Propagation. *Nat. Neurosci.* 13, 1283–1291 (2010).
 170. Vincent, M. *et al.* The Difference between Electrical Microstimulation and Direct Electrical Stimulation - Towards New Opportunities for Innovative Functional Brain Mapping? *Rev. Neurosci.* 27, 231–258 (2016).
 171. Kim, D., Jun, S. C. & Kim, H.-I. Computational Study of Subdural and Epidural Cortical Stimulation of the Motor Cortex. *Conf Proc IEEE Eng Med Biol Soc* 2011, 7226–9 (2011).
 172. Nathan, S. S., Sinha, S. R., Gordon, B., Lesser, R. P. & Thakor, N. V. Determination of Current Density Distributions Generated by Electrical Stimulation of the Human Cerebral Cortex. *Electroencephalogr. Clin. Neurophysiol.* 86, 183–192 (1993).
 173. Telford, W. M., Geldart, L. P. & Sheriff, R. E. *Applied Geophysics.* Cambridge University Press 3, (1990).
 174. Wongsarnpigoon, A. & Grill, W. M. Computational Modeling of Epidural Cortical Stimulation. *J. Neural Eng.* 5, 443–454 (2008).
 175. Rattay, F. The Basic Mechanism for the Electrical Stimulation of the Nervous System. *Neuroscience* 89, 335–346 (1999).
 176. Leuthardt, E. C., Miller, K. J., Schalk, G., Rao, R. P. N. & Ojemann, J. G. Electrocorticography-Based Brain Computer Interface-The Seattle Experience. *IEEE Trans. Neural Syst. Rehabil. Eng.* 14, 194–198 (2006).
 177. Blakely, T., Miller, K. J., Zanos, S. P., Rao, R. P. N. & Ojemann, J. G. Robust, Long-Term Control of an Electrocorticographic Brain-Computer Interface with Fixed Parameters. *Neurosurg. Focus* 27, E13 (2009).
 178. Hermes, D., Miller, K. J., Noordmans, H. J., Vansteensel, M. J. & Ramsey, N. F. Automated Electrocorticographic Electrode Localization on Individually Rendered Brain Surfaces. *J. Neurosci. Methods* 185, 293–298 (2010).
 179. Wander, J. D. *et al.* Distributed Cortical Adaptation during Learning of a Brain-Computer Interface Task. *Proc. Natl. Acad. Sci.* 110, 10818–10823 (2013).
 180. Shannon, R. V. A Model of Safe Levels for Electrical Stimulation. *IEEE Trans. Biomed. Eng.* 39, 424–426 (1992).
 181. Kim, S. *et al.* Behavioral Assessment of Sensitivity to Intracortical Microstimulation of Primate Somatosensory Cortex. *Proc. Natl. Acad. Sci. U. S. A.* 112, 15202–15207 (2015).
 182. Kim, L. H., McLeod, R. S. & Kiss, Z. H. T. A New Psychometric Questionnaire for Reporting of Somatosensory Percepts. *J. Neural Eng.* 15, 013002 (2018).
 183. Rohrmann, B. *Verbal qualifiers for rating scales: Sociolinguistic considerations and psychometric data.* (2007).
 184. Leek, M. R. Adaptive Procedures in Psychophysical Research. *Percept. Psychophys.* 63, 1279–92 (2001).
 185. Levitt, H. Transformed Up-Down Methods in Psychoacoustics. *J. Acoust. Soc. Am.* 49, 467–477 (1971).
 186. Wichmann, F. A. & Hill, N. J. The Psychometric Function: I. Fitting, Sampling, and Goodness of Fit. *Percept. Psychophys.* 63, 1293–1313 (2001).

187. Wichmann, F. A. & Hill, N. J. The Psychometric Function: II. Bootstrap-Based Confidence Intervals and Sampling. *Percept. Psychophys.* 63, 1314–1329 (2001).
188. Ekman, G. Weber's Law and Related Functions. *J. Psychol.* 47, 343–352 (1959).
189. Gordon, B. *et al.* Parameters for Direct Cortical Electrical Stimulation in the Human: Histopathologic Confirmation. *Electroencephalogr. Clin. Neurophysiol.* 75, 371–377 (1990).
190. Spence, C. & Gallace, A. Recent Developments in the Study of Tactile Attention. *Can. J. Exp. Psychol.* 61, 196–207 (2007).
191. Butovas, S. & Schwarz, C. Detection Psychophysics of Intracortical Microstimulation in Rat Primary Somatosensory Cortex. *Eur. J. Neurosci.* 25, 2161–2169 (2007).
192. Horsager, A. *et al.* Predicting Visual Sensitivity in Retinal Prosthesis Patients. *Invest. Ophthalmol. Vis. Sci.* 50, 1483–91 (2009).
193. Merikle, P. M., Smilek, D. & Eastwood, J. D. Perception without Awareness: Perspectives from Cognitive Psychology. *Cognition* 79, 115–134 (2001).
194. Kovac, S. *et al.* Comparison of Bipolar versus Monopolar Extraoperative Electrical Cortical Stimulation Mapping in Patients with Focal Epilepsy. *Clin. Neurophysiol.* 125, 667–674 (2014).
195. Lele, B. P. P., Sinclair, D. C. & Weddell, G. The Reaction Time to Touch. *J. Physiol.* 123, 187–203 (1954).
196. Šidák, Z. Rectangular Confidence Regions for the Means of Multivariate Normal Distributions. *J. Am. Stat. Assoc.* 62, 626–633 (1967).
197. Dinno, A. & Newton, H. J. Nonparametric Pairwise Multiple Comparisons in Independent Groups Using Dunn's Test. *Stata J.* 1, 292–300 (2015).
198. Brown, M. B. & Forsythe, A. B. Robust Tests for the Equality of Variances. *J. Am. Stat. Assoc.* 69, 364–367 (1974).
199. Woodworth, R. S. & Schlosberg, H. *Experimental Psychology*. (New York, Holt, 1954).
200. Godlove, J. M., Whaite, E. O. & Batista, A. P. Comparing Temporal Aspects of Visual, Tactile, and Microstimulation Feedback for Motor Control. *J. Neural Eng.* 11, 046025 (2014).
201. Arber, C. & Li, M. Cortical Interneurons from Human Pluripotent Stem Cells: Prospects for Neurological and Psychiatric Disease. *Front. Cell. Neurosci.* 7, 1–11 (2013).
202. Markram, H. *et al.* Interneurons of the Neocortical Inhibitory System. *Nat. Rev. Neurosci.* 5, 793–807 (2004).
203. Butovas, S. & Schwarz, C. Spatiotemporal Effects of Microstimulation in Rat Neocortex: A Parametric Study Using Multielectrode Recordings. *J. Neurophysiol.* 90, 3024–3039 (2003).
204. Millard, D. C., Whitmire, C. J., Gollnick, C. A., Rozell, C. J. & Stanley, G. B. Electrical and Optical Activation of Mesoscale Neural Circuits with Implications for Coding. *J. Neurosci.* 35, 15702–15715 (2015).
205. Tehovnik, E. J., Tolias, A. S., Sultan, F., Slocum, W. M. & Logothetis, N. K. Direct and Indirect Activation of Cortical Neurons by Electrical Microstimulation. *J. Neurophysiol.* 96, 512–521 (2006).
206. Yazdan-Shahmorad, A., Kipke, D. R. & Lehmkuhle, M. J. Polarity of Cortical Electrical Stimulation Differentially Affects Neuronal Activity of Deep and Superficial Layers of Rat Motor Cortex. *Brain Stimul.* 4, 228–241 (2011).
207. Tehovnik, E. J. & Slocum, W. M. Depth-Dependent Detection of Microampere Currents Delivered to Monkey V1. *Eur. J. Neurosci.* 29, 1477–89 (2009).
208. Graczyk, E. L., Resnik, L., Schiefer, M. A., Schmitt, M. S. & Tyler, D. J. Home Use of a Neural-Connected Sensory Prosthesis Provides the Functional and Psychosocial Experience of Having a Hand Again. *Sci. Rep.* 8, 9866 (2018).
209. Makin, T. R., Holmes, N. P. & Ehrsson, H. H. On the Other Hand: Dummy Hands and Peripersonal Space. *Behav. Brain Res.* 191, 1–10 (2008).
210. Rohde, M., Di Luca, M., Ernst, M. O., Gibson, S. & Bradshaw, J. The Rubber Hand Illusion: Feeling of Ownership and Proprioceptive Drift Do Not Go Hand in Hand. *PLoS One* 6, e21659 (2011).
211. Ehrsson, H. H. *et al.* Upper Limb Amputees Can Be Induced to Experience a Rubber Hand as Their Own. *Brain* 131, 3443–52 (2008).
212. Schmalzl, L. *et al.* 'Pulling Telescoped Phantoms out of the Stump': Manipulating the Perceived Position of Phantom Limbs Using a Full-Body Illusion. *Front. Hum. Neurosci.* 5, 121 (2011).
213. Marasco, P. D., Kim, K., Colgate, J. E., Peshkin, M. A. & Kuiken, T. A. Robotic Touch Shifts Perception of Embodiment to a Prosthesis in Targeted Reinnervation Amputees. *Brain* 134, 747–58 (2011).

214. Kapadia, N., Zivanovic, V., Verrier, M. & Popovic, M. Toronto Rehabilitation Institute—Hand Function Test: Assessment of Gross Motor Function in Individuals With Spinal Cord Injury. *Top. Spinal Cord Inj. Rehabil.* 18, 167–186 (2012).
215. Weisz, N. *et al.* Prestimulus Oscillatory Power and Connectivity Patterns Predispose Conscious Somatosensory Perception. *Proc. Natl. Acad. Sci. U. S. A.* 111, E417-25 (2014).
216. Berglund, U. & Berglund, B. Adaptation and Recovery in Vibrotactile Perception. *Percept. Mot. Skills* 30, 843–853 (1970).
217. Tannan, V., Simons, S., Dennis, R. G. & Tommerdahl, M. Effects of Adaptation on the Capacity to Differentiate Simultaneously Delivered Dual-Site Vibrotactile Stimuli. *Brain Res.* 1186, 164–170 (2007).
218. Goble, A. K. & Hollins, M. Vibrotactile Adaptation Enhances Amplitude Discrimination. *J. Acoust. Soc. Am.* 93, 771–780 (1993).
219. Munson, W. A. Standardizing Auditory Tests. *J. Acoust. Soc. Am.* 22, 675 (1950).
220. Fechner, G. T. *Elements of psychophysics.* (Holt, Rinehart and Winston, 1966).
221. Swets, J. A. & Green, D. M. *Signal detection theory and psychophysics.* (Wiley, 1966).
222. Jogan, M. & Stocker, A. A. A New Two-Alternative Forced Choice Method for the Unbiased Characterization of Perceptual Bias and Discriminability. *J. Vis.* 14(3), 1–18 (2014).
223. Dosen, S., Schaeffer, M.-C. & Farina, D. Time-Division Multiplexing for Myoelectric Closed-Loop Control Using Electrotactile Feedback. *J. Neuroeng. Rehabil.* 11, 138 (2014).
224. Miller, L. E. & Weber, D. J. Brain Training: Cortical Plasticity and Afferent Feedback in Brain-Machine Interface Systems. *IEEE Trans. Neural Syst. Rehabil. Eng.* 19, 465–467 (2011).
225. Sun, H. *et al.* Sequential Activation of Premotor, Primary Somatosensory and Primary Motor Areas in Humans during Cued Finger Movements. *Clin. Neurophysiol.* 126, 2150–2161 (2015).
226. Semprini, M., Bencicelli, L. & Vato, A. A Parametric Study of Intracortical Microstimulation in Behaving Rats for the Development of Artificial Sensory Channels. in *Conf Proc IEEE Eng Med Biol Soc* 799–802 (2012). doi:10.1109/EMBC.2012.6346052
227. Graziano, M. S. A. & Botvinick, M. M. How the Brain Represents the Body: Insights from Neurophysiology and Psychology. in *Common mechanisms in perception and action* (eds. Prinz, W. & Hommel, B.) 19, 136–157 (2002).
228. Spence, C., Pavani, F., Maravita, A. & Holmes, N. Multisensory Contributions to the 3-D Representation of Visuotactile Peripersonal Space in Humans: Evidence from the Crossmodal Congruency Task. *J. Physiol. Paris* 98, 171–89 (2004).
229. Van der Biest, L., Legrain, V., De Paepe, A. & Crombez, G. Watching What’s Coming near Increases Tactile Sensitivity: An Experimental Investigation. *Behav. Brain Res.* 297, 307–314 (2016).
230. Frey, J. N. *et al.* The Tactile Window to Consciousness Is Characterized by Frequency-Specific Integration and Segregation of the Primary Somatosensory Cortex. *Sci. Rep.* 6, 20805 (2016).
231. Foxe, J. J. & Snyder, A. C. The Role of Alpha-Band Brain Oscillations as a Sensory Suppression Mechanism during Selective Attention. *Front. Psychol.* 2, 154 (2011).
232. van Ede, F., de Lange, F., Jensen, O. & Maris, E. Orienting Attention to an Upcoming Tactile Event Involves a Spatially and Temporally Specific Modulation of Sensorimotor Alpha- and Beta-Band Oscillations. *J. Neurosci.* 31, 2016–2024 (2011).
233. Palva, S. & Palva, J. M. Functional Roles of Alpha-Band Phase Synchronization in Local and Large-Scale Cortical Networks. *Front. Psychol.* 2, 204 (2011).
234. Ray, S., Niebur, E., Hsiao, S. S., Sinai, A. & Crone, N. E. High-Frequency Gamma Activity (80-150Hz) Is Increased in Human Cortex during Selective Attention. *Clin. Neurophysiol.* 119, 116–33 (2008).
235. Bauer, M., Oostenveld, R., Peeters, M. & Fries, P. Tactile Spatial Attention Enhances Gamma-Band Activity in Somatosensory Cortex and Reduces Low-Frequency Activity in Parieto-Occipital Areas. *J. Neurosci.* 26, (2006).
236. Illes, J. & Bird, S. J. Neuroethics: A Modern Context for Ethics in Neuroscience. *Trends Neurosci.* 29, 511–517 (2006).
237. Glannon, W. Ethical Issues in Neuroprosthetics. *J. Neural Eng.* 13, 021002 (2016).
238. Klein, E. & Ojemann, J. Informed Consent in Implantable BCI Research: Identification of Research Risks and Recommendations for Development of Best Practices. *J. Neural Eng.* 13, 043001 (2016).
239. Klein, E., Brown, T., Sample, M., Truitt, A. R. & Goering, S. Engineering the Brain: Ethical Issues and the

- Introduction of Neural Devices. *Hastings Cent. Rep.* 45, 26–35 (2015).
240. Williams, N. R. & Okun, M. S. Deep Brain Stimulation (DBS) at the Interface of Neurology and Psychiatry. *J. Clin. Invest.* 123, 4546–56 (2013).
 241. Blabe, C. H. *et al.* Assessment of Brain-Machine Interfaces from the Perspective of People with Paralysis. *J. Neural Eng.* 12, 043002 (2015).
 242. Goering, S., Klein, E., Dougherty, D. D. & Widge, A. S. Staying in the Loop: Relational Agency and Identity in Next-Generation DBS for Psychiatry. *AJOB Neurosci.* 8, 59–70 (2017).
 243. Bonaci, T., Calo, R. & Chizeck, H. J. App Stores for the Brain : Privacy and Security in Brain-Computer Interfaces. *IEEE Technol. Soc. Mag.* 34, 32–39 (2015).
 244. Fisher, C. E. *et al.* The Ethics of Research on Deep Brain Stimulation for Depression: Decisional Capacity and Therapeutic Misconception. *Ann. N. Y. Acad. Sci.* 1265, 69–79 (2012).
 245. Taylor, P., Esnouf, J. & Hobby, J. The Functional Impact of the Freehand System on Tetraplegic Hand Function. Clinical Results. *Spinal Cord* 40, 560–566 (2002).
 246. Hobby, J., Taylor, P. N. & Esnouf, J. Restoration of Tetraplegic Hand Function by Use of the Neurocontrol Freehand System. *J. Hand Surg. Br. Eur. Vol.* 26, 459–464 (2001).
 247. Underwood, E. Brain Implant Trials Raise Ethical Concerns. *Science* 348, 1186–7 (2015).
 248. Bergstein, B. Paralyzed Again. *MIT Technology Review* (2015).
 249. Its Alive. *Google Groups: Freehand Users Group* (2017). Available at: <https://groups.google.com/forum/#!topic/freehand-users-group/k9rRiYkA1iQ>.
 250. Holtzheimer, P. E. *et al.* Subcallosal Cingulate Deep Brain Stimulation for Treatment-Resistant Depression: A Multisite, Randomised, Sham-Controlled Trial. *Lancet Psychiatry* 4, 839–888 (2017).
 251. Underwood, E. Brain Implant Trials Spur Ethical Discussions. *Science* 358, 710 (2017).
 252. Lázaro-Muñoz, G., Yoshor, D., Beauchamp, M. S., Goodman, W. K. & McGuire, A. L. Continued Access to Investigational Brain Implants. *Nat. Rev. Neurosci.* 19, 317–318 (2018).